

UC Merced

UC Merced Electronic Theses and Dissertations

Title

Reductions mediated by diboron with palladium and towards conformationally dynamic emissive materials based on the stimuli responsive DBCOD scaffold.

Permalink

<https://escholarship.org/uc/item/8hg7h9dz>

Author

Spaller, William

Publication Date

2023

Peer reviewed|Thesis/dissertation

William Carl Spaller

Reductions mediated by diboron with palladium and towards conformationally dynamic emissive materials based on the stimuli responsive DBCOD scaffold.

Table of Contents

Chapter 1 – Diboron (4) mediated reductions involving palladium

Introduction to diboron(4) compounds.....	1
Introduction and background on palladium catalysis in organic synthesis	2
Background on generation of palladium (0) complexes in catalysis.....	3
Established methods for the synthesis of Pd(P ^t Bu ₃).....	4
Synthesis of Pd(P ^t Bu ₃) ₂ using tetrahydroxydiboron as the reducing agent ,.....	7
Conclusion for synthesis of Pd(P(<i>t</i> Bu) ₃) ₂ by B ₂ (OH) ₄ reduction.....	12
Attempted development of a diboron (4) mediated homogeneous palladium catalyzed hydrogenation of olefins.....	13
Introduction to palladium catalyzed diboron (4) mediated reductions.....	14
Traditional and newer catalytic methods for deoxygenation of ketones.....	17
Introduction to tetrahydroxydiboron mediated palladium catalyzed deoxygenation of aromatic ketones.....	20
Deoxygenation of 4-acetylbiphenyl (1a) in THF- <i>d</i> ₈	22
Deoxygenative deuteration of select substrates.....	25
Deuteration of 4-acetylbiphenyl (1a) with D ₂ O and B ₂ (pin).....	26
Failed substrates under optimized conditions.....	27
Evidence of borate ester intermediate in the deoxygenation of aromatic ketones under anhydrous conditions.....	28
Post catalytic H/D exchange experiment on 4-ethylbiphenyl (2a).....	32
Putative catalytic cycle for the deoxygenation of aromatic ketones with tetrahydroxydiboron.....	33
Conclusions from Chapter 1.....	34
General procedure for the evaluation of the scope of the deoxygenation reaction.....	35
Experimental section for synthesis of Pd(P ^t Bu ₃) ₂	36
References for Chapter 1	37
Tabulated spectroscopic data from Chapter 1 (2a-2q).....	40
References for NMR data collected in chapter 1.....	46
NMR spectra of substrates in Chapter 1.....	47

Chapter 2 - Synthesis and characterization of anthracene and pyrene containing DBCOD compounds.....	68
Chapter 2 Abstract.....	68
Introduction to DBCOD based materials.....	68
Background on excimer formation in pyrene.....	72
Background of anthracene excimer in solution.....	73
Synthesis of tetramethyldibenzocyclooctadiene (TM-DBCOD) scaffold.....	74
Synthesis and characterization of 1-PryeneAmide.....	75
Results and discussion on 1-PyreneAmide.....	76
NMR Characterization of 1-PyreneAmide.....	78

Synthesis of 2-AnthraAmide	83
Results and discussion on 2-AnthraAmide.....	85
1-AnthraAmide initial results.....	89
Conclusions on chapter 2.....	90
References for chapter 2.....	91

Chapter 3. Borohydride mediated reduction of trans-stilbene and discovery of an benzo-oxetenes side product - Side Projects	93
Hydride mediated alkene hydrogenation	93
Isolation and identification of a novel benzo-oxetane product.....	96
Conclusions to Chapter 3.....	101
References for Chapter 3.....	101

List of Tables, Images, and Figures

Chapter 1

Table 1.1. Influence of Additives on Synthesis of Pd(P ^t Bu ₃) ₂
Table 1.2. B ₂ (OH) ₄ Mediated Pd/C Catalyzed Transfer Hydrogenation of Olefins with Stoichiometric Water Used as a Hydrogen Atom Source
Table 1.3. Probing the Role of the Diboron (4) Mediator in Pd-catalyzed Ketone Deoxygenations
Table 1.4. Evaluation of the Generality of the Reductive Deoxygenation of Aryl Ketones
Table 1.5. Evaluations of the Deuteration of Aromatic Ketones Using B ₂ (OD) ₄
Table 1.6. Full Optimization of the Deoxygenation Reaction.

List of Images

Image 1.1. Left – Difference in observed color of reaction where B₂(OH)₄ is omitted (left) and included (right). A clear yellow color is observed when B₂(OH)₄ is omitted, indicating no reaction is occurring

List of Figures

- Figure 1.1.** The structure of tetrahydroxydiboron, bis(pinacolato)diboron, and bis(catecholato) diboron
- Figure 1.2** Generally accepted mechanism of palladium cross coupling reactions between aryl halides and aryl boronate. Arrow feeding into cycle represents the reduction of the precatalyst to the active catalyst.
- Figure 1.3.** Pathways for the generation of zero valent palladium from Pd(II) precatalyst under catalytic conditions
- Figure 1.4 .** Triaryl phosphines as a reducing agent in formation of Pd(0) as described by Amatore and coworkers.
- Figure 1.5.** Skeletal structure of bis tritertbutyl phosphine palladium (0)
- Figure 1.6.** Synthetic utility of Pd(P^tBu₃)₂ in cross coupling reactions.
- Figure 1.7** Published methods for the generation of Pd(P^tBu₃)₂ and this work

Figure 1.8. Proposed base mediated mechanism of reduction of Pd(COD)Br₂ and synthesis of palladium (0) bisphosphines

Figure 1.9. Suspected cyclometalated Pd species observed in crude reaction mixtures.

Figure 1.10. Proposed mechanism for the tetrahydroxydiboron mediated reduction of Pd(OAc)₂ to Pd(P^tBu₃)₂

Figure 1.11. Control reaction in which Pd(Cl)₂ was employed and NaOAc added

Figure 1.12. ³¹P NMR (202 MHz, hexanes) of Figure 1.11 reaction with included NaOAc revealing some conversion of PdCl₂ to Pd(P^tBu₃)₂

Figure 1.13. Control reaction in which Pd(Cl)₂ was employed and no NaOAc added.

Figure 1.14. ³¹P-NMR (202 MHz, hexanes) of Figure 1.13 reaction without added NaOAc revealing trace conversion of PdCl₂ to Pd(P^tBu₃)₂

Figure 1.15. Proposed mechanism of palladium catalyzed diboron mediated transfer hydrogenation of alkenes using water as a stoichiometric hydrogen atom donor.

Figure 1.16. Attempts to develop a homogeneous B₂(OH)₄ mediated method of olefin hydrogenation with Pd(P^tBu₃)₂

Figure 1.17. Select examples of palladium catalyzed diboron(4) mediated reductions

Figure 1.18. Proposed mechanism for the palladium catalyzed evolution of H₂ using B₂(pin)₂ and water (left) or methanol (right).

Figure 1.19. Diboron-assisted palladium-catalyzed transfer hydrogenation of *N*-heteroaromatics in water

Figure 1.20 (Top) Deoxygenation of amine and pyridine *N*-Oxides with tetrahydroxydiboron (Bottom) Proposed mechanism.

Figure 1.21 Clemmensen and Wolf-Kishner - traditional methods of deoxygenation that use harsh conditions

Figure 1.22. Recent examples of palladium catalyzed deoxygenations of ketones using silanes as hydrogen atom donors

Figure 1.23. Example of palladium-catalyzed transfer deoxygenation of ketones. (Top). An example showing slow B₂(OH)₄-mediated catalytic transfer semi-reduction of ketones in 1,2-dichloroethane. (Bottom) This work: B₂(OH)₄-mediated catalytic ketone transfer deoxygenation in THF, with key putative mechanistic intermediates

Figure 1.24. Deoxygenation of **1a** conducted in THF-d₈ yielded no detectable deuteration

Figure 1.25. ¹H NMR (500 MHz in THF-d₈) of 4-ethylbiphenyl (**2a**)

Figure 1.26. ¹³C NMR (125 MHz, THF-d₈) of 4-ethylbiphenyl (**2a**)

Figure 1.27 Method for the synthesis of B₂(OD)₄ as reported by Cummins et al.²⁰

Figure 1.28. ¹H NMR (500 MHz, DMSO-d₆) of B₂(OD)₄ used in this work

Figure 1.29. Deoxygenative deuteration **1a** with B₂(pin)₂ and D₂O

Figure 1.30. ¹H NMR (500 MHz in CDCl₃) of deoxygenative deuteration of 4-acetyl biphenyl using B₂(pin)₂ and D₂O.

Figure 1.31. Substrates that failed to undergo diboron(4) mediated deoxygenation.

Figure 1.32. Reaction scheme devised for the detection of borate ester (**4a**)

Figure 1.33. Comparing ¹H NMR (500 MHz in CDCl₃) before (blue) and after (red) addition of D₂O of reaction depicted in **Figure 1.33**. Small signal at 5.30 ppm is attributed to DCM.

Figure 1.34. ¹H NMR (500 MHz in CDCl₃) of reaction depicted in Figure 1.32 before addition of D₂O.

Figure 1.35 ¹H NMR (500 MHz in CDCl₃) of reaction depicted in Figure 1.32 after addition of D₂O

Figure 1.36. Hydrogen gas observed by ¹H NMR in anhydrous THF by mixing B₂(OH)₄ and Pd/C

Figure 1.37. ^1H NMR (500 MHz, CDCl_3) spectrum showing H_2 gas evolved from Pd/C and $\text{B}_2(\text{OH})_4$ in anhydrous THF

Figure 1.38. Experiment showing post catalytic H/D exchange in the benzylic position of 4-acetylbiphenyl with $\text{B}_2(\text{OD})_2$

Figure 1.39. ^1H NMR (500 MHz in CDCl_3) spectrum of partially deuterated **2a** by post-catalytic exchange. Inset – zoomed into the methylene signal showing splitting due to incorporated deuterium atoms.

Figure 1.40. Putative catalytic cycle for the palladium catalyzed tetrahydroxydiboron mediated deoxygenation of aromatic ketones.

Figure 1.41. ^{31}P NMR spectrum (202 MHz, unreferenced) of recrystallized $\text{Pd}(\text{P}^t\text{Bu}_3)_2$ in toluene

Chapter 2

List of Figures

Figure 2.1. Top : Chemical structure of a DBCOD Unit and Possible Substitution Positions on the Phenyl Rings (1–10) Bottom: Energy vs. Conformational state diagram of boat to chair conformational change.

Figure 2.2. Chemical structures of TM-BDCOD (left) 1,10-di-Ph-amide (middle) and 1,10-di-PhEster (right)

Figure 2.3. ^1H NMR spectra of 2 mg/mL 1,10-di-Ph-amide in different deuterated solvents at 23 °C. B and C denote the Boat and Chair conformations, respectively.

Figure 2.4. Strategy for reversible excimer formation in TM-BDCOD based scaffolds. 2-AnthraAmide is depicted here as the model compound.

Figure 2.5. Top - Simplified orbital description of excimer formation in pyrene. Bottom - Example spectra showing both the emissions of monomer and excimer.

Figure 2.6. Top: Skeletal representation of octaacid and anthracene host guest interaction giving rise to excimer emissions. Bottom: emission of anthracene as a function of octaacid concentration showing increase in redshifted band attributed to excimer.

Figure 2.7. Photodimerization of anthracene to dianthracene and thermally reversibility of dimerization

Figure 2.8. Oxidation and photoisomerization of DAB

Figure 2.9. Synthetic Scheme for the synthesis of DBCOD based compounds appended with pyrene or anthracene.

Figure 2.10 Skeletal structure of 1-PyreneAmide

Figure 2.11. Variable temperature fluorescence of 1- PyreneAmide in DMSO (10 μM) and 340 nm excitation 1 mm slit width.

Figure 2.12. ^1H NMR (500 MHz, CDCl_3) spectrum of 1-PyreneAmide

Figure 2.13 ^1H - ^{13}C HSQC (500 MHz, CDCl_3) of 1,10-PyreneAmide in the aromatic region

Figure 2.14. ^1H - ^{13}C HSQC (500 MHz, CDCl_3) of 1-PyreneAmide in the methylene and methyl region

Figure 2.15. ^1H - ^1H COSY (500 MHz, CDCl_3) of 1-Pyrene Amide

Figure 2.16. High resolution mass spectrum of 1-PyreneAmide

Figure 2.17. Variable temperature ^1H NMR (500 MHz, CDCl_3) of 1-PyreneAmide

Figure 2.18. Skeletal structure of 2-AnthraAmide

Figure 2.19. High resolution mass spectrum of 2-AnthraAmide confirming the molecular weight as 703.32 g/mol.

Figure 2.20. VT- ^1H NMR (500 MHz, DMSO- d_6) of aromatic region of 2-AnthraAmide

Figure 2.21. VT- ^1H NMR (500 MHz, DMSO- d_6) of methyl region of 2-AnthraAmide

Figure 2.22. Variable temperature ($^{\circ}\text{C}$) fluorescence spectrum of 2-Anthraamide in N-Methylpyrrolidone (NMP)

Figure 2.23. Fluorescence spectrum of 2-amide anthracene in various solvents. 1 nm slit width and 345 nm excitation.

Figure 2.24. 2-AnthraAmide ^1H -NMR in DMSO- d_6 . Middle : after irradiation at 365 nm for 24 hr. Bottom - After heating at 160 $^{\circ}\text{C}$ in oil bath for 48 hr. New peaks at ~ 4.5 ppm are ascribed to photo-isomer shown in Figure 2.22 below.

Figure 2.25. Proposed structure of the photo-isomer of 2-AnthraAmide.

Figure 2.26. Skeletal structure of 1-AnthraAmide

Figure 2.27. VT ^1H NMR (500 MHz, CDCl_3) of 1-AnthraAmide

Figure 2.28. Fluorescence spectrum of 1-AnthraAmide in DCM and DMSO.

Chapter 3

List of Tables

Table 3.1. Optimization and Proposed mechanism of H-Bin/ KO^tBu Palladium Catalyzed Hydrogenation of Trans-Stilbene

List of Images

Image 3.1 . Picture of TLC plate of reaction depicted in **Figure 3.4 bottom** in the left most lane. The other lanes are from fractions of the column chromatography used to isolate the unknown product. Eluent - EtOAc:Hexanes (1:4).

List of Figures

Figure 3.1. β -diketiminato iron (II) catalyzed hydrogenation of alkenes using H-Bin

Figure 3.2. Nucleophile promoted decomposition of HBpin to form BH_3 as demonstrated by Thomas

Figure 3.3. (Top) Sulfuryl fluoride mediated synthesis of benzo-oxetes from 2'-acetophenones. (Bottom) Side product of benzo-oxetane when MeCN is employed as solvent.

Figure 3.4. ^1H NMR (500 MHz, CDCl_3) of isolated **5a**

Figure 3.5 ^{13}C NMR (101 MHz, CDCl_3) of isolated **5a**

Figure 3.6 ^{13}C - ^1H HSQC (500 MHz, CDCl_3) of **5a**.

Figure 3.7 ^{13}C - ^1H HMBC (500 MHz, CDCl_3) of **5a**.

List of Abbreviations

BDE- Bond dissociation energy

$\text{B}_2(\text{OH})_4$ - tetrahydroxydiboron

dba – benzylideneacetone

cod – cyclooctadiene

B₂(pin)₂ – Bispinacolato diborane
B₂(OH)₄ – Tetrahydroxodiboron
B₂(cat)₂ – bis(catecholato) diboron
TM-DBCOD - 2,3,8,9-tetramethyl-5,6,11,12-tetrahydrodibenzo[a,e][8]annulene
DBCOD - dibenzo[a]cyclooctadiene
An – Anthracene
DiAn – Dianthracene
Py – Pyrene
DAB - 1,2-di(9-anthryl)benzene
DCB – 1,2-dichlorobenzene
NMP – N-Methylpyrrolidone

Curriculum Vita

William Carl Spaller

Northrop Grumman

Principal Research Scientist (Jan 2023-Present) – Motor Health and Management Group

University of California, Merced (June 2017-present)

Graduate Research Associate Nguyen Group, Department of Chemistry and Biochemistry (Aug 2022 - Dec2022)

Graduate Research Associate Lu Group, Department of Materials Science (August 2020-July 2022)

Graduate Research Associate Stokes Group, Department of Chemistry and Biochemistry (June 2017-August 2020)

Research accomplishments

- Developed a robust diboron(4) reagents mediated palladium catalyzed deoxygenation of aromatic ketones, as well as elucidated a key intermediate in the reaction pathway giving mechanistic insight (Stokes Group)
- Developed a novel method for the synthesis of the ubiquitous catalyst Pd(P^tBu)₃ using inexpensive starting materials (Stokes Group)
- Successfully synthesized several DBCOD (dibenzo[a]cyclooctadiene) compounds (Lu Group)

Colorado State University (Jan 2015 - May 2017, Shores Group)

Education

University of California, Merced

PhD Candidate, Chemistry and Biology

Summer 2023

Thesis Title: Reductions mediated by diboron with palladium and towards conformationally dynamic emissive materials based on the stimuli responsive DBCOD scaffold.

Colorado State University

BA in Microbiology 2008-2012

BA in Chemistry 2015-2017

Awards/Recognitions

Nancy Levinger Summer Undergraduate Fellowship – Summer 2016 (Colorado State University)

MACES Graduate Research Fellow – August 2018 - May 2020 (UC Merced)

Publications

William Spaller.; Jennifer Q. Lu.; Benjamin J. Stokes, Tetrahydroxydiboron-Mediated Palladium-Catalyzed Deoxygenative Transfer Hydrogenation of Aryl Ketones. *Adv. Synth. Catal.* **2022**, 364, 2571-2575

Pin Liu; Randy Espinoza; Md. Imran Khan; **William C. Spaller**; Sayantani Ghosh; Son C. Nguyen, Mechanistic insight into deep holes from interband transitions in Palladium nanoparticle photocatalysts. *iScience* 25, 103737, February 18, **2022**

Ozumerzifon T. J.; Bhowmick, I.; **Spaller, W. C.**; Rappé A. K.; Shores, M. P. Toward Steric Control of Guest Binding Modality: A Cationic Co(II) Complex Exhibiting Cation Binding and Zero-Field Relaxation. *Chem. Commun.* **2017**, 53, 4211–4214

References

1. **Dr. Benjamin Stokes** – Assistant Professor of Chemistry at Santa Clara University
2. **Dr. Jennifer Lu** - Professor of Materials Science and Engineering
3. **Dr. Son Nguyen** – Assistant Professor of Chemistry at University of California, Merced

Abstract

In Chapter 1, tetrahydroxydiboron ($B_2(OH)_4$) is shown to effect 2 novel reductions involving palladium. First, we demonstrate a novel synthesis of $Pd(P^tBu_3)_2$ using $B_2(OH)_4$ as a reducing agent. Next, I discuss the attempted development of the diboron(4) reagent mediated homogeneous system for the hydrogenation of olefins catalyzed by $Pd(P^tBu_3)_2$, which was unsuccessful. Subsequently, I found and developed a Pd/C catalyzed deoxygenation of aromatic ketones in which $B_2(OH)_4$ is the sole reductant and hydrogen atom donor. I demonstrated the hydrogen atoms originating on the hydroxyl moieties of $B_2(OH)_4$ were incorporated into the final deoxygenated product, which had never been demonstrated previously. A small scope of deuterated products is presented using the deuterated $B_2(OD)_4$. A key intermediate postulated to be a borate ester was identified and a putative mechanism is proposed, including a key hydrogenolysis of a borate ester.

In Chapter 2, I disclose attempts to synthesize thermally responsive emissive compounds based on the TM-DBCOD scaffold. The unique ability of the DBCOD scaffold to exist stably in both the Boat and Chair conformers allows for the potential to design thermally responsive materials. I attempted to exploit this conformational change to reversibly form a species capable of excimer formation based on the spatial separation of the pendant excimer formers, both anthracene and pyrene. Three novel compounds with pendant anthracene or pyrene were synthesized and examined for their photophysical properties. These compounds were designated 1-PyreneAmide, 1-AnthraAmide, and 2-AnthraAmide. 1-PyreneAmide exhibited exclusively excimer emission, indicating spatial separation of $\sim 10\text{\AA}$ could not be achieved in this system, regardless of temperature. 2-AnthraAmide exhibited an interesting dependence on solvent polarity indicating an end-to-end overlap excimer may be forming, as a function of solvent polarity. Additionally, 2-AnthraAmide was shown to isomerize into the intramolecular [4+4] photo isomer. Thermal reversion of the proposed photo isomer was observed. Initial results were collected on the 1-AnthraAmide showing probable excimer formation, but further experiments are needed to characterize its behavior.

In Chapter 3, I discuss two side projects arising from observations made in the chapter 1 work. First, I discuss the development of a hydride mediated palladium catalyzed hydrogenation of alkenes. A combination of potassium tertbutoxide and pinacol borane effectively mediated hydrogenation of C=C bonds under palladium catalysis. I demonstrated the addition of a stoichiometric oxidant allowed for closure of the catalytic cycle. Next, I discuss the isolation and identification of a benzo oxetane product discovered during the diboron(4) mediated deoxygenation of aromatic ketones work.

Chapter 1. Diboron(4) mediated reductions involving palladium

Abstract

The following dissertation chapter discusses the use of tetrahydroxydiboron ($B_2(OH)_4$) as an effective reducing agent in the synthesis of $Pd(P^tBu_3)_2$. This novel preparation of $Pd(P^tBu_3)_2$ offers bench chemists a convenient synthesis of this useful catalyst. A diboron mediated palladium catalyzed deoxygenation of aromatic ketones was developed, intermediates identified, and a reaction pathway proposed. In this chemistry, the sole reductant and hydrogen atom donor is $B_2(OH)_4$.

Introduction to diboron(4) compounds

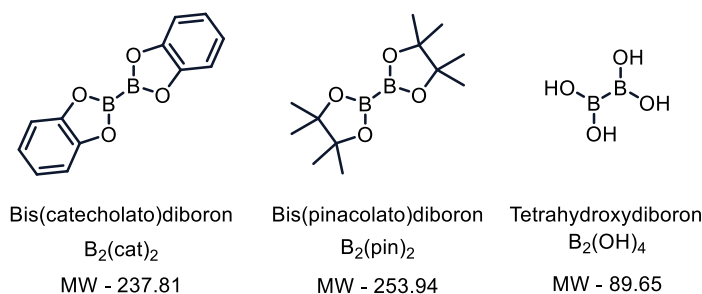


Figure 1.1. The structure of tetrahydroxydiboron, bis(pinacolato)diboron, and bis(catecholato)diboron

Diboron tetrachloride was synthesized in 1925 by striking an arc across zinc electrodes immersed in boron trichloride and isolation in 1% yield. Thankfully since then more efficient routes have been devised to forming B-B bonds leading to many derivatives.¹ Figure 1.1 shows the most relevant of these compounds to this dissertation. The electropositive nature of boron leads to the B-B bond being electron rich. These electrons can be unlocked in a myriad of synthetically useful ways. With an estimated BDE of 68 kcal/mol the B-B in diboron (4) reagents and the very stable B-O bond being 120 kcal/mol the thermodynamic driving force to make B-O bonds is quite large. Coupled with the $\sim\Delta H$ 180 kcal/mol for the formation of two B-O bonds the thermodynamic driving force to drive reactions is present.² The hybridization of the B-B varies from $sp^{1.25}$ in $B_2(OH)_4$ to $sp^{1.89}$ in tetrakis(pyrrolidino)diborane, with $B_2(pin)_2$ and $B_2(cat)_2$ falling between at $sp^{1.47}$ and $sp^{1.32}$ respectively. Increasing the donating ability of the ligands on the boron increases the p character and weakens the B-B bond.³ A typical B-B is 1.70Å making it relatively long for a single bond. Simple hydrolysis of $B_2(OH)_4$ with water releases H_2 and $B(OH)_3$ and is a well-established process.⁴ For these reasons diboron (4) reagents have emerged as versatile useful reducing agents in recent years.

Tetrahydroxydiboron ($B_2(OH)_4$) is the simplest of the diboron (4) reagents that contain a B-B single bond. Originally conceived as borylating agents, they have found great utility as a reducing agent in recent years as reductants, especially under palladium

catalysis. While the chemistry of bis(pinacolato)diboron ($B_2(\text{pin})_2$) is significantly more developed it's is much less atom economical, considering the large amount of carbon it contains as empty mass. Additionally, it can be troublesome as it decomposes into pinacol which is difficult to remove from reaction mixtures. $B_2(\text{OH})_4$ is significantly cheaper than $B_2(\text{pin})_2$. Analysis (December 2022) of both reagents bought at the 25 g scale from supplier Sigma Aldrich prices out $B_2(\text{OH})_4$ to cost \$0.79/mmol while $B_2(\text{pin})_2$ costs \$2.43/mmol. Clearly, there is an economical and practical incentive to replace $B_2(\text{pin})_2$ with $B_2(\text{OH})_4$ wherever possible. Leveraging the strong propensity of boron to form bonds with oxygen methods can be developed for both inorganic synthesis and reduction of unsaturated organic moieties. While the exact role of palladium in some of these systems remains up for debate, our understanding of diboron (4) chemistry is rapidly advancing, allowing us to utilize it in more useful organic transformations.

Introduction and background on palladium catalysis in organic synthesis

The discovery and emergence of palladium catalyzed cross coupling reactions in the 1970's revolutionized synthetic chemistry by giving chemists new ways to construct C-C and C-N bonds. Among the many reactions like the Suzuki-Miyaura, Stille, Negishi, Heck, Sonagashira, Buchwald-Hartwig with electrophiles (often abbreviated as Ar-X) such as aryl halides, aryl triflates, and sulfonyl chlorides among other coupling partners.⁵ The general mechanistic scheme is shown in Figure 1.2. Overall, the zero valent palladium is generated from a Pd(II) precatalyst (or Pd (0) is pre-formed) followed by an oxidative addition of the aryl electrophile and subsequent transmetalation to give a biaryl palladium that undergoes reductive elimination affording the biaryl coupled product. Pd (0) is necessary for the initial oxidative addition step and must be generated by some manner of reduction. In many procedures, *in situ* reduction of a Pd (II) precatalyst such as $Pd(\text{OAc})_2$ to the active Pd(0) must occur before the oxidative addition. In a catalytic reaction in which a Pd (II) salt (e.g. $Pd(\text{OAc})_2$ or $PdCl_2$) *in situ* reduction to the active Pd(0) species is well studied.⁵ However, translation to synthesis and isolation of a Pd (0) complex is rarely described. This is due to the fact bisphosphine palladium (0) complexes are typically air sensitive making them difficult to store and synthesize. Methods to efficiently generate the active catalyst in cross coupling reaction help alleviate the ambiguity in the *in-situ* reduction of the precatalyst to active catalyst. The general steps of and methods for the generation of the active catalysts are of the utmost importance in developing more efficient catalytic species and much effort is dedicated to such understanding. Figure 1.3 illustrates the generally accepted and described pathways for the reduction of Pd(II) under catalytic conditions.

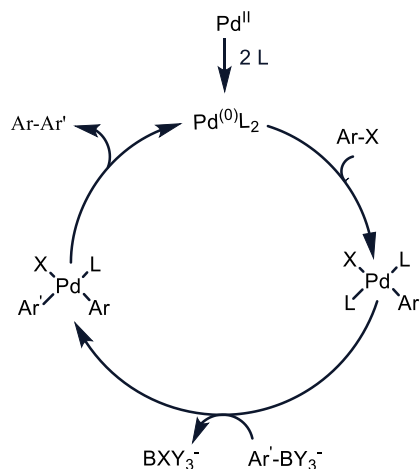


Figure 1.2 Generally accepted mechanism of palladium cross coupling reactions between aryl halides and aryl boronate. Arrow feeding into cycle represents the reduction of the precatalyst to the active catalyst.

Background on generation of palladium (0) complexes in catalysis

Generally, two strategies are employed when employing palladium in cross coupling reactions. First is to use a Pd(0) precatalyst such as Pd(dba)₂ and desired ligand. This strategy has the palladium already in the desired oxidation state and able to immediately perform an oxidative addition and begin the catalytic cycle. Other known Pd(0) species that can be isolated and used in catalytic reactions include Pd(PCy₃)₂, Pd(P^tBu₃)₂, and Pd(Po-tol₃)₂.

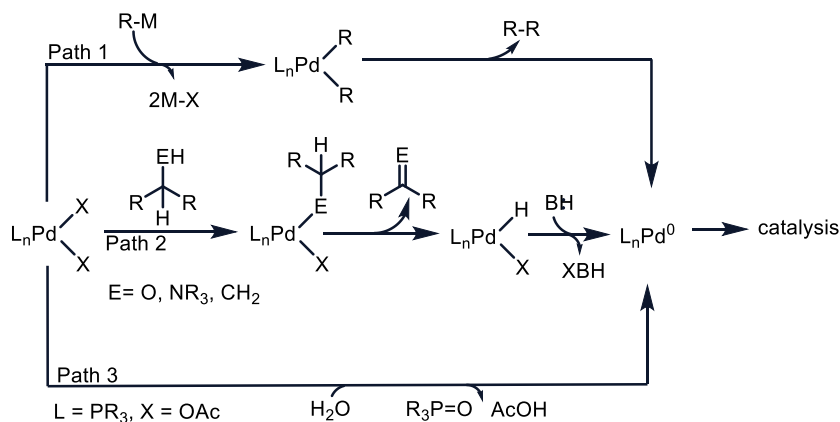


Figure 1.3. Pathways for the generation of zero valent palladium from Pd(II) precatalyst under catalytic conditions

Generation of Pd (0) from Pd (II) precursors is described under a myriad of different catalytic conditions.⁶ Figure 1.3 provides an overview of the commonly invoked pathways for the reduction of Pd(II). Path 1 involves an organometallic coupling partner such as

Grignard reagent or alkyl lithium reagents. Two successive transmetalations followed by a reductive elimination furnishes Pd(0). Path 2 involves β -hydride elimination of coordinated group such as an alcohol amine, or alkane followed by base promoted reductive elimination. Path 3 involves reduction by a phosphine ligand reliant upon the presence of water. Figure 1.4 illustrates the proposed mechanism in Path 3. Pioneering work by Amatore showed PPh_3 can act as the reducing agent to form $\text{Pd}^0(\text{PPh}_3)_4$ when $\text{Pd}(\text{OAc})_2$ is employed as the starting material.⁷ They postulate $\text{Pd}^{\text{II}}(\text{PPh}_3)_2(\text{OAc})_2$ reduces by an intramolecular mechanism and the acetate ion proves to be crucial in the reduction step. Water also appeared to be necessary for hydrolysis of the triphenyl phosphonium acetate byproduct. The PPh_3 acts as both the ligand and reducing agent in this system with an equivalent of triphenyl phosphine oxide produced serving as evidence to this claim. Amatore and coworkers additionally demonstrated for bidentate phosphine ligands an amine, phosphine, and water were all required to produce a final Pd(0) species in bidentate phosphine systems.⁷

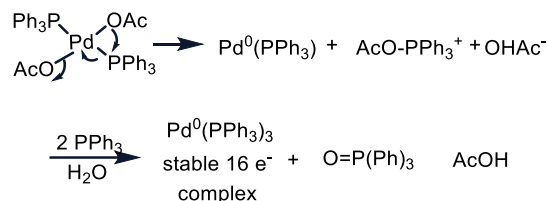


Figure 1.4 . Triaryl phosphines as a reducing agent in formation of Pd(0) as described by Amatore and coworkers.

While these 3 paths describe the mechanism for the generation of Pd(0) in under catalytic conditions, the principals are seldom applied to the synthesis and isolation of the complexes themselves. Mechanistic understanding of these pathways can help guide the development of methods to independently synthesize these valuable catalysts.

Established methods for the synthesis of $\text{Pd}(\text{P}^t\text{Bu}_3)_2$

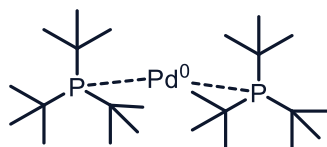


Figure 1.5. Skeletal structure of bis tritertbutyl phosphine palladium (0)

$\text{Pd}(\text{P}^t\text{Bu}_3)_2$ is a crystalline white air sensitive compound that must be handled in an inert atmosphere. $\text{Pd}(\text{P}^t\text{Bu}_3)_2$ is among the most useful bisphosphine Pd(0) compounds as it catalyzes an extremely wide range of cross coupling reactions. See Figure 1.6 below for a select review of the synthetic utility.^{8,9} Its bulky and electron rich tertiary alkyl phosphine ligands both promote the oxidative addition and reductive elimination steps of the catalytic cycle in cross coupling reactions shown in Figure 1.2. Although not the most widely used of the palladium catalysts $\text{Pd}(\text{P}^t\text{Bu}_3)_2$ has been found to catalyze some specialized reactions as shown in Figure 1.6. Coupling between alkyl lithium reagents and

aryl- and alkenyl bromide, synthesis of acid chlorides forgoing the use of SOCl_2 , and synthesis of chromates through a diastereoselective carboidination are all reported with $\text{Pd}(\text{P}^t\text{Bu}_3)_2$. It has also been shown to effectively couple many specialized coupling partners such as alkylgermanes, alkali-metal silanolates and triorgano-indium reagents.⁸ These are important tools for chemists constructing new molecules.

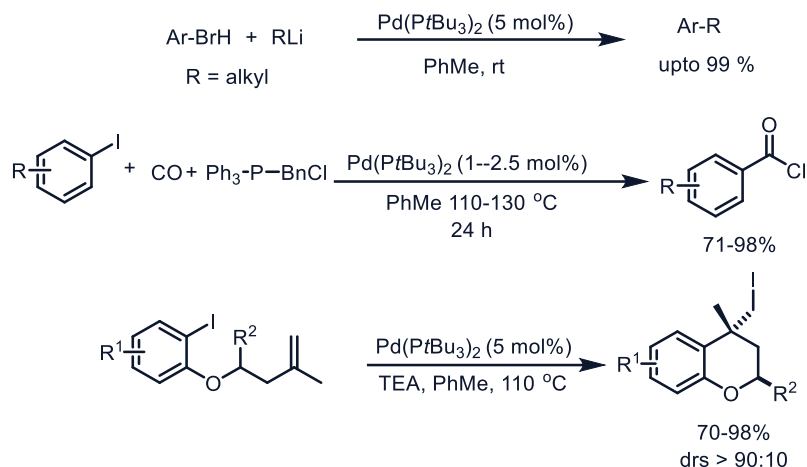
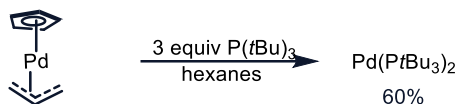


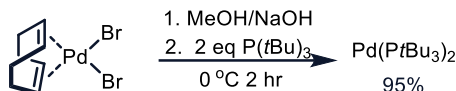
Figure 1.6. Synthetic utility of $\text{Pd}(\text{P}^t\text{Bu}_3)_2$ in cross coupling reactions.

The first synthesis and isolation of $\text{Pd}(\text{P}^t\text{Bu}_3)_2$ was reported in 1976 by reacting P^tBu_3 with $[\text{Pd}(\eta^5\text{-C}_5\text{H}_5)(\eta^3\text{-C}_3\text{H}_5)]$ in hexanes in a 60% isolated yield (top, Figure 1.7).¹⁰ The authors remarked it exhibited a rich reactivity and forthcoming investigations were ongoing. Unfortunately, the starting material $[\text{Pd}(\eta^5\text{-C}_5\text{H}_5)(\eta^3\text{-C}_3\text{H}_5)]$ is very moisture and air sensitive, as well as very expensive, compared to other palladium precursors, such as $\text{Pd}(\text{OAc})_2$. A mechanism for this reduction could not be found and doesn't appear to have been studied though one could envision a path where P^tBu_3 acts as the reducing agent, hence explaining why 3.0 equivalents are necessary. The instability and volatility of $[\text{Pd}(\eta^5\text{-C}_5\text{H}_5)(\eta^3\text{-C}_3\text{H}_5)]$ can be alleviated by reacting with NaC_6H_5 to form $\text{Pd}(\eta^5\text{-C}_5\text{H}_5)(\eta^3\text{-1-PhC}_3\text{H}_4)$, which serves a more stable and easily handled replacement for generation of bis-phosphine palladium(0) complexes.⁸ While this serves to make palladium precursors more easily handled, the cost of such reagents is still restrictive for a chemist looking to synthesize $\text{Pd}(\text{P}^t\text{Bu}_3)_2$ in a cost effective manner.

Otsuka 1975 - First report



Li 2010 - General route to Pd(0)L₂



This Work : Tetrahydroxydiboron mediated synthesis

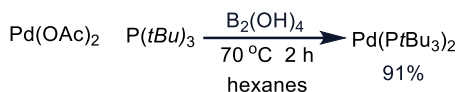


Figure 1.7 Published methods for the generation of Pd(P^tBu)₃)₂ and this work

Reports of methods to isolate Pd(P^tBu)₃)₂ since its initial report are rare and have yet to be reported using Pd(OAc)₂ as the starting material. The most practical synthesis came from Li and coworkers who demonstrated Pd(COD)Br₂ could be used and does not require a sacrificial phosphine.⁹ A stepwise pathway to the generation the Pd(PR₃)₂ product in which the olefin ligand cyclooctadiene (COD) ligand plays a crucial role, thus Pd(OAc)₂ could not be substituted under these conditions. This was evidenced by the observed formation of (1E,5Z)-1-methoxycycloocta-1,5-diene indicating the coordinated alkene ligand undergoes nucleophilic attack by a methoxide anion to generate the species di-μ-dibromobispalladium species depicted in **Figure 1.8**. Base mediated reductive elimination gives the final Pd (0) product. This methodology was used to synthesize a handful of bistrialkylpalladium phosphine (0) complexes in good yield.

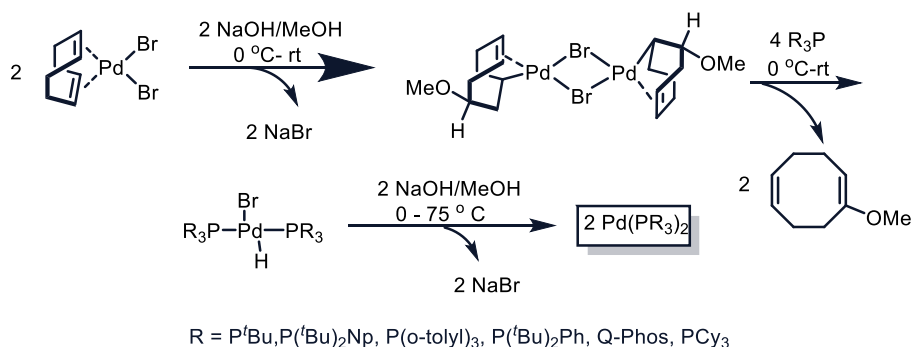


Figure 1.8. Proposed base mediated mechanism of reduction of Pd(COD)Br₂ and synthesis of palladium (0) bisphosphines

Wei and coworkers demonstrated reacting Pd(PCy₃)₂(OAc)₂ with B₂(pin)₂ the zero valent Pd(PCy₃)₂ is produced.¹⁰ Additionally, the authors demonstrated in the Miyaura

borylation that ‘pre-aging’ the Pd(Pcy₃)(OAc)₂ precatalyst with an equivalent of B₂(pin)₂ could eliminate an induction period precluding product formation. The mechanism of the Miyaura borylation is known to begin with an oxidative addition to an aryl halide by Pd(0). The authors concluded the B₂(pin)₂ acts as an efficient reducing agent to furnish Pd(0) complexes useful for catalysis. The authors never reported a procedure to isolate the zero valent species, instead characterized the products by ³¹P-NMR. The authors proposed a base promoted phosphine mediated path that lead to formation of monoligated Pd(PR₃) which disproportionate to one equivalent each of Pd(PR₃)₂ and Pd black. Isolation of Pd(P^tBu₃)₂ from these conditions would have likely been complicated by the presence of pinacol.

While PPh₃ is a suitable reducing agent for the generation of Pd(0) under the conditions reported by Amatore, its alkyl counterpart P^tBu₃ is unable to perform an analogous reduction described in Figure 1.8 and simply mixing P^tBu₃ with Pd(OAc)₂ doesn’t result in and reduction to Pd(0), nor the formation of O=P(^tBu)₃. An external reducing agent is required if Pd(OAc)₂ is to be employed. Diboron(4) reagents were proven effective in this manner, thus were screened for this purpose.

Synthesis of Pd(P^tBu₃)₂ using tetrahydroxydiboron as the reducing agent

To my knowledge since the first report, the synthesis and isolation of Pd(P^tBu₃)₂ has been reported through one novel method and one derivative as discussed above.^{8,9} We envisioned a clean production of Pd(P^tBu₃)₂ using B₂(OH)₄ as the reducing agent, the byproducts of would be soluble in polar protic solvents. In an argon filled dry box combining 3.0 equivalents P^tBu₃, Pd(OAc)₂, and 10 equivalents of B₂(OH)₄ in hexanes the resulted in formation of Pd(P^tBu₃)₂ in excellent yield of 91% after purifications(entry 1, Table 1.1). Interestingly, the reaction mixture turned from yellow/orange to clear and colorless through the course of the reaction (Image 1.1), suggesting the Pd(II) species is being consumed and a Pd(0) species is produced. The ³¹P NMR shifts of the known complexes have been reported by Colacot et al and were used to confirm the identity and purity of Pd(P^tBu₃)₂. Although recrystallization out of hot methanol can achieve pure product, simply removing the solvent and under vacuum and rinsing with methanol also affords pure Pd(P^tBu₃)₂. Lowering the equivalents of B₂(OH)₄ to 5.0 led to a slight drop in isolated yield (Table 1.1, entry 2). Lowering both the P^tBu and B₂(OH)₄ to 2.1 equivalents resulted in a lower but fair yield of 77% (Table 1.1, entry 3) When 2.5 equivalents of B₂(OH)₄ and 2.1 P^tBu were employed a drop in yield was observed, and interestingly new peaks upfield of zero in the ³¹P NMR were starting to be observed, indicating C-H activation products were forming.

Table 1.1. Influence of Additives on Synthesis of Pd(P^tBu)₂

Entry	Pd Source	P ^t Bu ₃ (x equiv)	B ₂ (OH) ₄ (equiv)	temp (°C)	t (h)	yield [%] ^a
1	Pd(OAc) ₂	3	10	70	12	91
2	Pd(OAc) ₂	3	5	70	12	85
3	Pd(OAc) ₂	2.1	2.1	60	1	77
4	Pd(OAc) ₂	2.1	2.5	60	1	69
5 ^b	Pd(OAc) ₂	3	0	70	12	0 ^b
6	Pd(MeCN) ₂ Cl ₂	3	10	70	12	15
7	PdCl ₂	3	10	70	12	0
8 ^c	Pd(OAc) ₂	2.1	5	70	1	nd ^c

- a. All yields are isolated, and all reactions run on 0.3 mmol scale in an argon filled glovebox b. Analysis by ³¹P NMR revealed trace product but attempts to purify failed c. Precipitation of Pd black observed



Image 1.1. Left – Difference in observed color of reaction where B₂(OH)₄ is omitted (left) and included (right). A clear yellow color is observed when B₂(OH)₄ is omitted, indicating no reaction is occurring.

A control experiment omitting B₂(OH)₄ did not result in the same color change and only trace product was detected with ³¹P-NMR (Table 1.1, entry 5). The presence of an acetate counter ion appeared essential for reaction success. Considering the driving force of this reaction is formation of a B-O bond, this is unsurprising. Pd(II) salts lacking an

acetate gave drastically lower yields (Table 1.1, entries 6,7) or failed entirely. The lowered solubility of PdCl₂ and Pd(MeCN)₂Cl₂ could also be responsible for the drop in yield. This result agrees with reports that B₂(pin)₂ fails to reduce [(Cy₃P)₂PdCl₂] to Pd(PCy₃)₂.¹³ Computational studies of transmetalation suggest the high energy of the B-Cl (as opposed to B-OAc) product makes a transmetalation unlikely to occur on a Pd-Cl species.¹⁴ Highest results were observed with 3.0 equivalents of likely due to the propensity of Pd(OAc)₂ to form cyclometalated species with P^tBu₃ mentioned above. When the P^tBu₃ equivalents are lowered to 2.1 with respect to the Pd(OAc)₂ cyclometalated side products were observed in the ³¹P-NMR but the major product is still Pd(P^tBu₃)₂. The ³¹P-NMR peaks up field of zero observed indicated the cyclometalated species, explored by Henderson and coworkers (Figure 1.9).¹⁵ Regarded as off-cycle catalytic species, cyclometalated species were tested for catalytic performance in Buchwald-Hartwig coupling reactions and they exhibited decreased activity, with yields ranging from 6-34%. The authors showed a cyclometalated species could be synthesized with 1:1 stoichiometry Pd(OAc)₂ to P^tBu₃ (Figure 1.9). The lowered equivalent of P^tBu₃ likely allows for the deleterious C-H activation leading to cyclometallation, eroding the yield and complicating purification. When lowered equivalents of P^tBu is used with excess B₂(OH)₄ the precipitation of Pd black is observed after about 30 minutes of stirring at 60 °C in hexanes. This may be due to the rapid disproportionation of monoligated Pd-P^tBu₃ to Pd black and Pd(P^tBu₃)₂.¹³

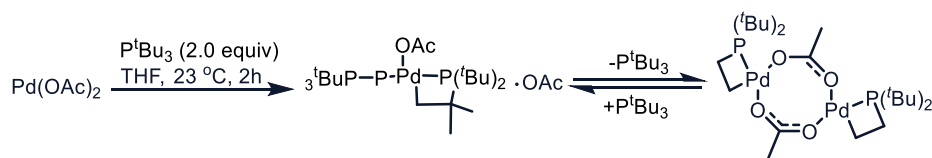


Figure 1.9. Suspected cyclometalated Pd species observed in crude reaction mixtures.

Although all results reported were using the trimer Pd₃(OAc)₆, it is worth noting that both polymeric [Pd(OAc)₂]_n and trimeric Pd₃(OAc)₆ are suitable Pd sources for this reaction and both exhibited practically identical reactivity. This is relevant considering the possible differences in reactivity exhibited by different Pd(OAc)₂ in recent works, showing [Pd(OAc)₂]_n may be unsuitable for use certain cross coupling reactions.¹⁶ Additionally, this method benefits from being run in the solvent the phosphine is commonly sold in making for easy operating procedure and easy removal of solvent during purification. It is worth noting that B₂(cat)₂ was also observed to produce Pd(P^tBu₃)₂ but its cost and atom economy brings no benefit.

The proposed mechanism is given in Figure 1.10. Transmetalation to produce a palladium boryl species and reductive elimination both of which produce an equivalent of

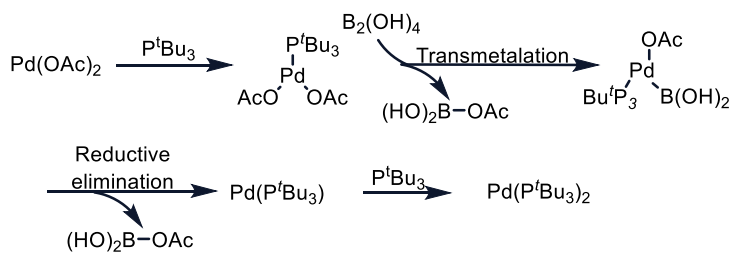


Figure 1.10. Proposed mechanism for the tetrahydroxydiboron mediated reduction of Pd(OAc)_2 to $\text{Pd(P}^t\text{Bu}_3)_2$

$(\text{OH})_2\text{-B-Oac}$. Studies of the Miyaura borylations suggest the presence of an acetate promotes a transmetalation. Bases such as acetate, as well as fluoride, alkoxides, N-heterocyclic carbenes, substituted pyridines, and phosphines are known to create transient $\text{sp}^2\text{-sp}^3$ Lewis base-diboron adducts rendering the sp^2 boron nucleophilic.¹⁷ When PdCl_2 is employed as the starting material and 5.0 equivalents of NaOAc is included a significant amount of $\text{Pd(P}^t\text{Bu}_3)_2$ is observed through $^{31}\text{P-NMR}$ (Figure 1.1) Additionally, the $^{31}\text{P-NMR}$ spectrum revealed the presence of cyclometalated species (-14.4 and -12.6 ppm) and small unidentified peaks at 68.4 ppm and 70.3 ppm. External addition of acetate promoting product formation suggests a transmetalation like the Miyaura borylation is operative, but side reactivity leading to the cyclometalated complexes cannot be suppressed, rendering PdCl_2 an ineffective starting material. Only trace $\text{Pd(P}^t\text{Bu}_3)_2$ was detected when PdCl_2 was substituted for Pd(OAc)_2 under standard conditions (Table 1.1, entry 7). An unidentified product at 82.29 ppm was also observed.

Attempts to extend this method to other bulky monodentate phosphines were unsuccessful, notably Pcy_3 failed as a ligand to afford the bisphosphine complex with $\text{B}_2(\text{OH})_4$. $[\text{Pd}(\text{PCy}_3)_2(\text{OAc})_2]$ proved unreactive under these conditions and no $\text{Pd}(\text{PCy}_3)_2$ was detected using TB as a reducing agent. Sterically and electronically similar, the divergent reactivity between PCy_3 and P^tBu_3 is difficult to rationalize. The formation of $\text{O=P}^t\text{Bu}_3$ was never observed when oxygen was rigorously excluded from the reaction mixture. This observation is of note because previous mechanisms for generation of $\text{Pd}(0)$ invoke a phosphine as the reducing agent, but clearly that is not operative reduction conditions. $\text{B}_2(\text{OH})_4$ is the sole reductant in this transformation.

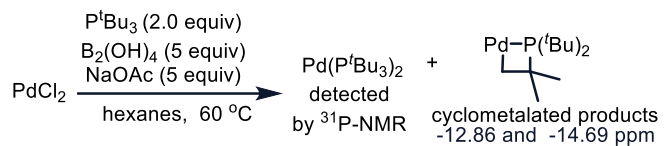


Figure 1.11. Control reaction in which $\text{Pd}(\text{Cl})_2$ was employed and NaOAc added

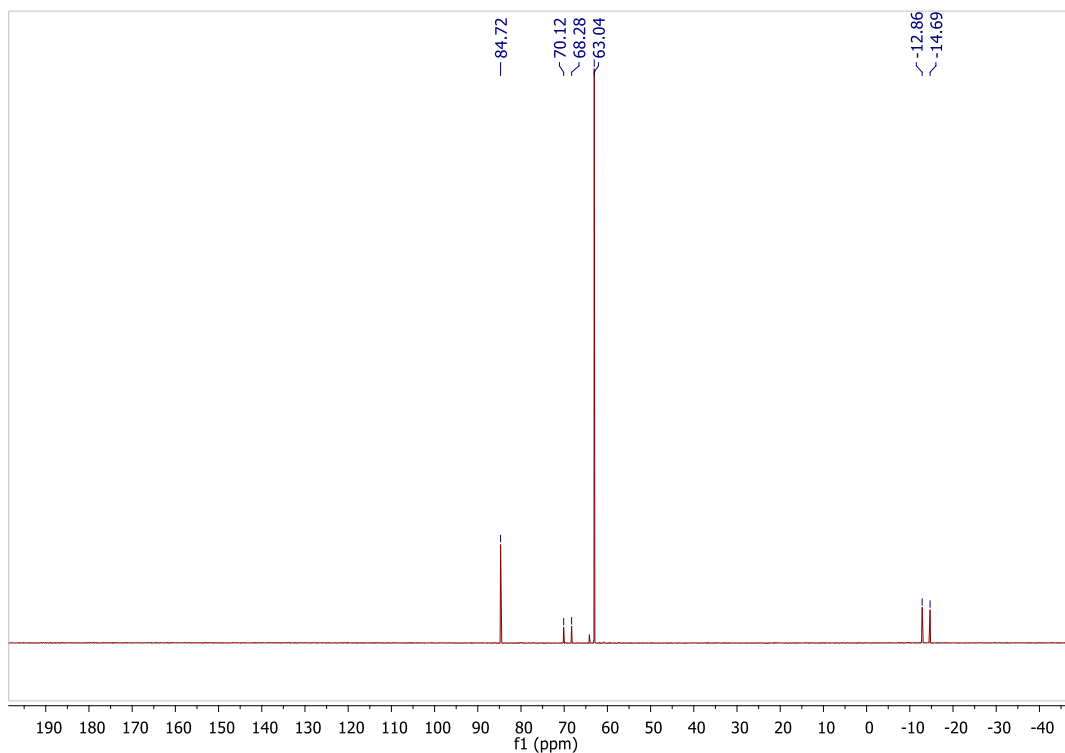


Figure 1.12. ^{31}P NMR (202 MHz, hexanes) of Figure 1.11 reaction with included NaOAc revealing some conversion of $\text{Pd}(\text{Cl})_2$ to $\text{Pd}(\text{P}^t\text{Bu}_3)_2$



Figure 1.13. Control reaction in which Pd(Cl)₂ was employed and no NaOAc added.

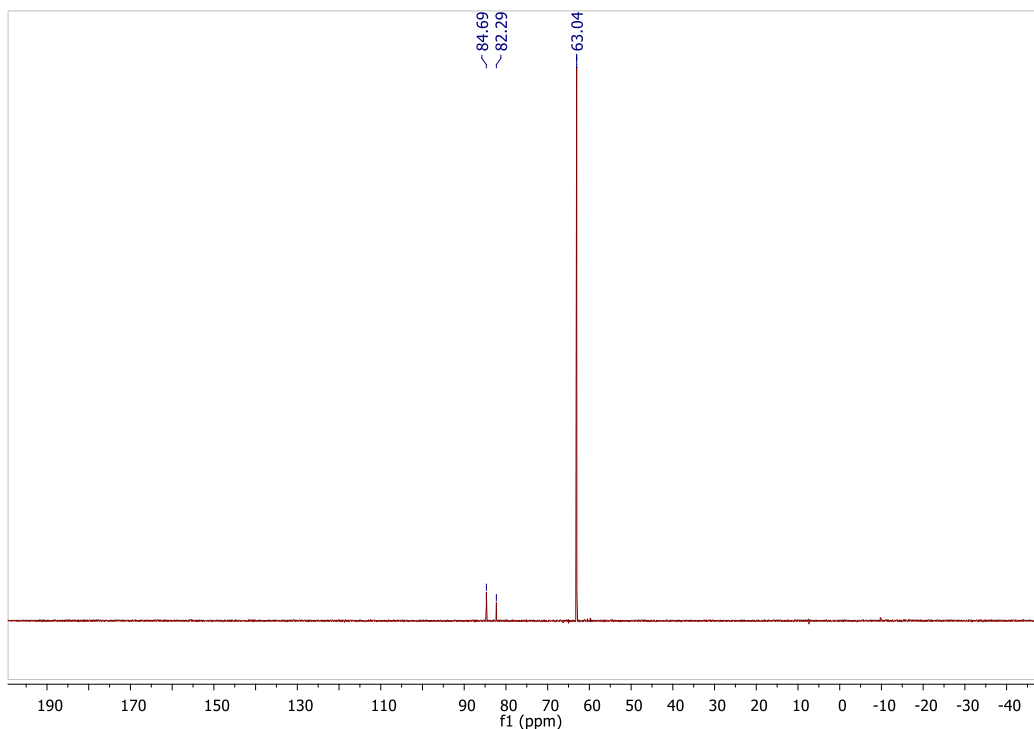


Figure 1.14. ³¹P-NMR (202 MHz, hexanes) of Figure 1.13 reaction without added NaOAc revealing trace conversion of PdCl₂ to Pd(P^tBu)₃₂

Conclusion for synthesis of Pd(P(^tBu)₃)₂ by B₂(OH)₄ reduction

B₂(OH)₄ can be effectively and cleanly used to reduce a mixture of Pd(OAc)₂ and P^tBu into the corresponding bisphosphine palladium(0) complex. An excess of phosphine is required to obtain a high yield. This is the first method to synthesize Pd(P(^tBu)₃)₂ that utilizes the ubiquitous Pd(OAc)₂ starting material. This method provides bench chemists with a facile way to prepare this useful catalyst from an easily handled palladium source. Acetate plays an important role in the transformation and deleterious C-H bond activations produce unwanted cyclometalated Pd complexes, which have been identified as off-cycle complexes in Pd cross coupling reactions.

Attempted development of a diboron (4) mediated homogeneous Pd-catalyzed hydrogenation of olefins

In 2016, Cummins and coworkers reported a $B_2(OH)_4$ mediated Pd/C catalyzed transfer hydrogenation of olefins using water as a stoichiometric hydrogen atom donor.¹⁸ The proposed mechanism is given in Figure 1.15. The original goal of all the aforementioned work was to use a homogeneous catalyst to catalyze this reaction. Subsequent studies suggested $B_2(OH)_4$ could reduce $Pd(OAc)_2$ in the presence of $P(tBu)_3$ to give $Pd(P^tBu_3)_2$, but a method for the isolation was not yet developed and the reaction was not achieved. Now with a facile method to synthesize the desired catalyst in-hand, I set out to develop a homogeneous variant to the reaction depicted in Figure 1.16.

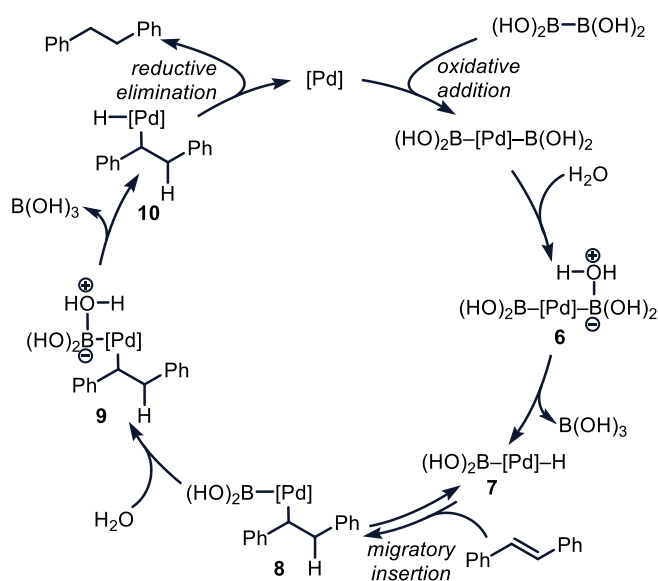


Figure 1.15. Proposed mechanism of palladium catalyzed diboron mediated transfer hydrogenation of alkenes using water as a stoichiometric hydrogen atom donor.

With interest in development of a homogeneous method of the above reaction to expand the published reaction, I began to investigate if such reducing conditions would allow for the retention of a discrete palladium complex and not formation of palladium particles. This could allow for spectroscopic analysis of palladium intermediates and kinetics experiments. Initially no reaction was observed (Figure 1.16, reaction 1) in an air-free glove box of argon when air was rigorously excluded from the reaction mixture in any solvent tested. This strongly suggested $Pd(P^tBu_3)_2$ was unreactive towards the diboron(4) reagents, as visually no change in color or hydrogenated product observed, even trace. The $14e^-$ complex was unable to engage with $B_2(OH)_4$ even at elevated temperatures (Figure 1.17, reaction 1). Only when a small amount of oxygen (air) was present a notable color change to orange/red was observed, high yields of hydrogenated product. The color change was ascribed to the presence of Pd (II) species participating in the catalytic cycle. Exposure to air likely oxidized the phosphine ligands, desaturating the palladium making it available

for catalysis. If this reaction was allowed to run to completion the mixture was observed to go clear with small black flake suspended in solution (Figure 1.16, reaction 2).

Finally, to test the true homogeneity, a mercury drop experiment gave a yield of hydrogenated product was practically zero when the mercury was added at the beginning of the reaction. Addition of excess elemental mercury to a heterogeneous reaction will poison the catalyst by binding up the active sites, thus preventing catalysis. In retrospect, this should have been the expected result since under reducing conditions palladium is known to aggregate and form large palladium particles and such larger particles would likely have lower catalytic activity due to the reduced surface area. This line of research was ceased when it became clear a homogeneous reaction was unlikely under these conditions.

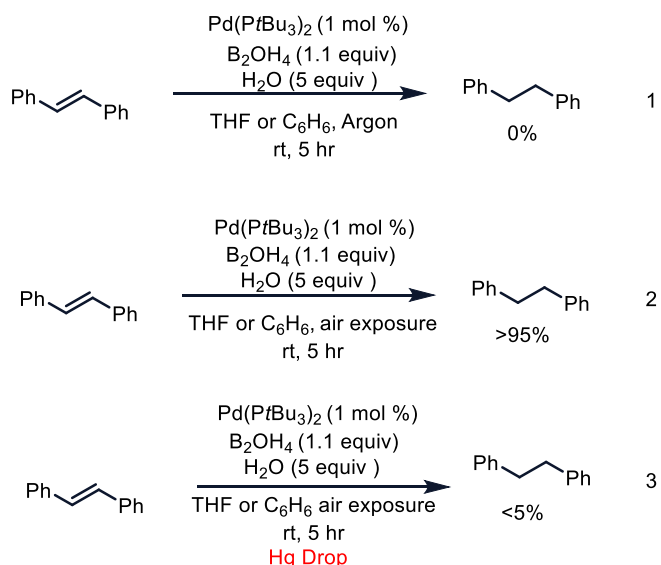


Figure 1.16. Attempts to develop a homogeneous $\text{B}_2(\text{OH})_4$ mediated method of olefin hydrogenation with $\text{Pd}(\text{P}^t\text{Bu}_3)_2$

Introduction to palladium catalyzed diboron (4) mediated reductions

Figure 1.17 shows three noteworthy examples of palladium catalyzed diboron (4) mediated reductions that exemplify this methodology. Note all three methods shown in Figure 1.18 were published within one year of each other (2016), highlighting the attention these reagents had begun to receive in this timeframe.

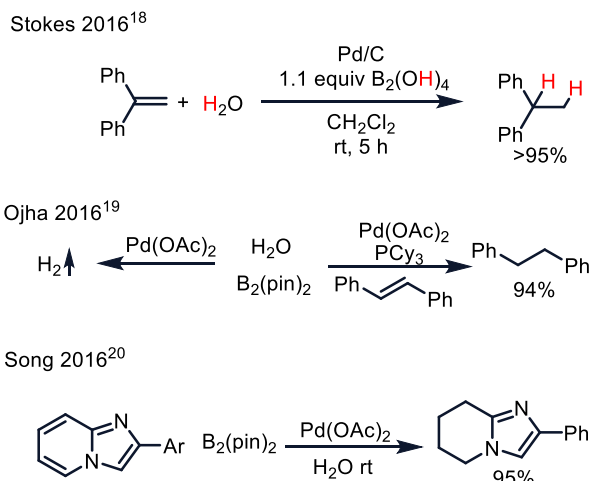


Figure 1.17. Select examples of palladium catalyzed diboron(4) mediated reductions

Generally, palladium catalyzed diboron(4) mediated reduction rely upon a protic hydrogen atom donor as in all three examples shown in Figure 1.17.^{2,26,27} Although the proposed mechanisms for all of these vary slightly, the overarching theme is the formation a boric acid derivative, $B(OR)_3$. An oxidative addition across the B-B is invoked in many of these reactions to form the key $(OR)_2$ -B-Pd-B $(OR)_2$ species but the nature of this oxidative addition is not well understood or described. Next a sigma bond metathesis for the formation of a Pd-H species as depicted in the transformation from II \rightarrow III and V \rightarrow III. The proposed mechanism in the bottom reaction follows a somewhat different path in which the initial Pd-B(pin) species is achieved through an acetate mediated transmetalation, not unlike the proposed mechanism in Figure 1.10 shown earlier. Next the Lewis acidity of the boryl ligand leads to sigma bond metathesis formation of palladium hydride III in Figure 1.19.

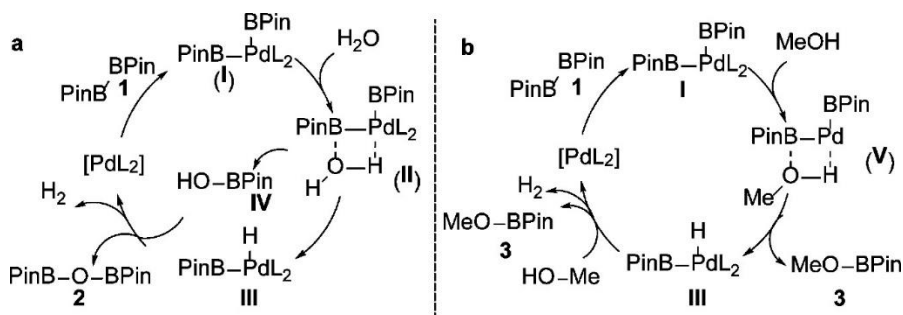


Figure 1.18. Proposed mechanism for the palladium catalyzed evolution of H_2 using $B_2(pin)_2$ and water (left) or methanol (right).

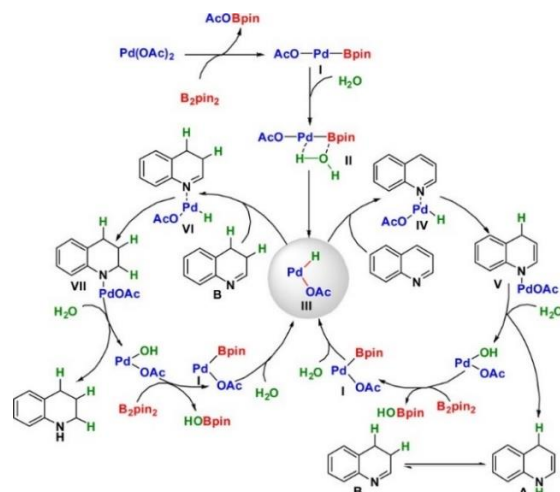


Figure 1.19. Diboron-assisted palladium-catalyzed transfer hydrogenation of *N*-heteroaromatics in water

Understanding the governing forces of this fundamental step would provide a much deeper understanding of these systems and would allow for the development of new methodologies. As discussed above, in 2015 Cummins and coworkers disclosed the first palladium catalyzed system for the hydrogenation of alkenes in which water was added as a stoichiometric hydrogen atom donor.¹⁸ Key findings from this publication are highlighted in **Table 1.2** below. Figure 1.15 shows the originally proposed mechanism by Cummins and coworkers including the same fundamental steps as also proposed by Song¹⁹ and Prabhu.²⁰

Table 1.2 B₂(OH)₄ Mediated Pd/C Catalyzed Transfer Hydrogenation of Olefins with Stoichiometric Water Used as a Hydrogen Atom Source

$\text{Ph}_2\text{C}=\text{CH}_2 + \text{H}_2\text{O} \xrightarrow[\text{solvent (0.3 M), rt, 18 h}]{\text{additive (1.1 equiv), catalyst (5 mol \%)}} \text{Ph}_2\text{CH}-\text{CH}_3$					
entry	catalyst	additive	solvent	H ₂ O (equiv)	Yield (%) ^b
1	Pd/C	B ₂ (OH) ₄	DCM	2.1	>95
2	Pd/C	B ₂ (OH) ₄	DCM	0	0
3	Pd/C	B ₂ (OH) ₄	MeOH	0	65
4	Pd/C	B₂(OH)₄	THF	0	50
5 ^c	Pd/C	B ₂ (OH) ₄	DCM	5	0
6	Pd(PPh ₃) ₄	B ₂ (OH) ₄	DCM	5	0
7 ^d	Pd/C	B ₂ (OH) ₄	DCM	5	10
8	Pd(OAc) ₂	B ₂ (OH) ₄	DCM	5	>95
9	Pd/C	B ₂ cat ₂	DCM	5	>95
10	Pd/C	B ₂ pin ₂	DCM	5	<5

These reactions employed untreated catalysts unless otherwise noted and were conducted on 0.2 mmol scale. In all cases, the substrate conversion matched the yield. ^Determined by ¹H NMR analysis of reaction mixtures upon filtration using 1,3,5-trimethoxybenzene as an internal standard. ^Reduced Pd/C was used in this experiment. ^d Reaction was conducted in the presence of 145 equivalents of Hg per Pd.

However, Cummins and coworkers noticed an intriguing result when THF was employed under anhydrous conditions. In THF with no added water a 50% yield of **2a** was observed. While not disproving the proposed pathways it strongly suggested alternative reaction modes were operative. This prompted us to investigate the nature of this ‘waterless’ reaction and seek to develop novel palladium catalyzed reductions with B₂(OH)₄ that don’t rely upon a protic hydrogen atom donor. We set out to investigate if B₂(OH)₄ could be utilized as the sole reductant under palladium catalysis.

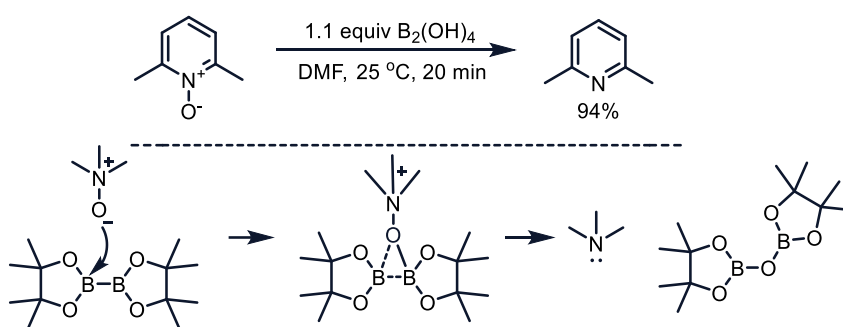


Figure 1.20 (Top) Deoxygenation of amine and pyridine N-Oxides with tetrahydroxydiboron (Bottom) Proposed mechanism.

Aside from metal catalyzed reductions, tetrahydroxydiboron can reduce certain organic moieties on its own. The oxophilic nature of boron suggests it could be used in deoxygenation, where presumably the removed oxygen would end up bound to boron. Indeed, B₂(pin)₂ was used in the deoxygenation of amine and pyridine N-Oxides (Figure 1.20) in which the driving force of the reaction is the formation of B-O bond.³ Knowing the strong tendency of boron to form stable bonds to oxygen, I envisioned a catalytic method in which ketones could be reduced using diboron reagents under palladium catalysis.

Traditional and newer catalytic methods for deoxygenation of ketones

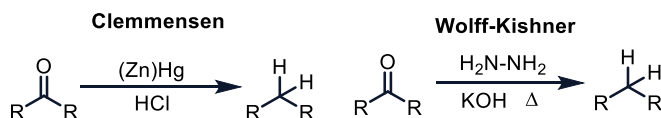


Figure 1.21 Clemmensen and Wolff-Kishner - traditional methods of deoxygenation that use harsh conditions

Before discussing the diboron mediated reaction, a discussion about the state of the deoxygenation of ketones is necessary. Deoxygenation of aromatic ketones provides a synthetic route to alkylated arenes, especially after a Friedel-Crafts acylation. Traditional methods ketone deoxygenation includes Wolff-Kishner (W-K) and Clemmensen reductions. These are associated with harsh conditions that limit their substrate scope.²¹ The most utilized non-catalytic method by far is the Wolff-Kishner which usually employs temperatures in excess of 150 °C in strongly basic conditions. Silylated hydrazine and catalytic Sc(OTf)₃ were shown to achieve the W-K reaction at room temperatures.²² The need for gentle catalytic methods of ketone deoxygenation is clear. Transition metal-catalyzed deoxygenations using H₂ gas involve either high reaction temperature or pressure, specialty non-commercial catalysts, or electrolytic H₂ generation.²³⁻³² Alternatively, catalytic transfer deoxygenation of ketones allows for reactions with simple, procedurally safe, and often mild operating conditions. Such transfer deoxygenation methods predominantly employ polymeric silanes as hydrogen atom donors.³³⁻³⁶ Notably, Adolfsson, and co-workers developed a heterogeneous palladium-catalyzed transfer deoxygenation of ketones at ambient temperature using polymethylhydrosiloxane (PMHS) as the hydride source (Figure 1.22).³³ Pd-catalyzed systems often require the addition of an acid or acid-generating co-catalyst (in this example chlorobenzene) to promote the hydrogenolysis of an alcohol intermediate. An Fe(Cl)₃ catalyzed deoxygenation requires high temperatures, high catalyst loading, and microwave irradiation to achieve deoxygenation.³⁵ Argouarch showed rhodium was capable of deoxygenation with silanes, but this method requires cooling the mixture to 0 °C and an extremely expensive catalyst in rhodium.³⁶ Borohydride reagents in carboxylic acid media (typically trifluoroacetic acid) have also been used to achieve ketone deoxygenation.³⁷

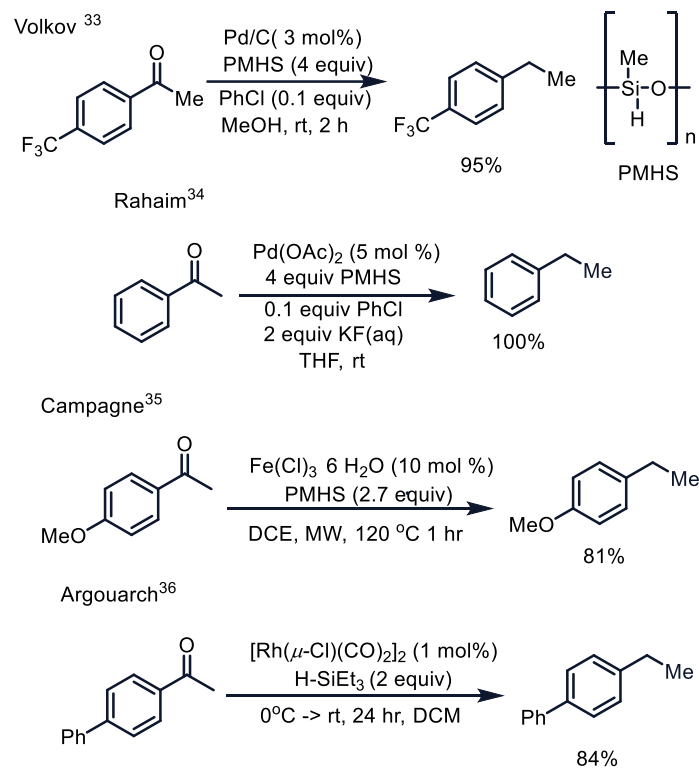


Figure 1.22. Recent examples of palladium catalyzed deoxygenations of ketones using silanes as hydrogen atom donors

Introduction to tetrahydroxydiboron mediated palladium catalyzed deoxygenation of aromatic ketones

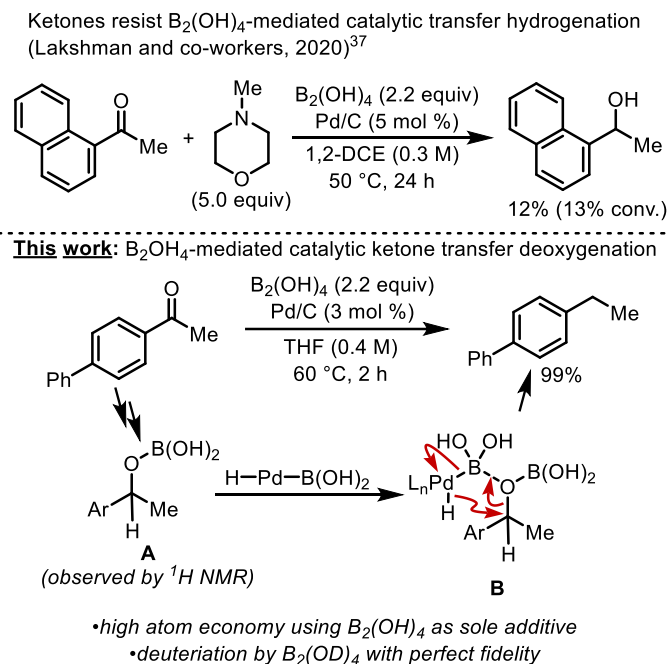
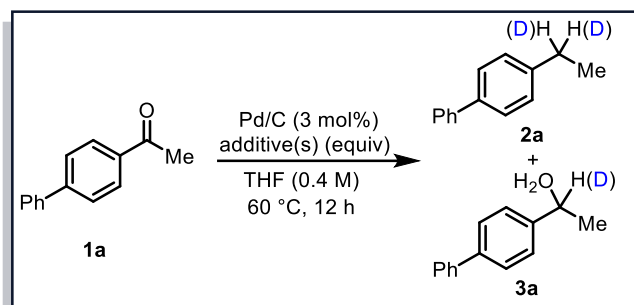


Figure 1.23. Example of palladium-catalyzed transfer deoxygenation of ketones. (Top). An example showing slow $B_2(OH)_4$ -mediated catalytic transfer semi-reduction of ketones in 1,2-dichloroethane. (Bottom) This work: $B_2(OH)_4$ -mediated catalytic ketone transfer deoxygenation in THF, with key putative mechanistic intermediates

As discussed above, tetrahydroxydiboron and other diboron(4) reagents have recently emerged as versatile reductants in palladium-catalyzed transfer hydrogenations, with tetrahydroxydiboron being the most atom economical.^{18-20,38-41} Lakshman and co-workers reported a Pd-catalyzed method that utilizes $B_2(OH)_4$ and N-methylmorpholine (NMM) to reduce a variety of functional groups including aryl halides, alkenes, and aldehydes, with aldehydes being semireduced to alcohols. Ketones were not readily reduced, and full deoxygenation was not reported (see Figure 1.23, top).³⁷ Diboron (4)-mediated ketone deoxygenation had never been reported, despite similar conditions being reported. Herein I describe a catalytic system for deoxygenation of aromatic ketones using $B_2(OH)_4$ as the sole source of H atoms (Figure 1.23 bottom). Mechanistically, the C–O bond cleavage of the indicated borate ester intermediate observed by 1H NMR and may occur via reductive elimination upon complexation with $H-Pd-B(OH)_2$.

Table 1.3. Probing the Role of the Diboron (4) Mediator in Pd-Catalyzed Ketone Deoxygenations.

entry	additive(s) (equiv)	yield 2a (%)	D in 2a (%)	yield 3a (%)
1	B ₂ (OH) ₄ (1.1)	20	n/a	54
2	B ₂ (OH) ₄ (2.2)	>95	n/a	0
3 ^a	B ₂ (OH) ₄ (2.2)	78	n/a	18
4 ^b	B ₂ (pin) ₂ (2.2)	trace	n/a	trace
5 ^b	B ₂ (pin) ₂ (2.2) + H ₂ O (5)	70	n/a	20
6 ^c	B ₂ (OD) ₄ (2.2)	>95	85	0
7	B ₂ (OH) ₄ (2.2) + D ₂ O (10)	>95	67	0
8 ^d	B ₂ (OH) ₄ (2.2)	>95	0	0

Reactions were conducted on 0.3 mmol scale in anhydrous THF (<25 ppm H₂O per Karl Fischer titration) under N₂ atmosphere in a sealed one-dram vial unless otherwise noted. Percent conversion, percent yield, and % deuterium incorporation were determined by ¹H NMR using 1,3,5-trimethoxybenzene as an internal standard. ^[a] Reaction was performed unsealed under a blanket of N₂ on 1.0 mmol scale. ^[b] Reaction was performed at 80 °C. ^[c] B₂(OD)₄ was prepared as 85% deuterium enriched. ^[d] Reaction was performed in d-8 THF.

Unreduced palladium on carbon was the best-performing catalyst that we evaluated, and THF the optimal solvent. Pd(OAc)₂ performed poorly in this reaction only giving up to 60% yield of **2a** despite increased catalyst loading and increased B₂(OH)₄ equivalents. Reactions employing Pd(OAc)₂ quickly exhibited black particles indicating aggregation into large insoluble catalytically inactive material. Other solvents led to significantly reduced conversion. Non-coordinating solvent 1,2-dichloroethane gave markedly lower yield and conversions. The coordinating nature of THF is postulated to help promote the reaction by perhaps activating the B₂(OH)₄ through a Lewis acid-base interaction. 60 °C gave the most consistent yields and was elected as the optimal temperature. See **Table 1.6** below for complete optimization details. A slight excess of B₂(OH)₄ afforded deoxygenated product **2a** and semireduced **3a** in 20% and 54% yield, respectively (entry 1, **Table 1.2**). Doubling the B₂(OH)₄ load afforded quantitative deoxygenation of **1a** to **2a** (entry 2). A reaction conducted under a blanket of nitrogen in an open system afforded 78% of **2a** and 18% of **3a**, indicating a closed flask is necessary for the success of the reaction. In stark contrast, the use of B₂(pin)₂ instead of B₂(OH)₄ leads to only trace reduction (entry 4), suggesting that the hydrogen atoms are transferred from B₂(OH)₄ and not some other source (such as THF). B₂(pin)₂ proved capable of mediating the deoxygenation if exogenous water is added, though 80 °C is required, and

pinacol byproduct complicate the purification (entry 5, Table 1.3). Importantly, 2.2 equivalents of $B_2(OD)_4$ (85% D) quantitatively deoxygenated **2a** with perfect 85% deuterium incorporation (entry 6); previous methods for deoxygenative deuteration include the use of expensive and typically pyrophoric reagents, such as $LiAlD_4$ or D_2 gas.^{31,42-44} When 10 equivalents of D_2O with $B_2(OH)_4$ were employed, quantitative deoxygenation with deuterium incorporation of 67% was observed (entry 7). This result indicates protons from $B_2(OH)_4$ and deuterons from water exchange and become available for reduction. Addition of 5.0 equivalents of D_2O resulted in quantitative deuteration but only 50% deuterium incorporation (not shown). Lastly, a reaction performed using d_8 -THF resulted in no deuterium incorporation (entry 8), indicating that THF is not a hydrogen atom donor in the reaction. The resultant spectra are presented in Figure 1.25 and Figure 1.26 below. Additionally, $B_2(cat)_2$ with addition of 5 equivalents of water was observed to mediate the reaction is high (91%) yield but due to the loss in atom economy was not pursued further.

Deoxygenation of 4-acetylbiphenyl (**1a**) in THF- d_8

This is the reaction corresponding to entry 8 in **Table 1.3**. The standard reaction was conducted in THF- d_8 with 4-acetylbiphenyl. The crude reaction was filtered through Celite and analyzed by 1H NMR and ^{13}C NMR in THF- d_8 (referenced to the residual THF solvent peaks at 1.73 ppm and 25.5 ppm, respectively). No deuterium incorporation was observed by either 1H -NMR or ^{13}C -NMR. >95% conversion to 4-ethylbiphenyl was observed with the remaining material (>5%) being converted to the alcohol (**3a**).

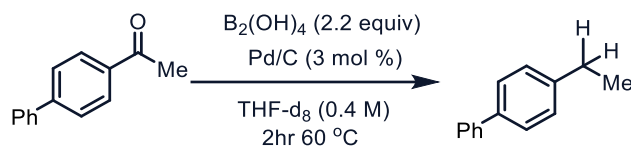


Figure 1.24. Deoxygenation of **1a** conducted in THF- d_8 yielded no detectable deuteration

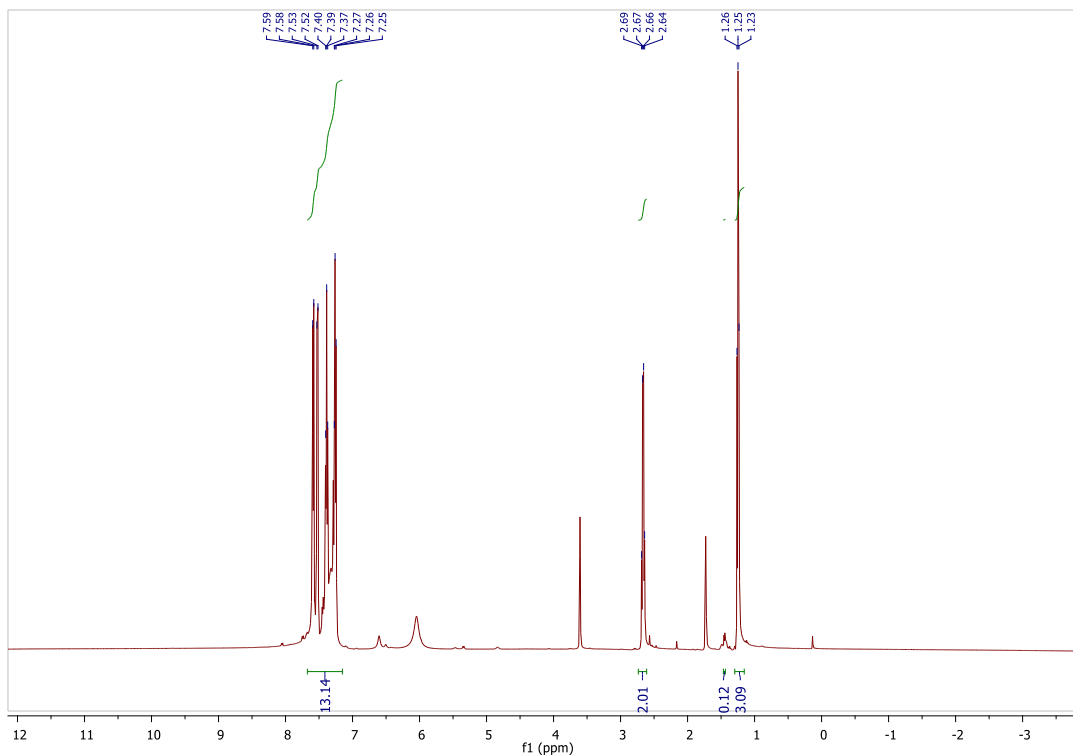


Figure 1.25. ^1H NMR (500 MHz in THF-d_8) of 4-ethylbiphenyl (**2a**)

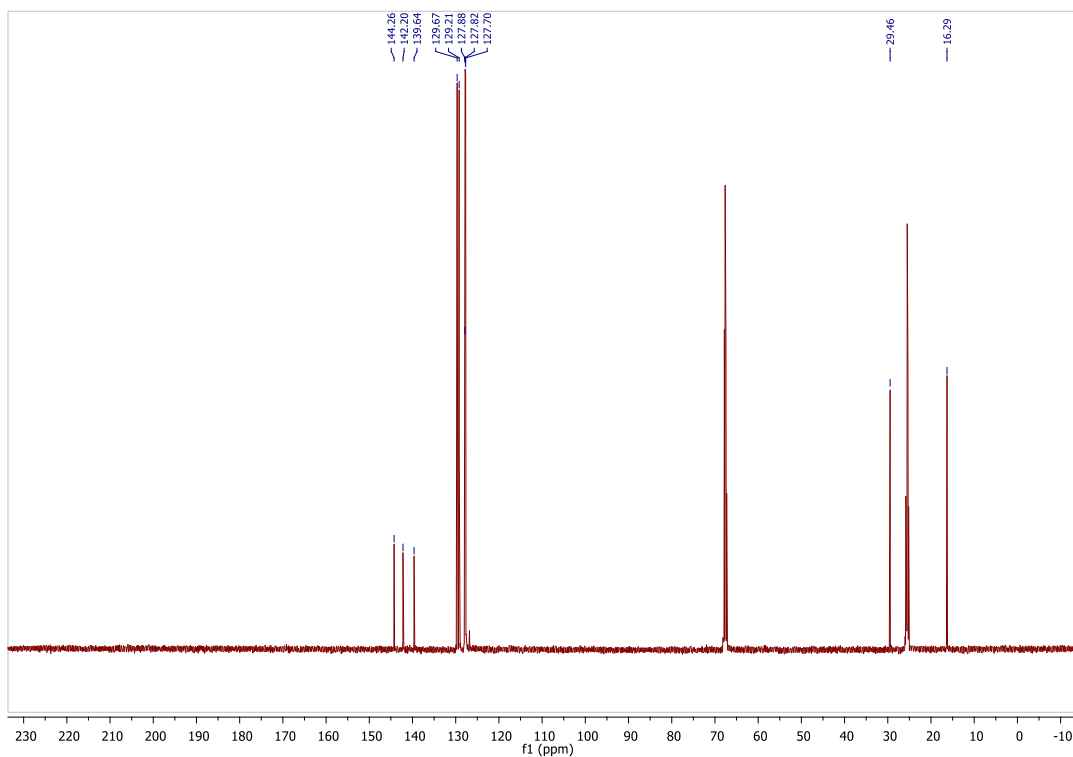
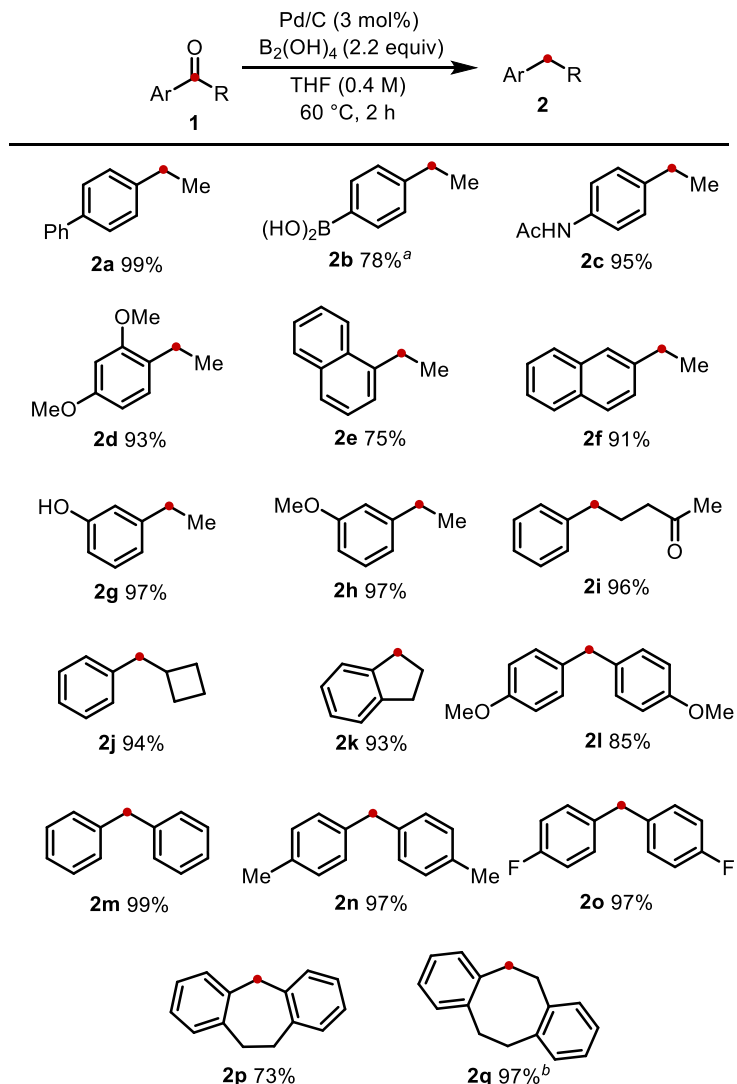


Figure 1.26. ^{13}C NMR (125 MHz, THF-d_8) of 4-ethylbiphenyl (**2a**)

Table 1.4. Evaluation of the Generality of the Reductive Deoxygenation of Aryl Ketones

Reactions were conducted on 0.5 mmol scale in anhydrous THF under air in a sealed one-dram vial unless otherwise noted. All yields are isolated unless otherwise noted. ^[a] Yield was determined using ¹H NMR with 1,3,5-trimethoxybenzene as an internal standard. ^[b] Reaction was performed on 4.70 g (21.2 mmol) scale.

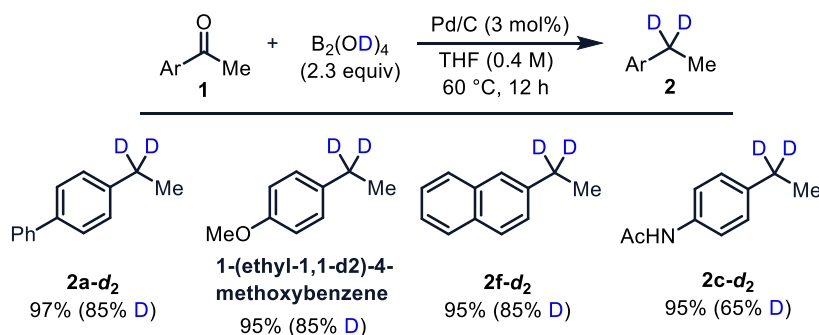
The optimized conditions of 2.2 equivalents of B₂(OH)₄ and 3 mol % of Pd/C in THF lend themselves to high yield transfer deoxygenation of a variety of aromatic ketones. *Para*-biphenyl-substituted methyl ketone **1a** was isolated in 99% yield on 0.5 mmol scale (Table 1.4). Other methyl phenyl ketones evaluated include *para*-boronic acid (**1b**) and *para*-acetamide (**1c**) derivatives, which were deoxygenated in high yield. *Ortho*-substituted methyl phenyl ketones were also tolerated, as exhibited by dimethoxyaryl substrate **1d** and 1-naphthyl substrate **1e**, the latter of which reacted more sluggishly giving yield of 75%. In contrast, 2-naphthyl ketone substrate **1f** afforded **2f** in 91% yield. Two meta-substituted methyl phenyl ketones were also cleanly deoxygenated, including free hydroxyl **1g** (97%

yield) and methyl ether **1h** (also 97% yield). Dialkyl ketones proved unreactive in this reaction as shown in the deoxygenation of diketone **1i**, wherein only the more easily reduced benzylic carbonyl is removed. Other alkyl aryl ketones that were cleanly reduced include cyclobutyl phenyl ketone **1j** (94%) and 1-indanone **1k** (93%). The retention of the cyclobutane of **1j** suggests that a benzylic radical is not formed during the reaction, as the cyclobutyl group would likely undergo a ring opening reaction if this were the case.⁴⁴ Additionally 4-CF₃ acetophenone was deoxygenated but required 80 °C and 3.0 equivalents of B₂(OH)₄ (not shown). Four symmetric diaryl ketones were also cleanly deoxygenated, name 4,4'-dimethoxybenzophenone (**1l**), benzophenone (**1m**), 4,4'-dimethylbenzophenone (**1n**), and 4,4'-difluorobenzophenone (**1o**). Conformationally inflexible dibenzosuberone **1p** proved slower to convert and resulted in attenuated yield of 73%. A multigram scale reaction was also performed in high yield using ketone **1q**, and we have been using the dibenzocyclooctadiene product **2q** as a precursor for a model monomer in functional polymer materials synthesis.^{46,47} Reducible functional groups such as aryl halides, alkenes, alkynes, nitro, and nitriles were not evaluated based on the understanding that competing reactions would dominate.^{18,37,41}

Deoxygenative deuteration of select substrates.

Deuteration of pharmaceuticals is an important tool the development of new and improved drugs. Deuterium substitution impedes oxidative metabolism thus allowing the drug to act longer. Methods to selectively deuterate molecules are extremely important in helping develop such drugs.⁴⁸ To that end we looked to exhibit the deoxygenative deuteration of some aromatic ketones. **1f** and *para*-acetylanisole were each subjected to these conditions, and both also incorporated deuterium with perfect fidelity. **1c** was screened and while near quantitative deoxygenation was observed, an eroded deuteration incorporation was observed, likely due to the exchangeable amide proton scrambling. **Table 1.5** summarizes these results. The limiting factor to achieving high deuteration incorporation is synthesis of B₂(OD)₄ of high isotopic purity. Additionally, when following Cummins procedure for the synthesis of B₂(OD)₄ dimethylamine hydrochloride (2.65 ppm) must be completely removed from the product as even the slightest of trace quantities shut down the reaction. This can be achieved by extensive washing with CDCl₃ and DCl:D₂O.

Table 1.5. Evaluation of the Deuteration of Aromatic Ketones Using B₂(OD)₄



The optimized protocol was followed but using 2.3 equivalents of $B_2(OD)_4$ as the diboron(4) source (**Table 1.5**). The deuterium incorporation was determined by integration and lack of signal at the known chemical shift in the 1H NMR. The spectral data is included below. The isotopic purity of $B_2(OD)_4$ was determined to be 85% D/15% H using 1,3,5-trimethoxybenzene as an internal standard. See Figure 1.28 for 1H NMR of material used in this work.

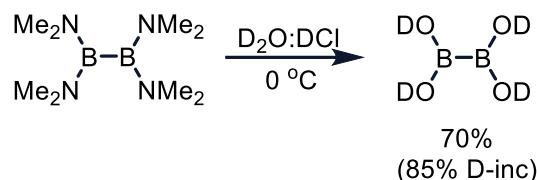


Figure 1.27 Method for the synthesis of $B_2(OD)_4$ as reported by Cummins et al.²⁰

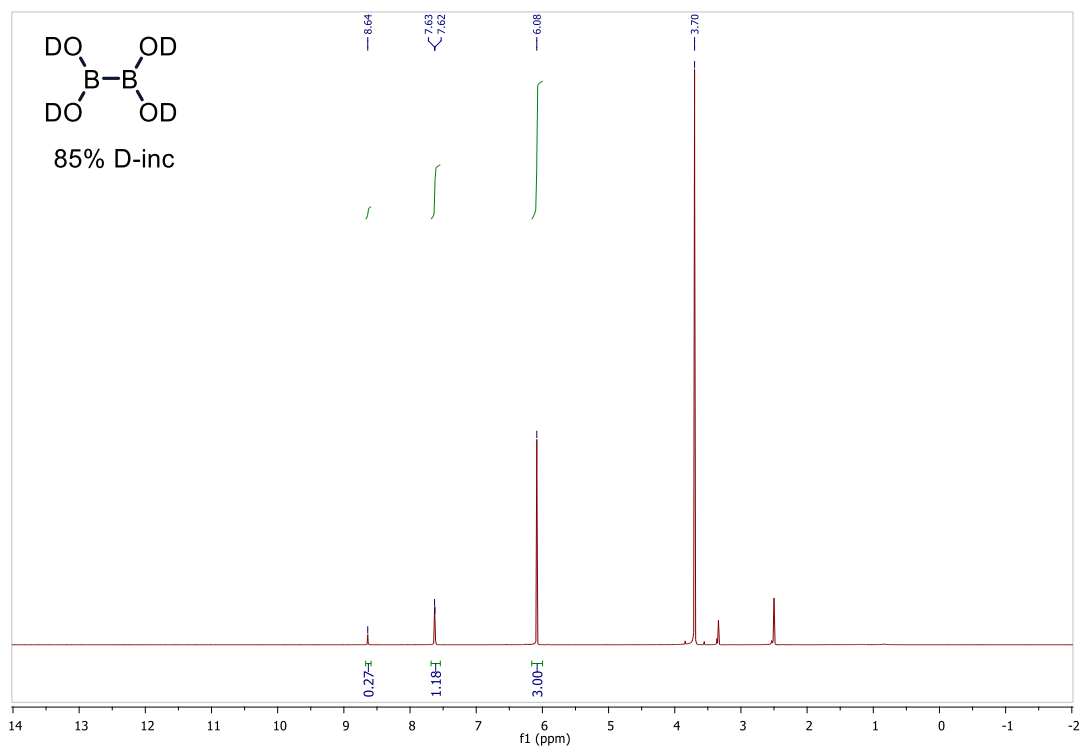


Figure 1.28. 1H NMR (500 MHz, $DMSO-d_6$) of $B_2(OD)_4$ used in this work

Deuteration of 4-acetylbiphenyl (**1a**) with D_2O and $B_2(\text{pin})_2$

60 mg of 4-acetylbiphenyl (**1a**), 163 mg of $B_2(\text{pin})_2$ and 50 μL D_2O were added to a one-dram vial and capped with a PTFE lined screw top cap. Then 0.75 mL of THF was added via syringe and the reaction was stirred at 80 $^\circ\text{C}$ for 12 h. The crude reaction mixture was passed through a silica/Celite plug followed by eluent removal using rotary evaporation. Near perfect deuteration was observed under these conditions. Palladium catalyzed hydrolysis of $B_2(\text{pin})_2$ has been described multiple times so it is possible simple

evolution of D_2 is operating in this reaction.¹⁹ Quantitative D_2 evolution under these conditions seems unlikely since the gas would escape the reaction mixture likely leading to a much lower yield than observed.

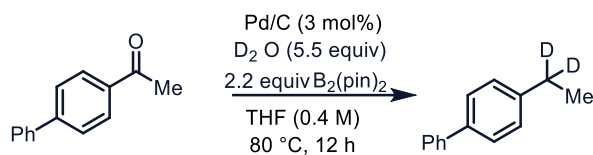


Figure 1.29. Deoxygenative deuteration **1a** with $B_2(\text{pin})_2$ and D_2O

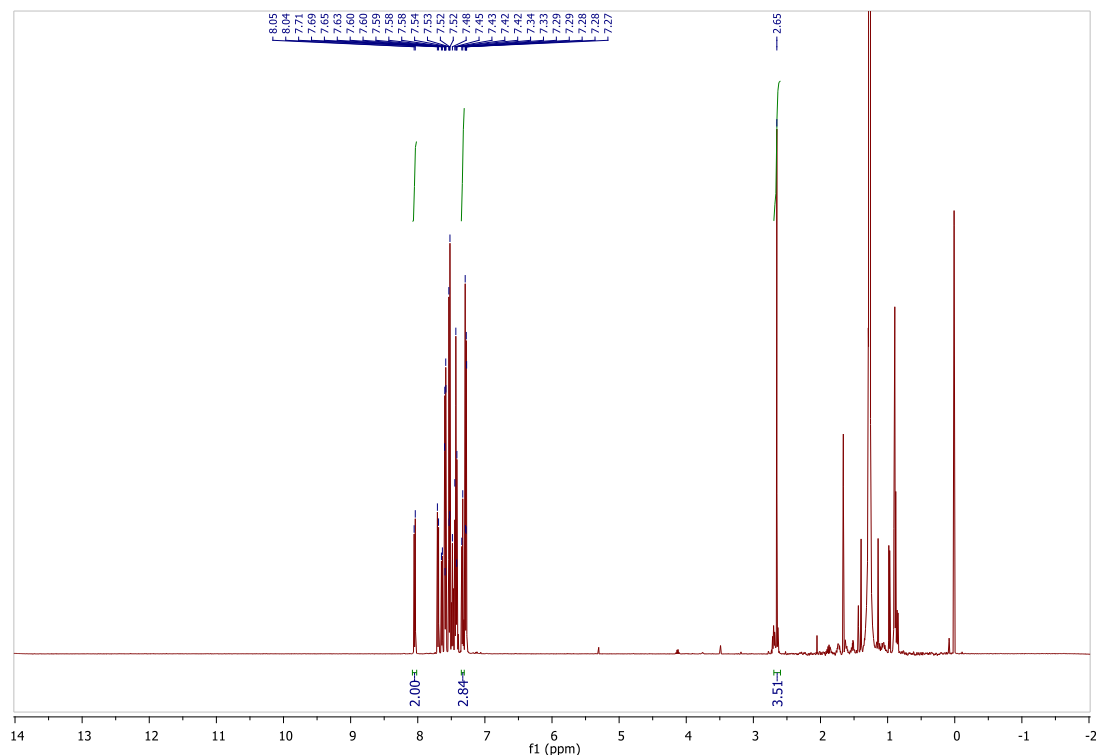


Figure 1.30. ^1H NMR (500 MHz in CDCl_3) of deoxygenative deuteration of 4-acetylbiphenyl using $B_2(\text{pin})_2$ and D_2O .

Failed substrates under optimized conditions

Figure 1.31 shows a handful of substrates that were tested but could not be deoxygenated under these conditions. The steric demanding substrate **1r** showed trace deoxygenation but isolation of **2r** was not attempted. 9-acylanthracene (**1s**) also proven unreactive to these conditions and was fully recovered from the reaction mixture. Interestingly **1t** proved unreactive, perhaps due to the B-N interaction disrupting the catalysis.

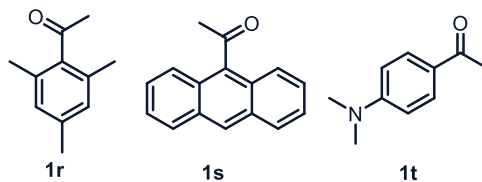


Figure 1.31. Substrates that failed to undergo diboron(4) mediated deoxygenation.

Evidence of borate ester intermediate in the deoxygenation of aromatic ketones under anhydrous conditions

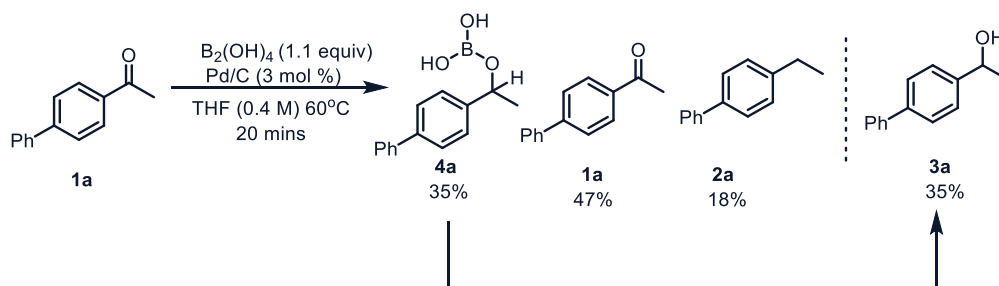


Figure 1.32. Reaction scheme devised for the detection of borate ester (**4a**)

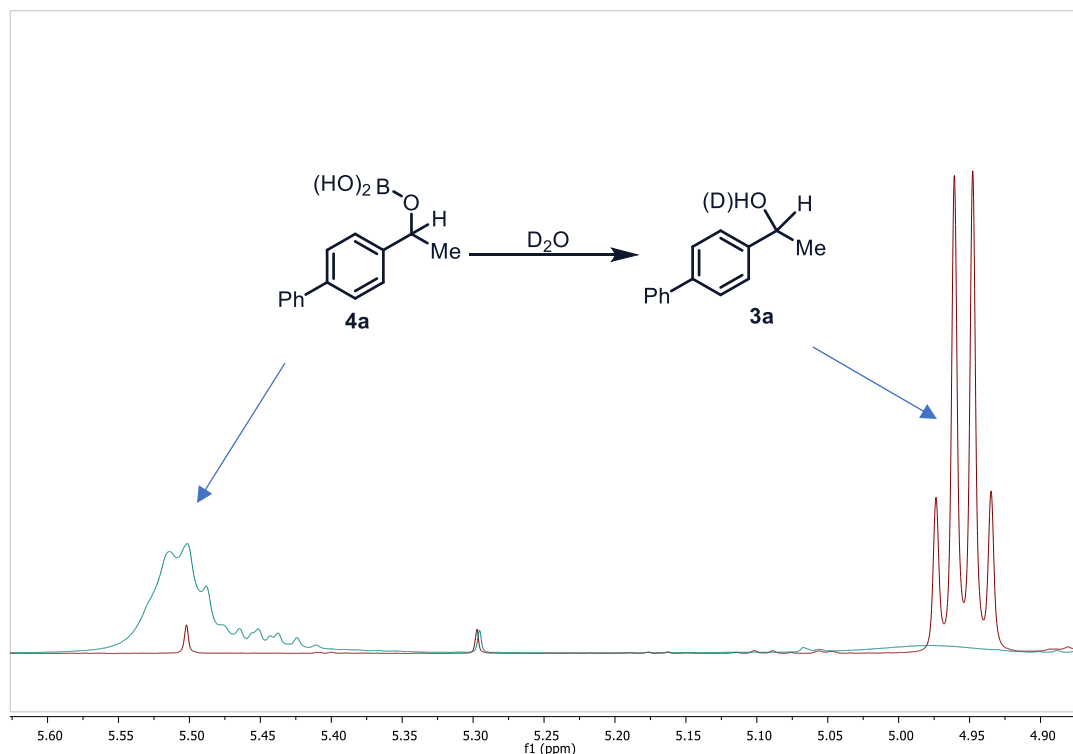


Figure 1.33. Comparing ^1H NMR (500 MHz in CDCl_3) before (blue) and after (red) addition of D_2O of reaction depicted in **Figure 1.33**. Small signal at 5.30 ppm is attributed to DCM.

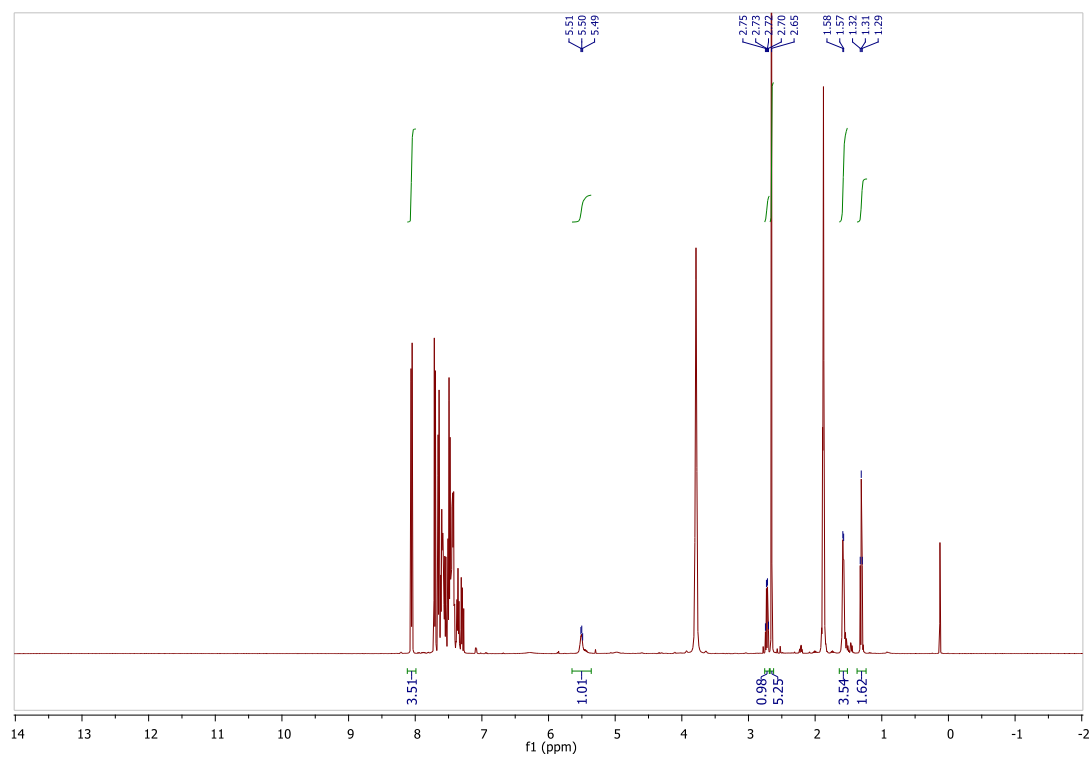


Figure 1.34. ¹H NMR (500 MHz in CDCl₃) of reaction depicted in **Figure 1.32** before addition of D₂O.

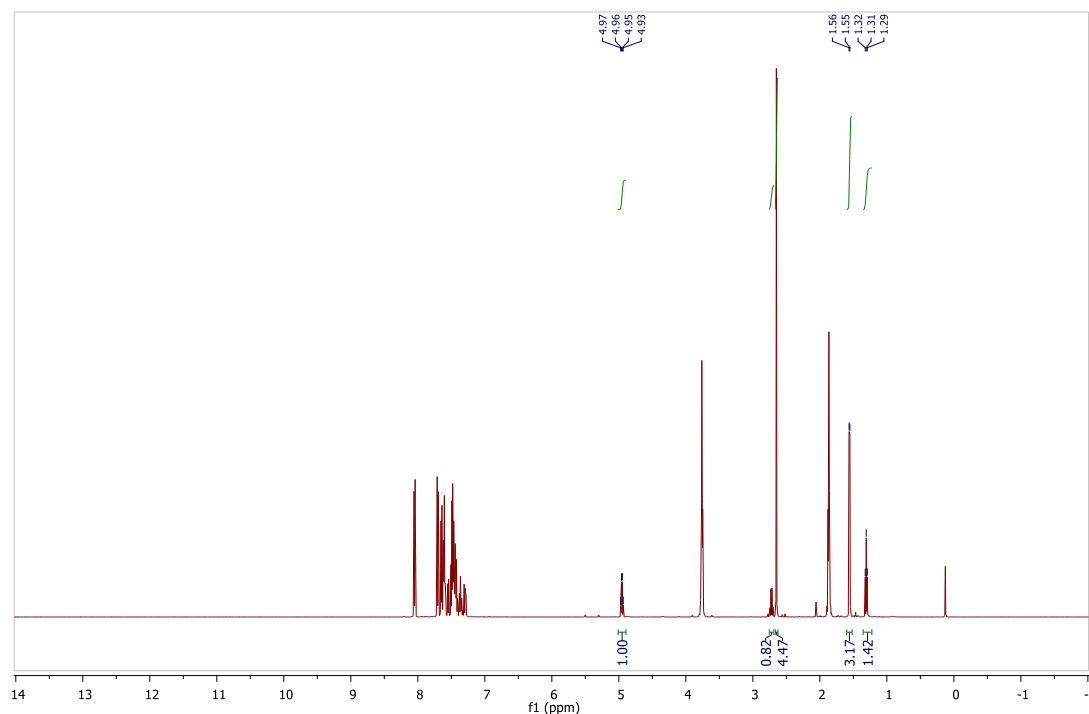


Figure 1.35 ^1H NMR (500 MHz in CDCl_3) of reaction depicted in **Figure 1.32** after addition of D_2O

The possibility of a hydroboration event leading to a borate ester was investigated using shortened reaction time and fewer equivalents of $\text{B}_2(\text{OH})_4$ to increase the chances of detecting semireduced intermediates (Figure 1.32). A standard reaction with **1a** using 1.1 equivalents of tetrahydroxydiboron and stirred at 60°C for 20 minutes. The reaction was filtered through a pad of Celite m and glass wool followed by eluent removal in vacuo and uptake of the residue in CDCl_3 for ^1H NMR analysis (500 MHz). After workup, ^1H NMR in CDCl_3 revealed a poorly resolved multiplet at 5.50 ppm that and the putative alcohol (**3a**) was not present. The ratio of the products was found to be 18% of 4-ethylbiphenyl (**2a**), 35% of the borate ester, and 47% of 4-acetylbiphenyl (**1a**). Upon addition of D_2O , a quartet resonance assigned to the benzylic proton of **3a** at 4.94 ppm appeared, indicating hydrolysis, shown in Figures 1.33-35. Integrations showed the starting material (**1a**) and alkane (**2a**) were unchanged. The benzylic protons of borate esters like **4a** are reported to have characteristic chemical shifts around 5.50 ppm in CDCl_3 .^{49,50} Isolation of the borate ester was unsuccessful, so further characterization was not possible. A similar experiment with benzophenone (**1m**) was also conducted revealing a similar suspected borate ester.

Hydrogen evolution has been reported for other transition metal-catalyzed reactions involving $\text{B}_2(\text{OH})_4$ although not under anhydrous or additive-free conditions.^{22,23,37,38} To probe H_2 evolution in our system, $\text{B}_2(\text{OH})_4$ and Pd/C were stirred in anhydrous THF at 60°C and the headspace was bubbled into CDCl_3 through a canula within an NMR tube, which then showed H_2 gas at 4.62 ppm in ^1H NMR.⁵¹ See Figure 1.37 for the spectroscopic evidence showing H_2 gas observed in ^1H NMR.

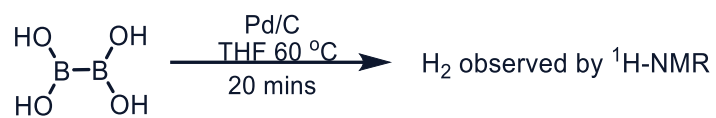


Figure 1.36. Hydrogen gas observed by ^1H NMR in anhydrous THF by mixing $\text{B}_2(\text{OH})_4$ and Pd/C

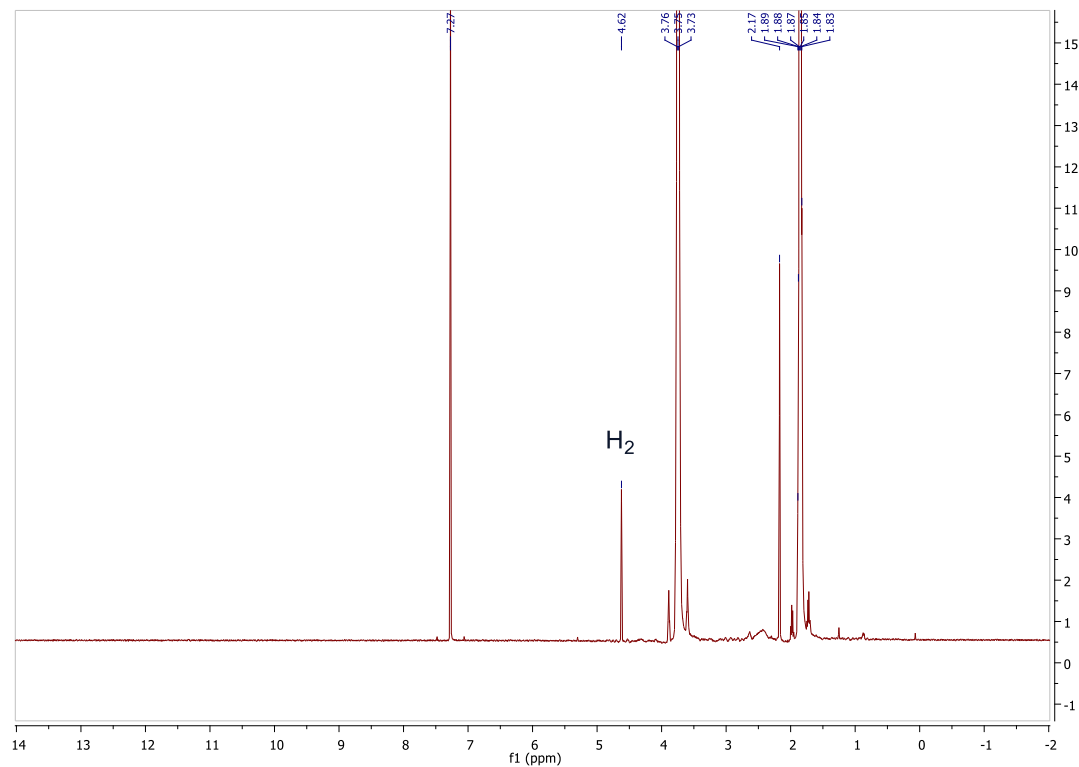


Figure 1.37. ^1H NMR (500 MHz, CDCl_3) spectrum showing H_2 gas evolved from Pd/C and $\text{B}_2(\text{OH})_4$ in anhydrous THF

Post catalytic H/D exchange experiment on 4-ethylbiphenyl (**2a**)

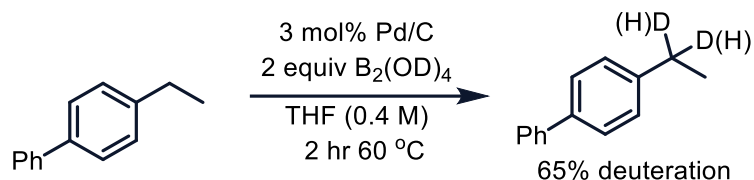


Figure 1.38. Experiment showing post catalytic H/D exchange in the benzylic position of 4-ethylbiphenyl with B₂(OD)₂

To examine the possibility of post-catalytic H/D exchange the following experiment was conducted. 54 mg of **2a**, 9 mg of 10% w/w Pd/C, 64 mg of B₂(OD)₄, 0.75 mL of THF, and a magnetic stir bar were charged to a one dram vial and capped with a PTFE lined screw top septum and stirred at 60 °C for 2 h. Filtration through Celite and removal of solvent revealed 56 mg of recovered **2a** which was analyzed by NMR in CDCl₃ (Figure 1.39) which shows 65% deuterium incorporation at the benzylic position. This result suggests that post catalytic H/D exchange is occurring in these reactions. Benzylic H/D exchange after Pd-catalyzed oxidative cleavage is established in the literature.⁵² Interestingly no appreciable deuterium appeared to be incorporated in the terminal methyl showing a greater selectivity over the published method that unselectively exchanges the isotopes through an alkyl chain, many carbons away.

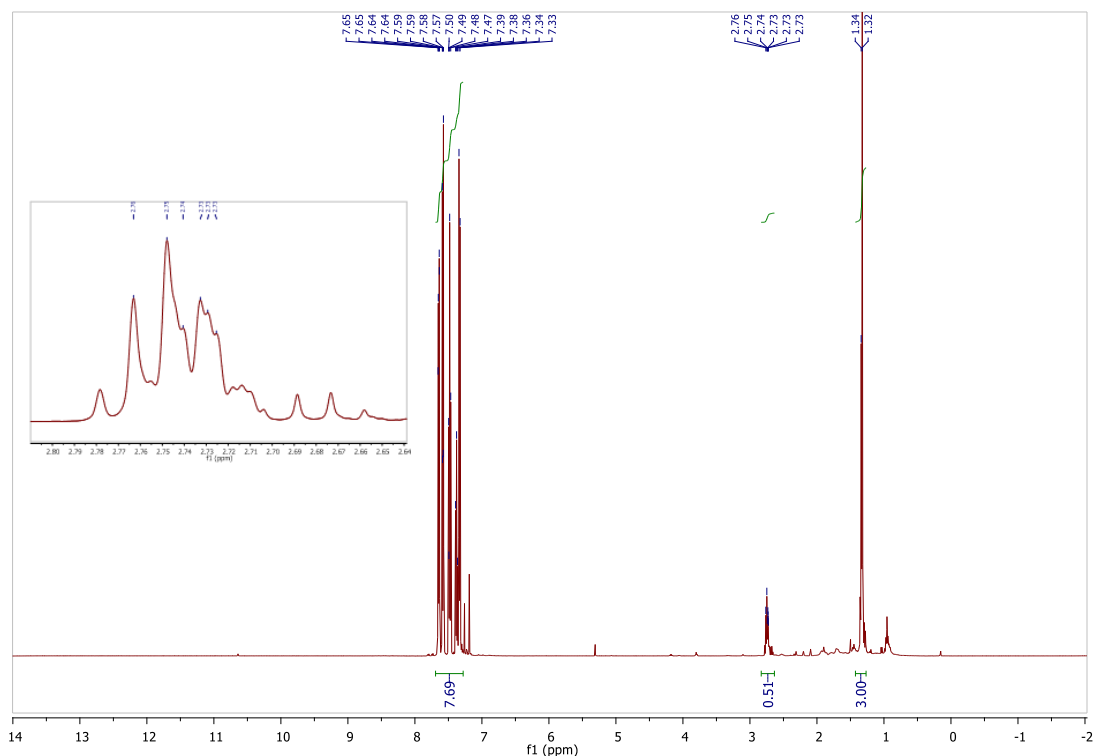


Figure 1.39. ^1H NMR (500 MHz in CDCl_3) spectrum of partially deuterated **2a** by post-catalytic exchange. Inset – zoomed into the methylene signal showing splitting due to incorporated deuterium atoms.

Putative catalytic cycle for the deoxygenation of aromatic ketones with tetrahydroxydiboron

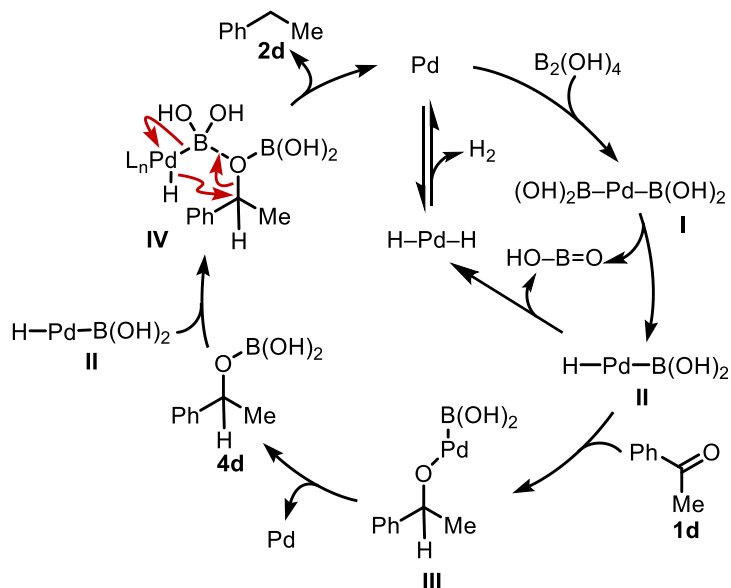


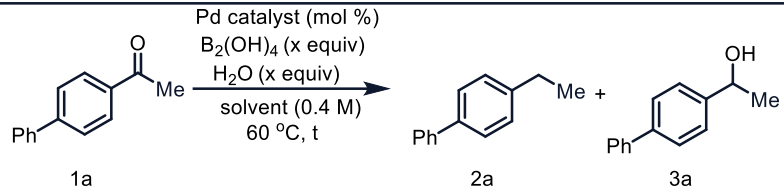
Figure 1.40. Putative catalytic cycle for the palladium catalyzed tetrahydroxydiboron mediated deoxygenation of aromatic ketones.

A putative mechanism is shown in Figure 1.40 using acetophenone (**1d**) as a model substrate. Oxidative addition across the B–B bond gives a diboryl complex **I** from which β -hydride elimination could yield H–Pd–B(OH)₂ species **II** and metaborate (HO–B=O), which has been suggested previously.^{25,42} Migratory insertion of the carbonyl into the Pd–H bond of **II** could afford alkoxy palladium intermediate **III**, from which reductive elimination could afford borate ester **4d**. Subsequent coordination of **4d** to **II** followed by a fragmenting reductive elimination via a five-membered transition state could afford **2d**. An analogous reductive elimination involving H–Pd–H instead of H–Pd–B(OH)₂ cannot be ruled out. Boric anhydride ((HO)₂–B–(OH)₂) was postulated as the side product of the product forming step but not characterized spectroscopically. Similarly, an alternative pathway from **1d** to **4d** could involve reaction of **1d** with PdH₂, as has previously been reported for Pd-catalyzed reduction of aldehydes and ketones to alcohols using HB(pin)⁴³ but this would be expected to afford an alcohol intermediate, which we did not observe *in situ*.

Chapter 1 conclusions

This work expanded the use of B₂(OH)₄ as a reducing agent to two novel processes. Both reactions relied upon the strongly oxophilic nature of boron and the formation of B–O bonds in their reaction pathways. In the synthesis of Pd(P^tBu₃)₂ this was formation of AcO–B(OH)₂ and in deoxygenation the formation of a borate ester and boric anhydride were integral in reaction success. We showed B₂(OH)₄ can act as the sole reducing agent as well as a hydrogen atom donor. While the formation of the palladium reducing species is unclear, the perfect fidelity of deuterium transfer unequivocally proves the origin of the hydrogen atoms is B₂(OH)₄. The mechanism of hydride transfer (Figure 1.40 I → II) is unknown and worthy of further investigation. This method is amenable to the development of selective benzylic perdeuteration of small molecules, an important tool in emerging pharmaceuticals. Additionally, the reagents B₂(OD)₄ holds much potential for selective H/D exchange reactions, with the selective installation of deuterium remaining a challenge. This work highlights that the hydroxyl moiety of B₂(OH)₄ is still far from understood. A detailed mechanistic study of the deoxygenation reaction would likely open the door to developing alternative chemistry. This work also further cements that diboron (4) reagents are much more than just borylating agents. There is a rich future in the field of B₂(OH)₄ and palladium chemical systems and those who chose to study it. I hope this work can lead to further discovery and innovation in the field.

During this work an interesting trace side product benzo-oxete was discovered. The isolation and characterization of this compound is discussed in chapter 3 of this thesis. The discovery of such a unique structure under such unassuming conditions serves as potent examples that the chemistry of diboron (4) reagents under palladium catalysis is far from developed, and new interesting chemistry are still to be discovered.

Table 1.6. Full Optimization of the Deoxygenation Reaction.


entry	solvent	B ₂ (OH) ₄ (x equiv)	time (h)	H ₂ O (x eq)	Pd catalyst (mol %)	conversion 1a	yield 2a (%)	yield 3a (%)
1	PhMe	3.0	12	0	Pd/C (3)	95	41	45
2	DCE	2.1	3	0	Pd/C (3)	80	19	58
3	DCE	2.1	3	5	Pd/C (3)	99	59	40
4	DCE	2.1	20	0	Pd/C (3)	64	22	20
5	DCE	2.1	20	5	Pd/C (3)	94	48	39
6	MeCN	2.1	3	0	Pd/C (3)	80	45	20
7	MeCN	2.5	3	5	Pd/C (3)	90	15	64
8	THF	2.1	12	5	Pd/C (3)	100	97	trace
9 ^a	THF	2.1	12	0	Pd/C (3)	97	86	11
10 ^b	THF	2.1	3	5	Pd/C (3)	98	83	15
11 ^a	THF	2.1	1	5	Pd/C (3)	99	77	21
12 ^a	THF	2.1	12	10	Pd/C (3)	95	80	7
13	THF	2.1	12	5	Pd/C (3)	97	8	85
14	THF	2.1	12	5	Pd/C (3)	99	8	92
15	THF	1.1	5	5	Pd/C (3)	80	20	54
16	THF	2.1	12	5	Pd/C (3)	100	90	10
17	THF	2.2	12	5	Pd/C (3)	100	71	18
18	THF	2.3	12	5	Pd/C (3)	100	75	15
19 ^b	THF	2.2	12	0	Pd/C (3)	100	100	0
20	THF	2.2	12	5	Pd/C (3)	99	94	5
21	THF	2.2	12	2.1	Pd/C (3)	100	93	4
22 ^c	THF	3.0	6	0	Pd/C (5)	100	99	0
23	THF	3.0	6	0	Pd/C (1)	100	80	20
24	THF	3.0	6	0	Pd/C (3)	100	100	0
25	THF	2.5	6	0	Pd/C (1)	100	98	trace
26	THF	2.1	6	0	Pd/C (3)	97	92	5
27	THF	3	6	0	Pd(OAc) ₂ (5)	100	55	42
28	THF	5	6	0	Pd(OAc) ₂ (10)	100	60	40

a. All reactions were conducted on an on 0.3 mmol scale under N₂ in a closed flask unless otherwise noted. Yields were determined using 1,3,5-trimethoxy benzene as internal standard unless otherwise noted. *a* Reaction run at 50 °C. *b* Reaction run in closed vial under air *c.* Isolated yield.

General Procedure for the Evaluation of the Scope of the Deoxygenation Reaction

Reactions were carried out on 0.5 mmol scale unless otherwise noted. 16 mg of 10 weight % of unreduced Pd/C (3 mol%), 0.5 mmol of the ketone substrate, and 98 mg of tetrahydroxydiboron (2.2 equivalents), and a PTFE coated magnetic stir bar were charged to a one-dram vial and 1.25 mL (0.4 M) of dry and degassed THF was added. The vial was firmly capped with a PTFE-lined screw-top septum cap and the suspension stirred at 60 °C for 2 hours unless otherwise noted. The reaction was allowed to cool to room temperature and analyzed by TLC for completion. The crude mixture was passed through a mixed silica/Celite plug rinsing the reaction vial with 5% MeOH/95% DCM; the eluent was removed by rotary evaporation. Compounds **1d**, **1l**, and **1p** were not fully converted

after 2 hours, so column chromatography was employed to isolate the deoxygenated product.

Experimental section for synthesis of Pd(P^tBu₃)₂

A 3.7 ml dram vial in argon filled glove box was charge with 67mg (0.3mmol) of Pd(OAc)₂, 135 mg of B₂(OH)₄, and 1.82 g (3.0 eq) of P(*t*Bu)₃ 10 weight% in hexanes (2.67 ml). The vial was sealed with a teflons septa and stirred for 12 hours at 70 °C, during with time the reaction became lighter in color and a precipitate produced. After allowing the mixture to cool, the vial was opened and the supernatant passed through a 0.2 micron - syringe filter and the solvent was removed under reduced pressure, yielding a white crystalline solid. After the all the solvent was removed the remaining solid was washed 2x with dry degassed methanol. For further purification 1 ml of hexanes was added and the vial was resealed. The solution was heated at 70 °C until all the solids were solubilized and it was placed in a glovebox freezer (-35 °C) overnight, yielding 138 mg (91%) of Pd(P(*t*Bu)₃)₂ as colorless crystals. The recrystallization step can be substituted for washing the crude material with rigorously degassed methanol. This step will remove any yellow color from the white powder and furnish spectroscopically pure Pd(P^tBu₃)₂ shown in Figure 1.41. ³¹P NMR – 89.64 ppm. The controls experiments were conducted in the same manner and scale with Pd(Cl)₂ and NaOAc.

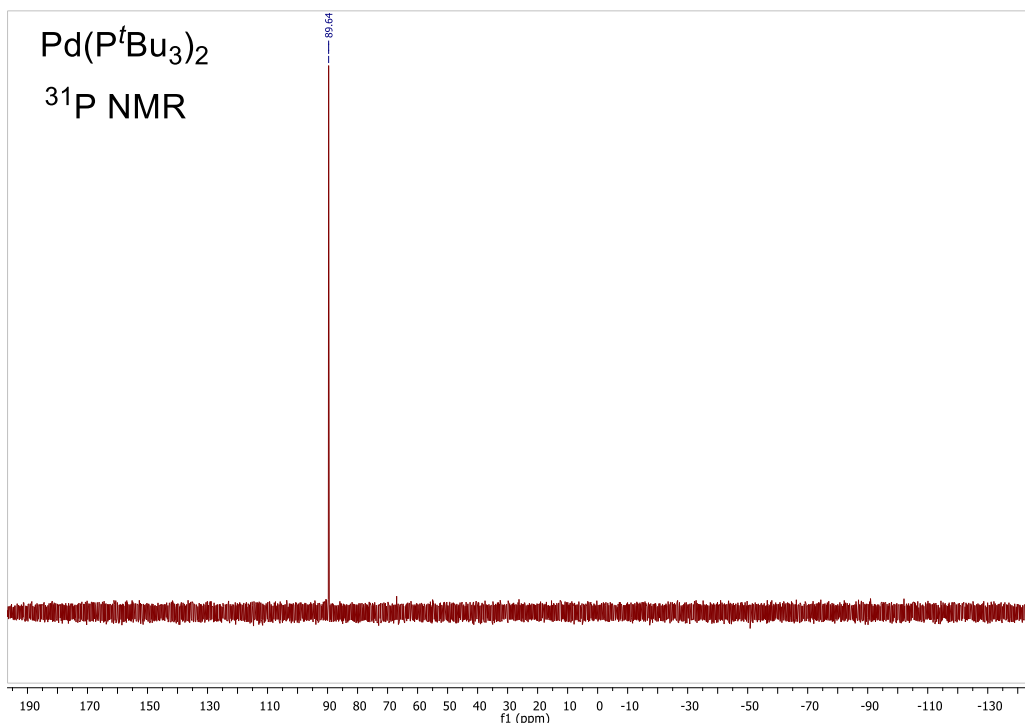


Figure 1.41. ³¹P NMR spectrum (202 MHz, unreferenced) of recrystallized Pd(P^tBu₃)₂ in toluene

References for Chapter 1

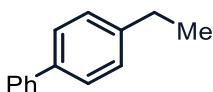
1. Neeve, E. C.; Geier, S. J.; Mkhaliid, I. A. I.; Westcott, S. A.; Marder, T. B. Diboron(4) Compounds: From Structural Curiosity to Synthetic Workhorse. *Chem. Rev.* **2016**, *116*, 9091-9161
2. Kokatla, H. P.; Thomson, P. F.; Bae, S.; Doddi, V. R.; Lakshman, M. K. Reduction of Amine N-Oxides by Diboron Reagents. *J. Org. Chem.* **2011**, *76*, 7842-784.
3. Perras, F. A.; Bryce, D. L. Boron-Boron/Coupling Constants Are Unique Probes of Electronic Structure: A Solid-State NMR and Molecular Orbital Study. *Chem. Sci.* **2014**, *5* (6), 2428-2437.
4. Liu, X.; Zhang, X.; Zhang, G.; Sun, S.; Li, D.-S. A Deeper Understanding of H₂ Evolution Entirely from Water via Diborane Hydrolysis. *ACS Materials Letters* **2023**, *5* (3), 783-797.
5. Biffis, A.; Centomo, P.; del Zotto, A.; Zecca, M. Pd Metal Catalysts for Cross Couplings and Related Reactions in the 21st Century: A Critical Review. *Chem. Rev.* **2018**, *118*, 2249-2295
6. Shaughnessy, K. H. Development of Palladium Precatalysts that Efficiently Generate LPd (0) Active Species. *Isr. J. Chem.* **2020**, *60*, 180-194
7. Amatore, C.; Jutand, A.; Thuilliez, A. Formation of Palladium(0) Complexes from Pd(OAc)₂ and a Bidentate Phosphine Ligand (Dppp) and Their Reactivity in Oxidative Addition. *Organometallics* **2001**, *20* (15), 3241-3249
8. Shaughnessy, K. H. Palladium, Bis[Tris(1,1-Dimethylethyl)Phosphine]. *Encyclopedia of Reagents for Organic Synthesis* **2008**.
9. He, L.-Y. Bis(Tri-Tert-Butylphosphine)Palladium(0) [Pd(t-Bu₃P)₂]. *Synlett.* **2015**, *26* (06), 851-852
10. Bis(tertiary phosphine)palladium(0) and -platinum(0) complexes: preparations and crystal and molecular structures Otsuka, S.; Yoshida, T.; Matsumoto, M.; Nakatsu, K. *J. Am. Chem. Soc.* **1976**, *98*, 585
11. Fraser, A. W.; Jaksic, B. E.; Batcup, R.; Sarsons, C. D.; Woolman, M.; Baird, M. C. Pd(η^3 -1-PhC₃H₄)(η^5 -C₅H₅), an Unusually Effective Catalyst Precursor for Heck-Mizoroki and Sonogashira Cross-Coupling Reactions Catalyzed by Bis-Phosphine Palladium(0) Compounds *Organometallics* **2013**, *32*, 9-11
12. Li, H.; Grasa, G. A.; Colacot, T. J. A Highly Efficient, Practical, and General Route for the Synthesis of (R₃P)₂Pd(0): Structural Evidence on the Reduction Mechanism of Pd(II) to Pd(0). *Organic Letters* **2010**, *12* (15), 3332-3335
13. Wei, C. S.; Davies, G. H. M.; Soltani, O.; Albrecht, J.; Gao, Q.; Pathirana, C.; Hsiao, Y.; Tummala, S.; Eastgate, M. D. The Impact of Palladium(II) Reduction Pathways on the Structure and Activity of Palladium(0) Catalysts. *Angewandte Chemie.* **2013**, *125* (22), 5934-5938.
14. Sumimoto, M.; Iwane, N.; Takahama, T.; Sakaki, S. Theoretical Study of Trans-Metalation Process in Palladium-Catalyzed Borylation of Iodobenzene with Diboron. *J. Am. Chem. Soc.* **2004**, *126* (33), 10457-1047
15. Henderson, W. H.; Alvarez, J. M.; Eichman, C. C.; Stambuli, J. P. Characterization, Reactivity, and Potential Catalytic Intermediacy of a Cyclometalated Tri-Tert-

- Butylphosphine Palladium Acetate Complex. *Organometallics* **2011**, 30 (18), 5038–5044.
16. Carole, W. A.; Bradley, J.; Sarwar, M.; Colacot, T. J. Can Palladium Acetate Lose Its “Saltiness”? Catalytic Activities of the Impurities in Palladium Acetate. *Org. Lett.* **2015**, 17, 5472–5475
 17. Wu, H.; Garcia, J. M.; Haeffner, F.; Radomkit, S.; Zhugralin, A. R.; Hoveyda, A. H. Mechanism of NHC-Catalyzed Conjugate Additions of Diboron and Borosilane Reagents of α,β -Unsaturated Carbonyl Compounds. *J. Am. Chem. Soc.* **2015**, 137, 10585–10602
 18. Cummings, S. P.; Le, T.-N.; Fernandez, G. E.; Quiambao, L. G.; Stokes, B. J. Tetrahydroxydiboron-Mediated Palladium-Catalyzed Transfer Hydrogenation and Deuteration of Alkenes and Alkynes Using Water as the Stoichiometric H or D Atom Donor. *J. Am. Chem. Soc.* **2016**, 138, 6107–6110.
 19. Ojha, D. P.; Gadde, K.; Prabhu, K. R. Generation of Hydrogen from Water: A Pd-Catalyzed Reduction of Water Using Diboron Reagent at Ambient Conditions. *Org. Lett.* **2016**, 18, 5062–5065
 20. Xuan, Q.; Song, Q. Diboron-Assisted Palladium-Catalyzed Transfer Hydrogenation of N-Heteroaromatics with Water as Hydrogen Donor and Solvent. *Org. Lett.* **2016**, 18, 4250–4253.
 21. Li, J. J. *Named Reactions: a Collection of Detailed Reaction Mechanisms*. **2009** Springer: Dordrecht
 22. Furrow, M. E.; Myers, A. G. Practical Procedures for the Preparation of N-tert Butyldimethyl silylhydrazones and Their Use in Modified Wolff–Kishner Reductions and in the Synthesis of Vinyl Halides and gem-Dihalides. *J. Am. Chem. Soc.* **2004**, 126, 5436
 23. Bejblová, M.; Zámotný, P.; Červený, L.; Čejka, J. Hydrodeoxygenation of Benzophenone on Pd Catalysts. *Appl. Catal. A* **2005**, 296, 169–175.
 24. Gong, S. W.; He, H. F.; Zhao, C. Q.; Liu, L. J.; Cui, Q. X. Convenient Deoxygenation of Aromatic Ketones by Silica-Supported Chitosan Schiff Base Palladium Catalyst. *Synth. Commun.* **2012**, 42, 574–581.
 25. Vannice, M. A.; Poondi, D. The Effect of Metal-Support Interactions on the Hydrogenation of Benzaldehyde and Benzyl Alcohol. *J. Catal.* **1997**, 169, 166–175.
 26. Murru, S.; Nicholas, K. M.; Srivastava, R. S. Ruthenium (II) Sulfoxides-Catalyzed Hydrogenolysis of Glycols and Epoxides. *J. Mol. Catal. A: Chem.* **2012**, 363–364, 460–464.
 27. Wang, W.; Yang, Y.; Luo, H.; Hu, T.; Liu, W. Amorphous Co–Mo–B Catalyst with High Activity for the Hydrodeoxygenation of Bio-Oil. *Catal. Commun.* **2011**, 12, 436–440.
 28. Ma, J.; Liu, S.; Kong, X.; Fan, X.; Yan, X.; Chen, L. A Continuous Process for the Reductive Deoxygenation of Aromatic Ketones over $\text{Cu}_{30}\text{Cr}_{10}/\gamma\text{-Al}_2\text{O}_3$. *Res. Chem. Intermed.* **2012**, 38, 1341–1349.

29. Zaccheria, F.; Ravasio, N.; Ercoli, M.; Allegrini, P. Heterogeneous Cu-Catalysts for the Reductive Deoxygenation of Aromatic Ketones Without Additives. *Tetrahedron Lett.* **2005**, *46*, 7743-7745.
30. Kogan, V.; Aizenshtat, Z.; Neumann, R. Polyoxometalates as Reduction Catalysts: Deoxygenation and Hydrogenation of Carbonyl Compounds. *Angew. Chem. Int. Ed.* **1999**, *38*, 3331-3334.
31. Ou, W.; Xiang, X.; Zou, R.; Xu, Q.; Loh, K. P.; Su, C. Room-Temperature Palladium-Catalyzed Deuterogenolysis of Carbon Oxygen Bonds Towards Deuterated Pharmaceuticals. *Angew. Chem. Int. Ed.* **2021**, *60*, 6357-6361.
32. Schwob, T.; Kunas, P.; de Jonge, N.; Papp, C.; Steinrück, H. P.; Kempe, R. General and Selective Deoxygenation by Hydrogen Using a Reusable Earth-Abundant Metal Catalyst. *Sci. Adv.* **2019**, *5*, eaav3680.
33. Volkov, A.; Gustafson, K. P. J.; Tai, C.-W.; Verho, O.; Bäckvall, J.-E.; Adolfsson, H. Mild Deoxygenation of Aromatic Ketones and Aldehydes over Pd/C Using Polymethylhydrosiloxane as the Reducing Agent. *Angew. Chem. Int. Ed.* **2015**, *54*, 5122-5126.
34. Rahaim, R. J.; Maleczka, R. E. C-O Hydrogenolysis Catalyzed by Pd-PMHS Nanoparticles in the Company of Chloroarenes. .
35. Dal Zotto, C.; Virieux, D.; Campagne, J.-M. FeCl₃-Catalyzed Reduction of Ketones and Aldehydes to Alkane Compounds. *Synlett* **2009**, 276-278.
36. Argouarch, G. Mild and Efficient Rhodium-Catalyzed Deoxygenation of Ketones to Alkanes. *New J. Chem.* **2019**, *43*, 11041-11044.
37. Gribble, G. W. Sodium borohydride in carboxylic acid media: a phenomenal reduction system. *Chem Soc. Rev.* **1998**, *27*, 395-404
38. Korvinson, K. A.; Akula, H. K.; Malinchak, C. T.; Sebastian, D.; Wei, W.; Khandaker, T. A.; Andrzejewska, M. R.; Zajc, B.; Lakshman, M. K. Catalytic Reductions Without External Hydrogen Gas: Broad Scope Hydrogenations with Tetrahydroxydiboron and a Tertiary Amine. *Adv. Synth. Catal.* **2020**, *362*, 166-176.
39. Little, S.; Trice, J.; Kennedy, S. M. Tetrahydroxydiboron. In *Encyclopedia of Reagents for Organic Synthesis*. **2019** John Wiley & Sons, Ltd. DOI: 10.1002/047084289X.rn01382.pub2
40. Flinker, M.; Yin, H.; Juhl, R. W.; Eikeland, E. Z.; Overgaard, J.; Nielsen, D. U.; Skrydstrup, T. Efficient Water Reduction with sp³-sp³ Diboron(4) Compounds: Application to Hydrogenations, H-D Exchange Reactions, and Carbonyl Reductions. *Angew. Chem. Int. Ed.* **2017**, *56*, 15910-15915.
41. Zhou, Y.; Zhou, H.; Liu, S.; Pi, D.; Shen, G. Water as a Hydrogen Source in Palladium-Catalyzed Reduction and Reductive Amination of Nitroarenes Mediated by Diboronic Acid. *Tetrahedron* **2017**, *73*, 3898-3904
42. Ofosu-Asante, K.; Stock, L. M. A Convenient and Selective Method for Reductive Deuteration of Aryl Carbonyl Compounds. *J. Org. Chem.* **1987**, *52*, 2938-2939.
43. Austin, R. P.; Ridd, J. H. The Mechanism of Cyclisation of 1-Ethyl-2-Nitrobenzene to Give 3-Methylantranil in Trifluoromethanesulfonic Acid.

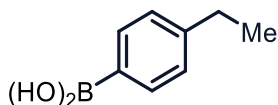
- Evidence for an Intramolecular Hydrogen Transfer. *J. Chem. Soc., Perkin Trans. 2*. **1993**, 1229-1232.
44. White, R. E.; Miller, J. P.; Favreau, L. V.; Bhattacharyya, A. Stereochemical dynamics of aliphatic hydroxylation by cytochrome P-450. *J. Am. Chem. Soc.* **1986**, *108*, 6024-6031.
 45. Ingold, K. U.; Maillard, B.; Walton, J. C. The ring-opening reactions of cyclobutylmethyl and cyclobutenylmethyl radicals. *J. Chem. Soc., Perkin Trans. 2* **1981**, 970-974.
 46. Fu, W.; Alam, T. M.; Li, J.; Bustamante, J.; Lien, T.; Adams, R. W.; Teat, S. J.; Stokes, B. J.; Yang, W.; Liu, Y.; Lu, J. Q. Arene Substitution Design for Controlled Conformational Changes of Dibenzocycloocta-1,5-dienes. *J. Am. Chem. Soc.* **2020**, *142*, 16651-16660.
 47. Wang, Z.; Huang, Y.; Guo, J.; Li, Z.; Xu, J.; Lu, J. Q.; Wang, C. Design and Synthesis of Thermal Contracting Polymer with Unique Eight-Membered Carbocycle Unit. *Macromolecules* **2018**, *51*, 1377-1385.
 48. DeWitt, S. H.; Maryanoff, B. E. Deuterated Drug Molecules: Focus on FDA-Approved Deutetrabenazine. *Biochemistry* **2018**, *57* (5), 472-473
 49. Jagt, R. B. C.; Toullec, P. Y.; de Vries, J. G.; Feringa, B. L.; Minnaard, A. Rhodium/phosphoramidite-catalyzed asymmetric arylation of aldehydes with arylboronic acids. *J. Org. Biomol. Chem.* **2006**, *4*, 773-775.
 50. Wang, W.; Luo, M.; Yao, W.; Ma, M.; Pullarkat, S. A.; Xu, L.; Leung, P.-H. Catalyst-free and solvent-free hydroboration of ketones. *New J. Chem.* **2019**, *43*, 10744-10749.
 51. Fulmer, G. R.; Miller, A. J. M.; Sherden, N. H.; Gottlieb, H. E.; Nudelman, A.; Stoltz, B. M.; Bercaw, J. E.; Goldberg, K. I. NMR Chemical Shifts of Trace Impurities: Common Laboratory Solvents, Organics, and Gases in Deuterated Solvents Relevant to the Organometallic Chemist. *Organometallics* **2010**, *29*, 2176-2179.
 52. H. Sajiki, F. Aoki, H. Esaki, T. Maegawa, K. Hirota, Efficient C-H/C-D Exchange Reaction on the Alkyl Side Chain of Aromatic Compounds Using Heterogeneous Pd/C in D₂O. *Org. Lett.* **2004**, *6*, 1485-1487.

Tabulated spectroscopic data from Chapter 1 (2a-2q)

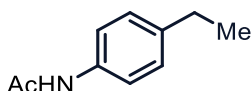


4-Ethylbiphenyl 2a. 98 mg of 4-acetylbiphenyl (**1a**) was subjected to the general procedure. Upon filtration and evaporation 90 mg (99%) of **2a** was isolated as a colorless solid. NMR data obtained matched the literature.² ¹H NMR (500 MHz, CDCl₃): δ 7.68 (d, *J* = 7.7 Hz, 2H), 7.62 (d, *J* = 8.1 Hz, 2H), 7.51 (d, *J* = 7.5 Hz, 2H), 7.41 (t, *J* = 7.5 Hz, 1H)

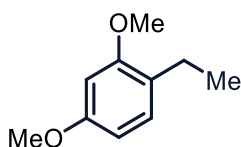
7.37 (d, $J = 8.0$ Hz, 2H), 2.79 (q, $J = 10$ Hz, 2H), 1.38 (t, $J = 7.5$ Hz, 3H); ^{13}C NMR (125 MHz, CDCl_3): δ 143.5, 141.3, 138.7, 128.8, 128.4, 127.2, 127.1 (2C), 28.7, 15.7.



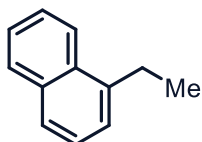
4-Ethylphenylboronic acid 2b. 82 mg of 4-acetylphenylboronic acid (**1b**) was subjected to the general procedure. Due to the acidity of the boronic acid, ^1H NMR yield was employed and revealed 78% yield. NMR data obtained matched literature.³ ^1H NMR (CDCl_3 , 400 MHz): δ 8.17 (d, $J = 8.0$ Hz, 2H), 7.35 (d, $J = 8.0$ Hz, 2H), 2.75 (q, $J = 8.0$ Hz, 2H), 1.31 (t, $J = 8.0$ Hz, 3H); ^{13}C NMR (100 MHz): δ 161.6, 149.3, 135.9, 127.7, 29.4, 15.5.



N-(4-Ethylphenyl)acetamide 2c. 88 mg of N-(4-acetylphenyl)acetamide (**1c**) was subjected to general procedure. Upon filtration and evaporation 78 mg (95%) of **2c** was isolated as a white solid. NMR data obtained matched literature.⁴ ^1H NMR (500 MHz, CDCl_3): δ 8.43 (s, 1H), 7.41 (d, $J = 8.3$ Hz, 2H), 7.10 (d, $J = 8.2$ Hz, 2H), 2.58 (q, $J = 7.5$ Hz, 2H), 2.11 (s, 3H), 1.19 (t, $J = 7.6$ Hz, 3H); ^{13}C NMR (125 MHz, CDCl_3): δ 169.2, 140.3, 135.7, 128.2, 120.5, 28.3, 24.2, 15.7.

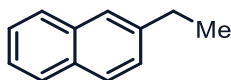


1-Ethyl-2,4-dimethoxybenzene 2d. 90 mg of 1-(2,4-dimethoxyphenyl)ethan-1-one (**1d**) was subjected to general procedure. Flash chromatography using EtOAc:Hexanes (9:1) as eluent gave 76 mg (93%) of **2d** as a white solid. NMR data obtained matched the literature.⁵ ^1H NMR (500 MHz, CDCl_3): δ 7.07 (d, $J = 8.5$ Hz, 1H), 6.47–6.44 (m, 2H), 3.82 (s, 3H), 3.81 (s, 3H), 2.60 (q, $J = 7.5$ Hz, 2H), 1.19 (t, $J = 7.5$ Hz, 3H); ^{13}C NMR (125 MHz, CDCl_3): δ 159.1, 158.3, 129.1, 125.2, 103.9, 98.6, 55.5, 55.4, 22.7, 14.6

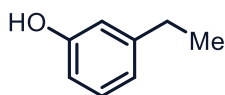


1-Ethylnaphthalene 2e. 85 mg of 1-acetylnaphthalene (**1e**) was subjected to general procedure. Upon filtration and evaporation 59 mg (75%) of **2t** was isolated as a clear oil.

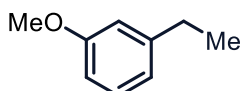
NMR data obtained matched literature.⁶ ¹H NMR (500 MHz, CDCl₃): δ 8.14 (d, *J* = 10 Hz, 1H), 7.94 (d, *J* = 10 Hz, 1H), 7.79 (d, *J* = 10 Hz, 1H), 7.54-7.61 (m, 2H), 7.49 (t, *J* = 5.0 Hz, 1H), 7.42 (d, *J* = 5.0 Hz, 1H), 3.20 (q, *J* = 5.0 Hz, 2H), 1.47 (t, *J* = 5.0 Hz, 3H); ¹³C NMR (125 MHz CDCl₃): δ 140.4, 134.0, 131.9, 128.9, 126.5, 125.8 (2C), 125.5, 125.0, 123.9, 26.0, 15.2.



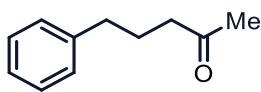
2-Ethylnaphthalene 2f. 85 mg of 2-acetylnaphthalene (**1f**) was subjected to the general procedure. Upon filtration and evaporation 71 mg (91%) of **2f** was isolated as a clear liquid. NMR data obtained matched the literature.⁷ ¹H NMR (500 MHz, CDCl₃): δ 7.91–7.86 (m, 3H), 7.73 (s, 1H), 7.56-7.44 (m, 3H), 2.91 (q, *J* = 7.5 Hz, 2H), 1.44 (t, *J* = 7.6 Hz, 3H), ¹³C NMR (100 MHz CDCl₃): δ 141.9, 133.8, 132.1, 127.9, 127.7, 127.5, 127.2, 125.9, 125.7, 125.1, 29.2, 15.7.



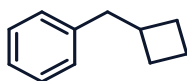
3-Ethylphenol 2g. 68 mg of 3-acetylphenol (**1g**) was subjected to the general procedure. Upon filtration and evaporation 60 mg (97%) of **2g** was isolated as a clear liquid. NMR data obtained matched the literature.⁴ ¹H NMR (500 MHz, CDCl₃): δ 7.18 (t, *J* = 7.5 Hz, 1H), 6.81 (d, *J* = 7.5 Hz, 1H), 6.72 (s, 1H), 6.69 (d, *J* = 8.0 Hz, 1H), 5.47 (s, 1H), 2.63 (q, *J* = 7.5 Hz, 2H), 1.24 (t, *J* = 7.5 Hz, 3H); ¹³C NMR (125 MHz, CDCl₃): δ 155.5, 146.4, 129.6, 120.6, 115.0, 112.7, 28.8, 15.5.



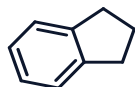
1-Ethyl-3-methoxybenzene 2h. 75 mg of 1-(3-methoxyphenyl)ethan-1-one (**1h**) was subjected to the general procedure. Upon filtration and evaporation 67 mg (97%) of **2h** was isolated as a clear liquid. NMR data obtained matched literature.⁴ ¹H NMR (500 MHz, CDCl₃): δ 7.26 (t, *J* = 7.8 Hz, 1H), 6.82 (s, 1H), 6.79 (d, *J* = 8.2 Hz, 1H), 3.85 (s, 3H), 2.70 (q, *J* = 7.6 Hz, 2H), 1.30 (t, *J* = 7.6 Hz, 3H); ¹³C NMR (125 MHz, CDCl₃): δ 159.8, 146.0, 129.4, 120.4, 113.8, 110.9, 55.2, 29.1, 15.6



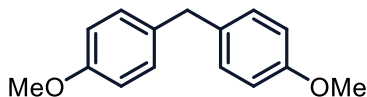
5-Phenylpentan-2-one 2i. 88mg of 1-phenyl-1,4 pentadienone (**1i**) was subjected to the general procedure. Upon filtration and evaporation 77mg (96%) of **2i** was isolated as a clear liquid. NMR data obtained matched literature.⁹ ¹H NMR (500 MHz, CDCl₃): δ 7.31-7.17 (m, 5H), 2.65 (t, *J* = 8.0 Hz, 2H), 2.46 (t, *J* = 8.0 Hz, 2H), 2.14 (s, 3H), 1.94 (p, *J* = 4.0 Hz, 2H); ¹³C NMR (125 MHz, CDCl₃): δ 208.7, 141.6, 128.5, 128.4, 126.0, 42.8, 35.0, 30.0zz25.2.



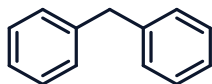
(Cyclobutylmethyl)benzene 2j. 80 mg of cyclobutyl(phenyl)methanone (**1j**) was subjected to the general procedure. Upon filtration and evaporation 69 mg (94%) of **2j** was isolated as a clear liquid. NMR data obtained matched literature.⁶ ¹H NMR (500 MHz, CDCl₃) δ 7.32-7.17 (m, 5H), 2.73 (d, *J* = 7.6 Hz, 2H), 2.60 (sep, *J* = 9.0 Hz, 1H), 2.09-2.05 (m, 2H) 1.94-1.71 (m, 4H); ¹³C NMR (125 MHz, CDCl₃): δ 141.4, 128.7, 128.3, 125.7, 43.2, 37.4, 28.4, 18.5.



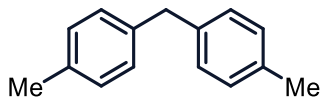
Indane 2k. 66mg of 1-indanone (**1k**) was subjected to the general procedure. Upon filtration and evaporation 54 mg (93%) of **2k** was isolated as a clear oil. NMR data obtained matched literature.¹⁰ ¹H NMR (500 MHz, CDCl₃): δ 7.25-7.27 (m, 2H), 7.15-7.17 (m, 2H), 2.95 (t, *J* = 7.5, 4H), 2.10 (q, *J* = 7.5 Hz, 2H). ¹³C NMR (125 MHz CDCl₃): δ 144.3, 126.1, 124.5, 33.0, 25.5.



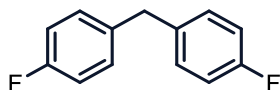
4,4'-Dimethoxydiphenylmethane 2l. 121 mg of 4,4'-dimethoxybenzophenone (**1l**) was subjected to the general procedure. TLC analysis revealed incomplete conversion to **2l** and column chromatography with EtOAc:Hex (2:8) afforded 98 mg (85%) of isolated **2l** as a clear solid. NMR data obtained matched literature.⁶ ¹H NMR (500 MHz, CDCl₃): δ 7.16 (d, *J* = 8.6 Hz, 2H), 6.89 (m, 2H), 3.93 (s, 2H), 3.83 (s, 6H); ¹³C NMR (125 MHz CDCl₃): δ 158.0, 133.8, 129.8, 113.9, 55.3, 40.2.



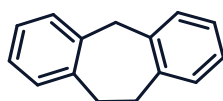
Diphenylmethane 2m. 91 mg of benzophenone (**1m**) was subjected to the general procedure. Upon filtration and evaporation 82 mg (99%) of **2m** was isolated as a clear solid. NMR data obtained matched literature.¹⁵ ¹H NMR (500 MHz, CDCl₃) 7.41-7.38 (m, 4 H) 7.32-7.30 (m, 6H), 4.1 (s, 2H); ¹³C NMR (125 MHz, CDCl₃) 141.2, 129.1, 128.6, 126.2, 42.1.



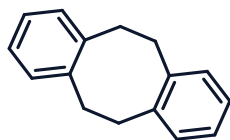
4,4'-Dimethyldiphenylmethane 2n. 105 mg of 4,4'-dimethylbenzophenone was subjected to the general procedure. Upon filtration and evaporation 95 mg (97%) of **2n** was isolated as a clear solid. NMR data obtained matched the literature.¹³ ¹H NMR (500 MHz, CDCl₃): δ 7.17-7.20 (m, 8H), 4.01 (s, 2H), 2.41 (s, 6H); ¹³C NMR (125 MHz, CDCl₃): δ 138.5, 135.5, 129.2, 128.9, 41.2, 21.1.



4,4'-Difluorodiphenylmethane 2o. 109 mg of 4,4'-difluorobenzophenone (**1o**) was subjected to the general procedure. Upon filtration and evaporation 99 mg (97%) of **2o** was isolated as a clear solid. NMR data obtained matched literature.¹⁴ ¹H NMR (400 MHz, CDCl₃) 7.12 (m, 4H), 6.91 (m, 4H), 3.94 (s, 2H). ¹³C NMR (100 MHz, CDCl₃) δ 161.5 (d, J_{CF} = 240 Hz), 136.6 (d, J_{CF} = 3.0 Hz), 130.3 (d, J_{CF} = 8.0 Hz), 115.4 (d, J_{CF} = 21 Hz), 40.4. ¹⁹F NMR (376 MHz, CDCl₃) δ -117.1.



10,11-Dihydro-5H-dibenzo[a,d][7]annulene 2p. 107 mg of dibenzosuberone (**1p**) was subjected to the general procedure using 134 mg (3.0 equiv) of B₂(OH)₄. TLC analysis revealed incomplete conversion and column chromatography with EtOAc:hexanes (1:9) afforded 70 mg (73%) of **2p** isolated as a white solid. NMR data obtained matched literature.¹⁵ ¹H NMR (500 MHz, CDCl₃): δ 7.26-7.17 (m, 8H), 4.19 (s, 2H), 3.25 (s, 4H); ¹³C NMR (125 MHz, CDCl₃): δ 139.4, 139.1, 129.7, 129.1, 126.7, 126.2, 41.1, 32.6.



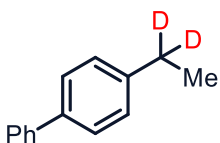
5,6,11,12-Tetrahydrodibenzo[a,e][8]annulene 2q. 4.70 grams (21.2 mmol) of **1q**, 4.18 grams (46.6 mmol) of B₂(OH)₄, 670 mg of 10% w/w Pd/C, and a magnetic stir bar was

charged to a 250 mL round bottom flask and fitted with a rubber septa. The septum was secured to the top of the flask by braiding with metal wire. 50 mL of THF was added through the septum and the reaction was placed in an oil bath preheated to 60 °C. Significant bubbling and buildup of pressure was observed. The reaction stirred for 2 hours and a needle was used to release the pressure through the septum. The reaction mixture was filtered through silica and the eluent was evaporated, leaving 4.26 g (97%) of **2q** as a white powder. NMR data obtained matched the literature.¹⁶ ¹H NMR (500 MHz, CDCl₃): δ 7.02–6.98 (m, 8H), 3.08 (s, 8H); ¹³C NMR (125 MHz, CDCl₃): δ 140.8, 129.8, 126.3, 35.3.

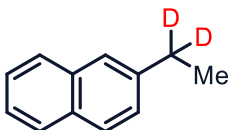
1. General Procedure for the Deoxygenative Deuteration of **1a**, **1f**, and *para*-acetylanisole .

0.3 mmol of ketone substrate, 2.3 equivalents (64 mg, 0.69 mmol) of B₂(OD)₄, 9 mg of 10% w/w Pd/C (3 mol %), and a magnetic stir-bar were charged to a one-dram vial. 0.75 mL of dry and degassed THF was added and the vial firmly capped with a PTFE-lined screw-top septum cap. The reaction was then stirred at 60 °C for 2 hours. The reaction mixture was filtered through mixed Celite and silica pipet plug rinsing the vial with methanol and DCM (5:95). The eluent was then removed by rotary evaporation and the residue was assessed using NMR spectroscopy.

2. Tabulated NMR Data of deuterated compounds **2a-d2**, **2f-d2**, and 1-(ethyl-1,1-d₂)-4-methoxybenzene.

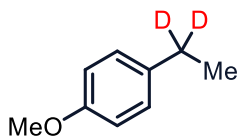


4-(ethyl-1,1-d₂)-1,1'-biphenyl 2a-d2. 59 mg of 4-acetylbiphenyl was subjected to the general procedure. Upon filtration and evaporation 54 mg (97%) of **2a-d2** was isolated as a white powder. NMR data obtained matched literature.¹⁷ ¹H NMR (500 MHz, CDCl₃): δ 7.63 (d, *J* = 7.0 Hz, 2H), 7.56 (d, *J* = 8.5 Hz, 2H), 7.46 (t, *J* = 8.0 Hz, 2H), 7.36 (t, *J* = 8.0 Hz, 1H), 7.31 (d, *J* = 8.5 Hz, 2H), 2.77-2.71 (m, 0.3H - 85% deuterium incorporation), 1.33 (m, 3H). (125 MHz, CDCl₃): δ 1243.5, 141.3, 138.8, 128.8, 128.4, 127.2, 127.2, 127.1, 28.5 - 27.8 (m), 15.7, 15.6.



2-(ethyl-1,1-d₂)naphthalene 2f-d2. 51mg of 2-acetylnaphthalene (**1f**) was subjected to the general procedure. Upon filtration and evaporation 45 mg (95%) of **2f-d2** was isolated as a colorless liquid. NMR data obtained matched literature.¹⁸ ¹H NMR (500 MHz, CDCl₃): δ 7.84-7.79 (m, 3H), 7.66 (s, 1H), 7.49-7.37 (m, 3H), 2.87-2.82 (m, 0.3H = 85% deuterium

incorporation), 1.36 (m, 3H). ^{13}C NMR (125 MHz, CDCl_3): δ 141.7, 133.7, 132.0, 127.8, 127.6, 127.4, 127.1, 125.8, 125.6, 125.0, 28.9–28.2 (m), 15.5, 15.4.



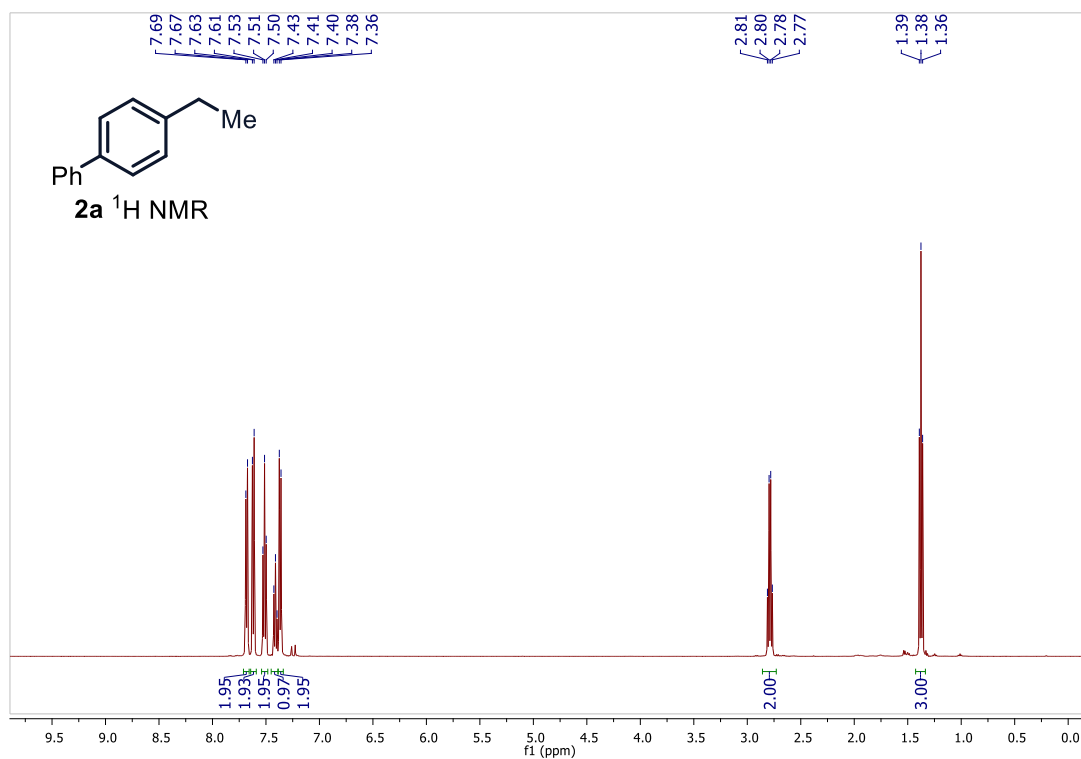
1-(ethyl-1,1-d₂)-4-methoxybenzene. 45 mg of *para*-acetylanisole was subjected to general procedure. Upon filtration and evaporation 39 mg (95%) of 1-(ethyl-1,1-d₂)-4-methoxybenzene was isolated as a clear liquid. NMR data obtained matched literature.¹⁹ ^1H NMR (500 MHz, CDCl_3): δ 7.12 (d, J = 8.5 Hz, 2H), 6.83 (d, J = 9.0 Hz, 2H), 2.60–2.55 (m, 0.3H = 85% deuterium incorporation), 1.20 (m, 3H). ^{13}C NMR (125 MHz, CDCl_3): δ 157.7, 128.8, 113.9, 55.4, 23.5 (suppressed due to splitting), 16.0, 15.9.

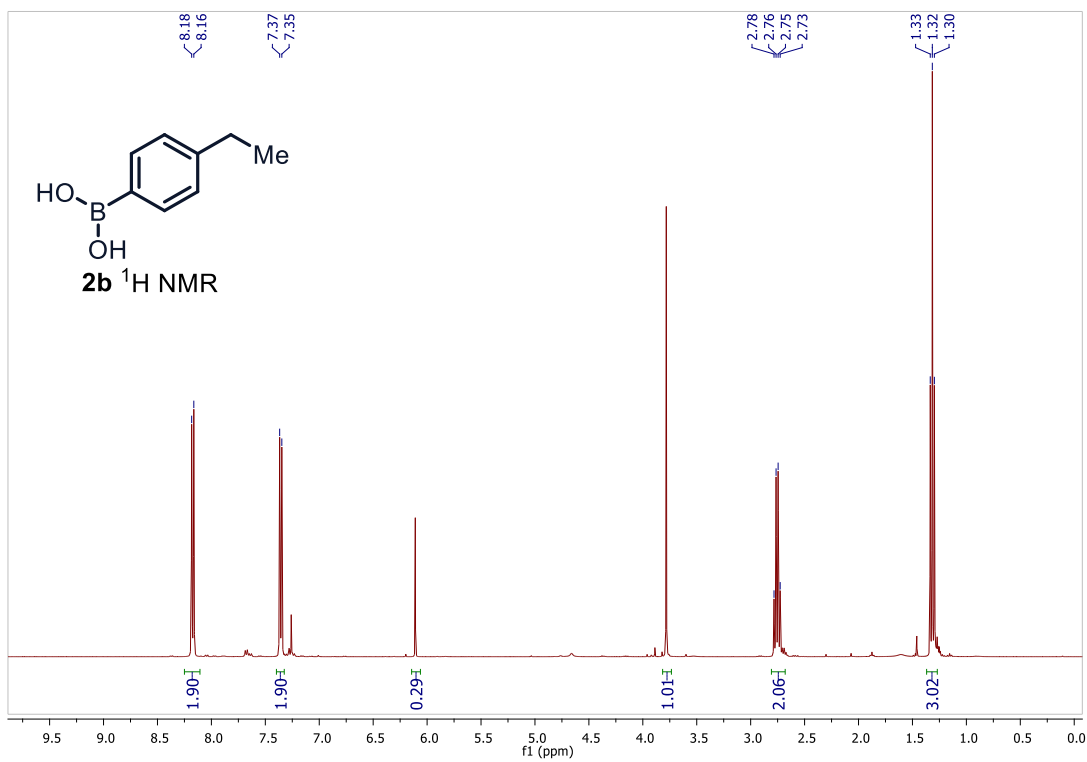
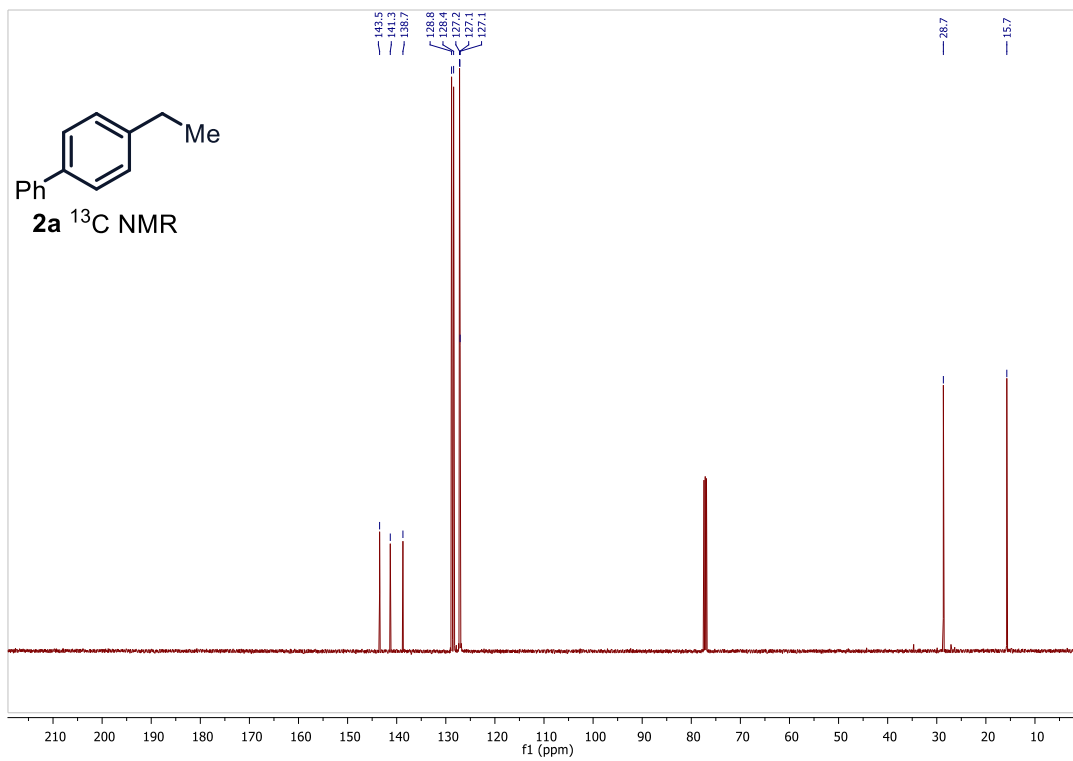
References for NMR data collected in chapter 1

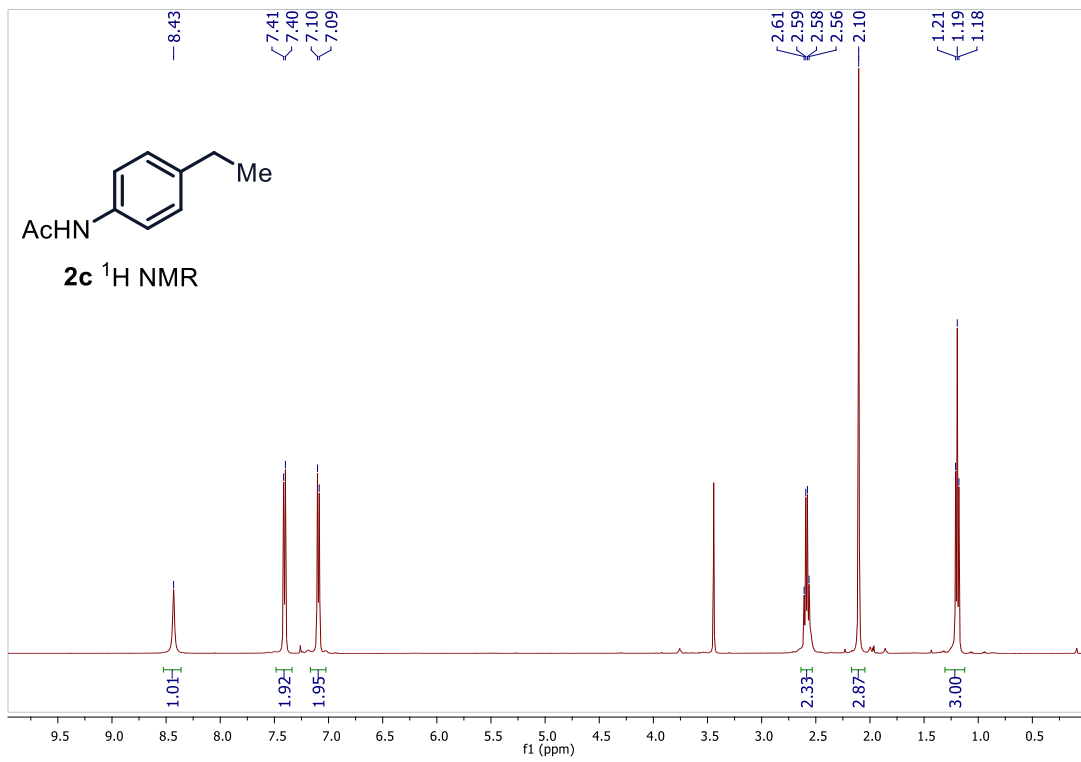
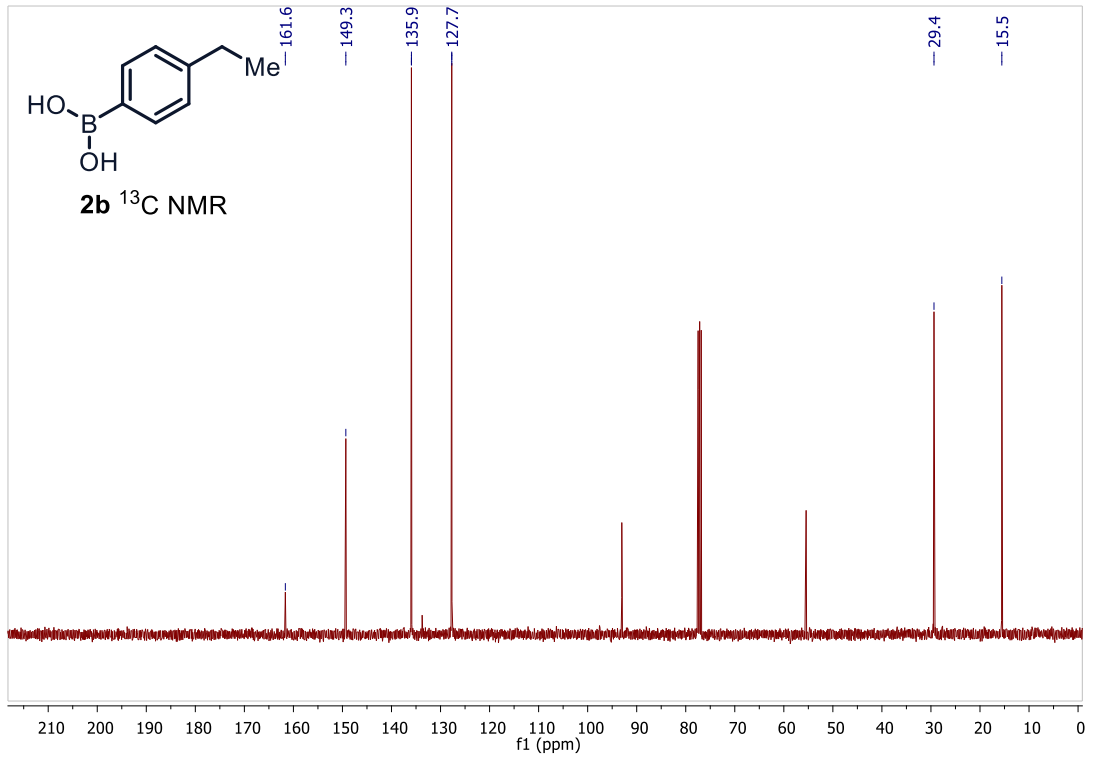
1. Cummings, S. P.; Le, T.-N.; Fernandez, G. E.; Quiambao, L. G.; Stokes, B. J. *J. Am. Chem. Soc.* **2016**, *138*, 6107–6110
2. Iglesias, M. J.; Prieto, A.; Nicasio, M. C. *Organic Letters* **2012**, *14*, 4318–4321
3. Flinker, M.; Yin, H.; Juhl, R. W.; Eikeland, E. Z.; Overgaard, J.; Nielsen, D. U.; Skrydstrup, T. *Angew. Chem. Int. Ed.* **2017**, *56*, 15910–15915
4. Shen, R.; Chen, T.; Zhao, Y.; Qiu, R.; Zhou, Y.; Yin, S.; Wang, X.; Goto, M.; Han, L.-B. *J. Am. Chem. Soc.* **2011**, *133*, 17037–17044
5. Jung, S.; Yoon, N.G.; Yang, S.; Kim, D.; Lee, W.S.; Choi, S.; Lee, C.; Kang, B.H.; Lee, J.H.; Kang, S. *Bioorg. Med. Chem. Lett.* **2020**, *30*, 126809
6. Rahaim, R. J.; Maleczka, R. E. *Org. Lett.* **2011**, *13* (4), 584–587
7. Guan, B. T.; Xiang, S. K.; Wang, B. Q.; Sun, Z. P.; Wang, Y.; Zhao, K. Q.; Shi, Z. *J. Am. Chem. Soc.* **2008**, *130*, 3268–3269
8. Betori, R. C.; May, C. M.; Scheidt, K. A. *Angew. Chem. Int. Ed.* **2019**, *58*, 16490–16494
9. Ochiai, M.; Tuchimoto, Y.; Higashiura, N. *Org. Lett.* **2004**, *6*, 1505
10. Bo, S.; Li, Y.; Hua, Z.; Jun-Li, H.; Huadong, W. *Organometallics* **2020**, *39*, 23, 4159–4163
11. Costanzo, M. J.; Patel, M. N.; Petersen, K. A.; Vogt, P. F. *Tetrahedron Lett.* **2009**, *50*, 5463–5466
12. Yoon, S.; Hong, M. C.; Rhee, H. *J. Org. Chem.* **2014**, *79*, 4206–4211
13. Cheng, Y.; Dong, W.; Wang, L.; Parthasarathy, K.; Bolm, C. *Org Lett.* **2014**, *16*, 2000–2002
14. Qian, X.; Kozak, C. M. *Synlett* **2011**, 852–856
15. Yamada, T.; Saito, K.; Akiyama, T. *Adv. Synth. Catal.* **2016**, *358*, 62–68
16. Wang, Z.; Huang, Y.; Guo, J.; Li, Z.; Xu, J.; Lu, J. Q.; Wang, C. *Macromolecules* **2018**, *51*, 1377–1385
17. Meng, Q.-Y.; Schirmer, T. E.; Berger, A. L.; Donabauer, K.; König, B. *J. Am. Chem. Soc.* **2019**, *141*, 11393–11397.

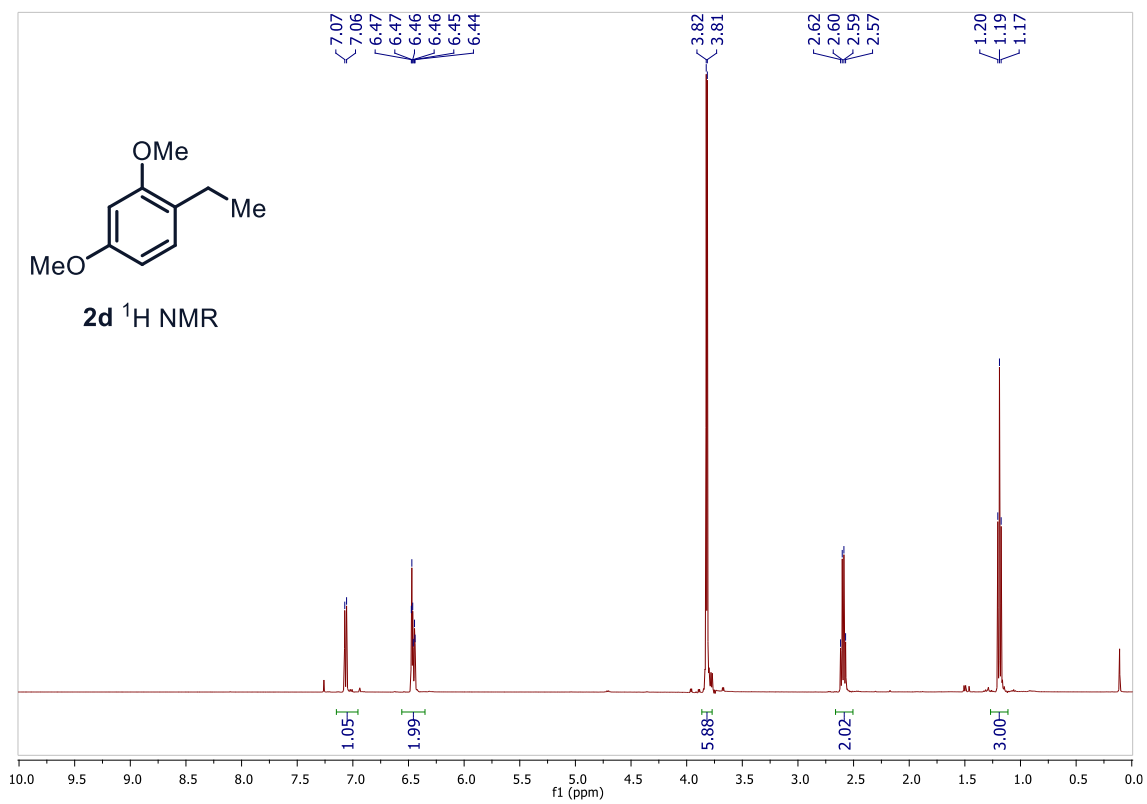
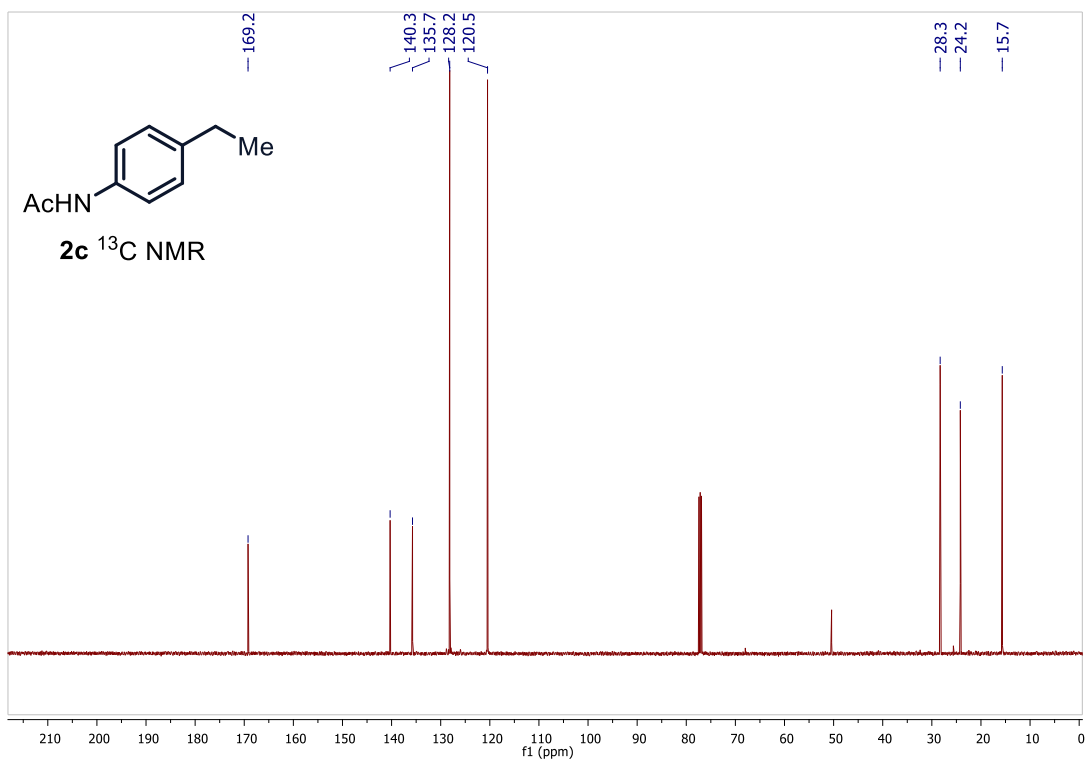
18. Saito, K.; Ando, K.; Akiyama, T. *Org. Lett.* **2015**, *17*, 3366–3369
19. Kurita, T.; Hattori, K.; Seki, S.; Mizumoto, T.; Aoki, F.; Yamada, Y.; Ikawa, K.; Maegawa, T.; Monguchi, Y.; Sajiki, H. *Chem. Eur. J.* **2008**, *14*, 664–673

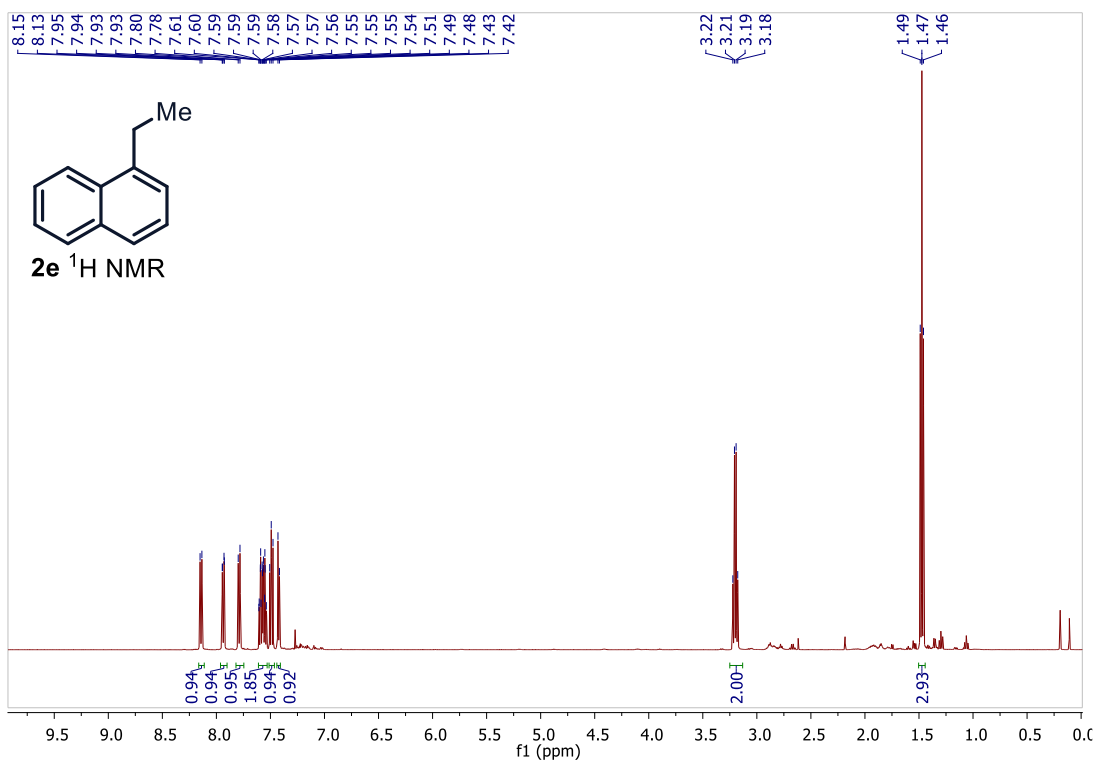
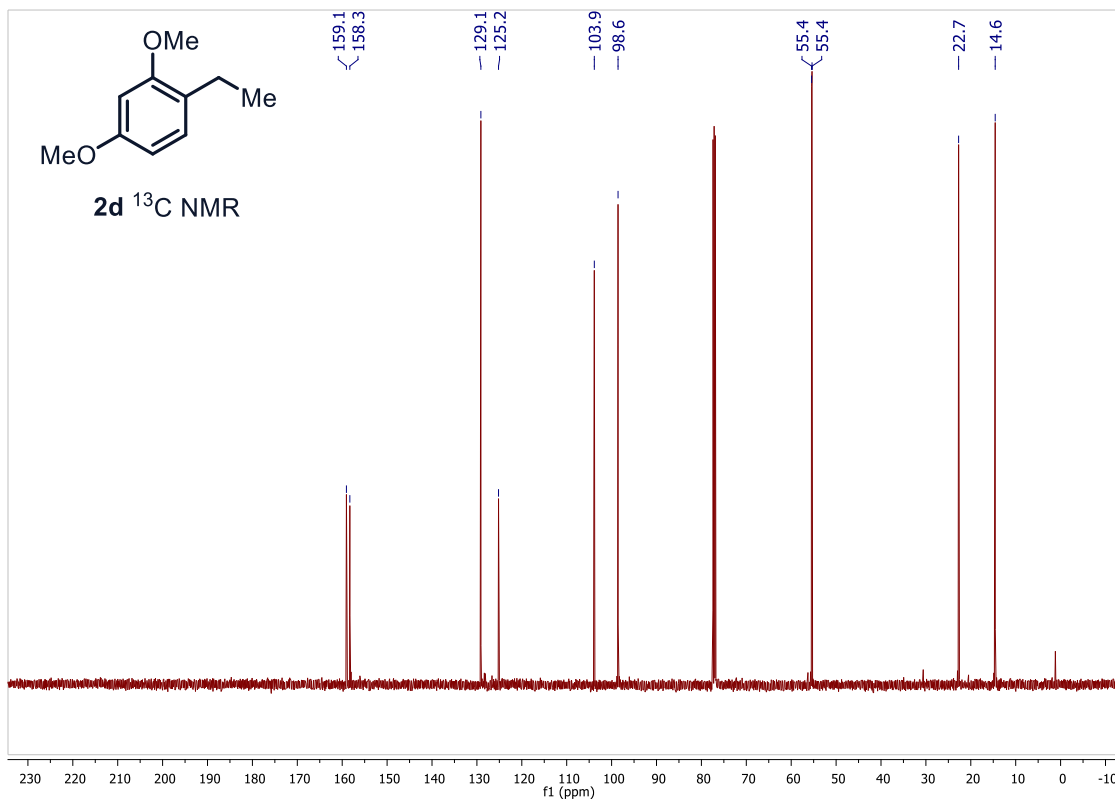
NMR spectra of substrates in Chapter 1

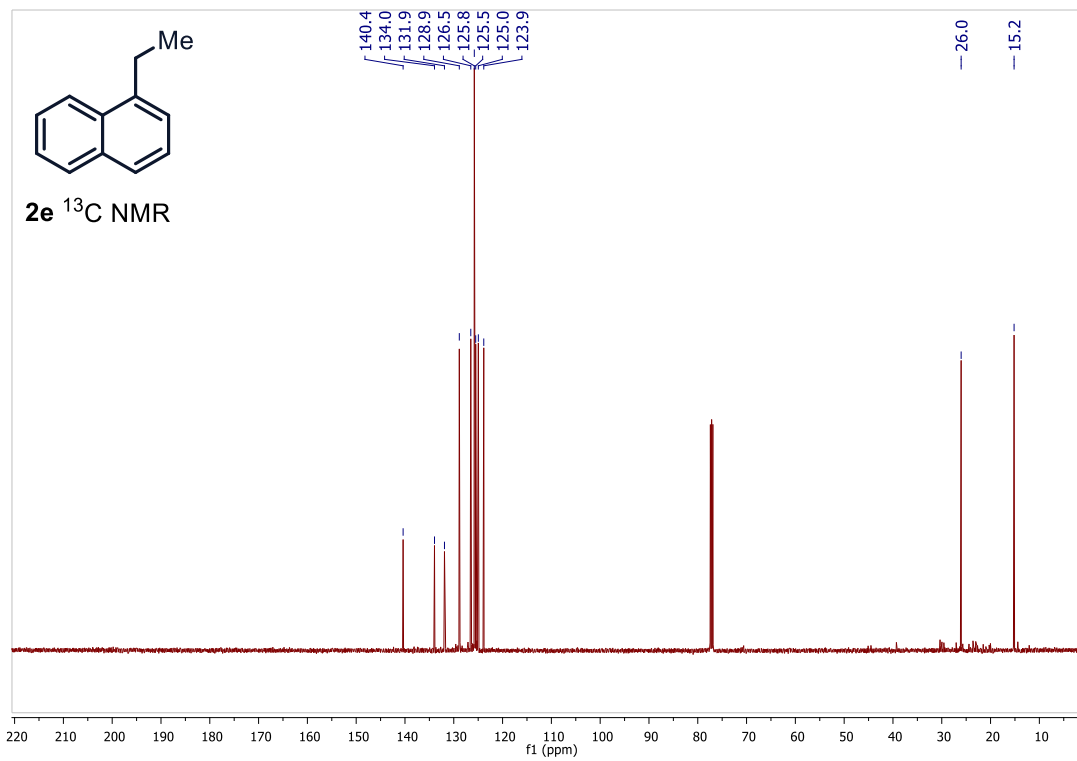


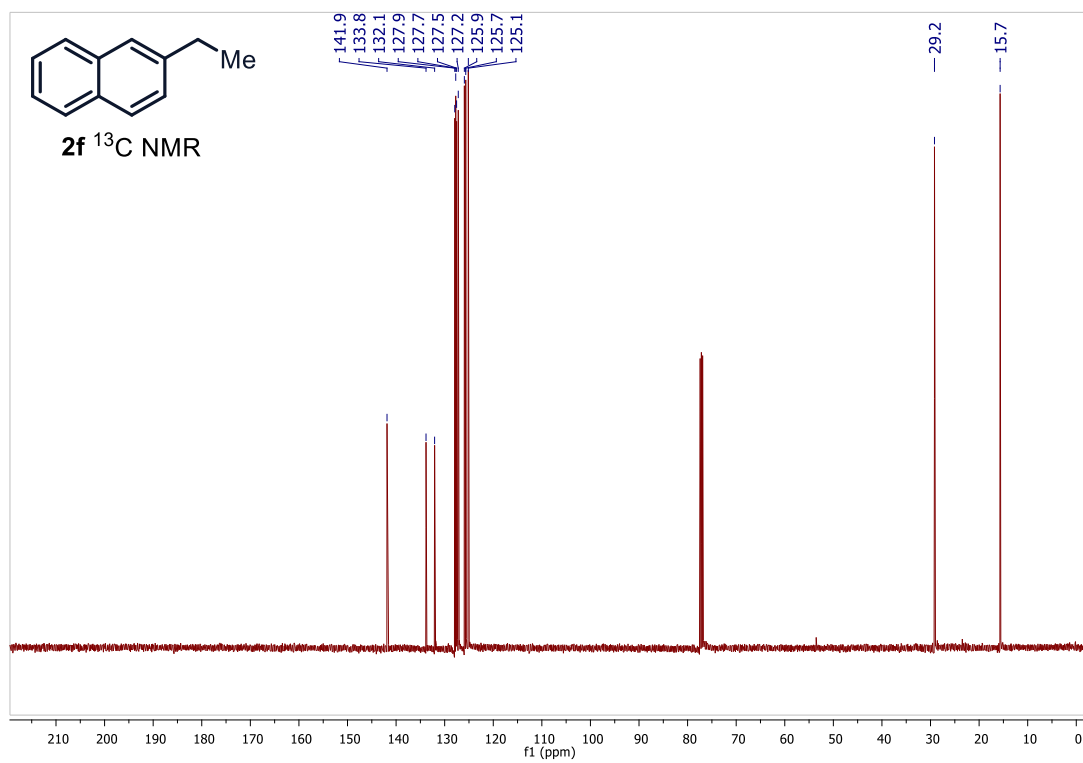
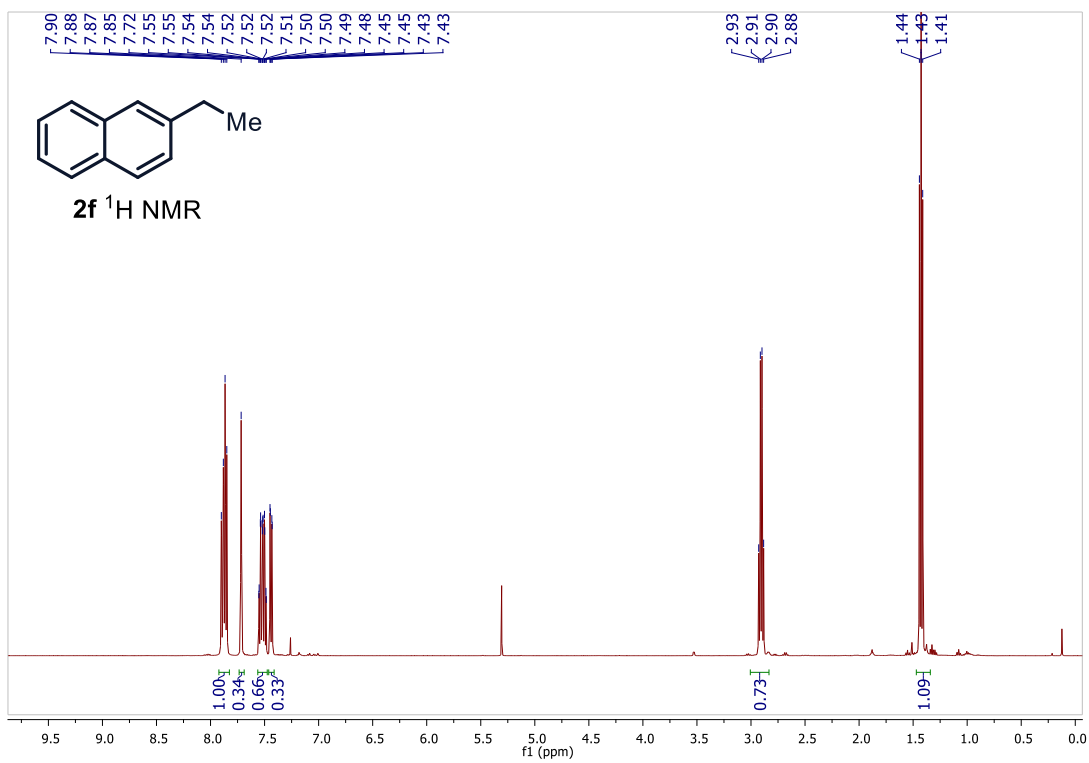


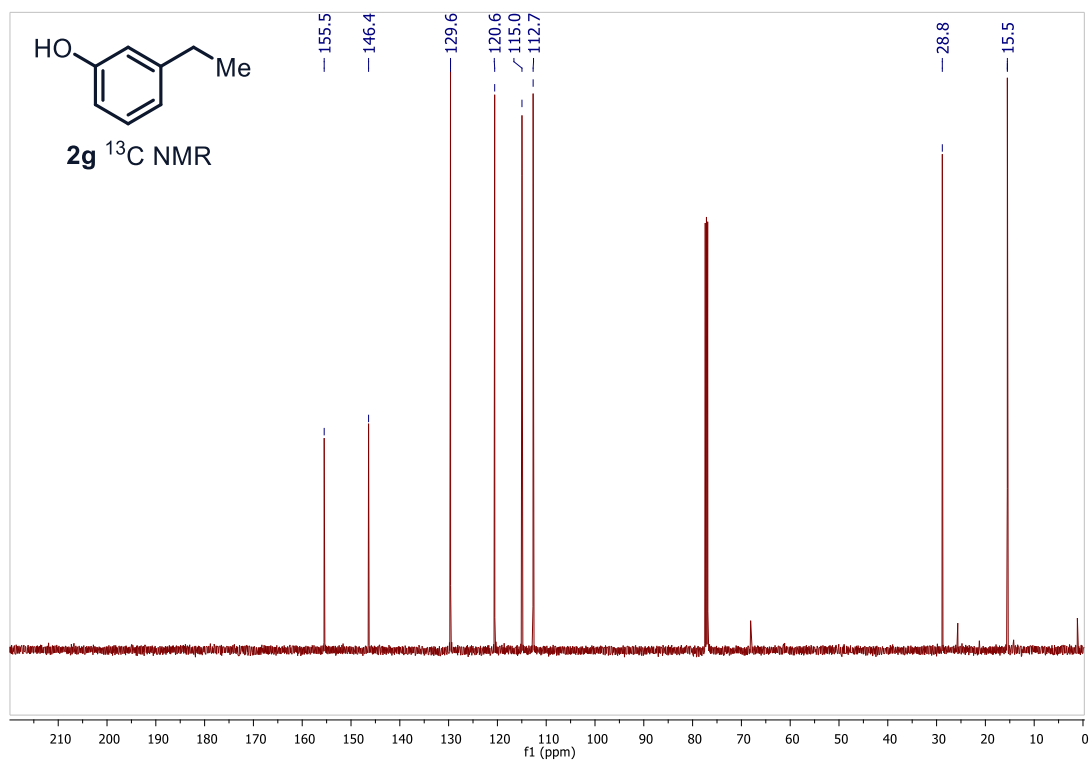
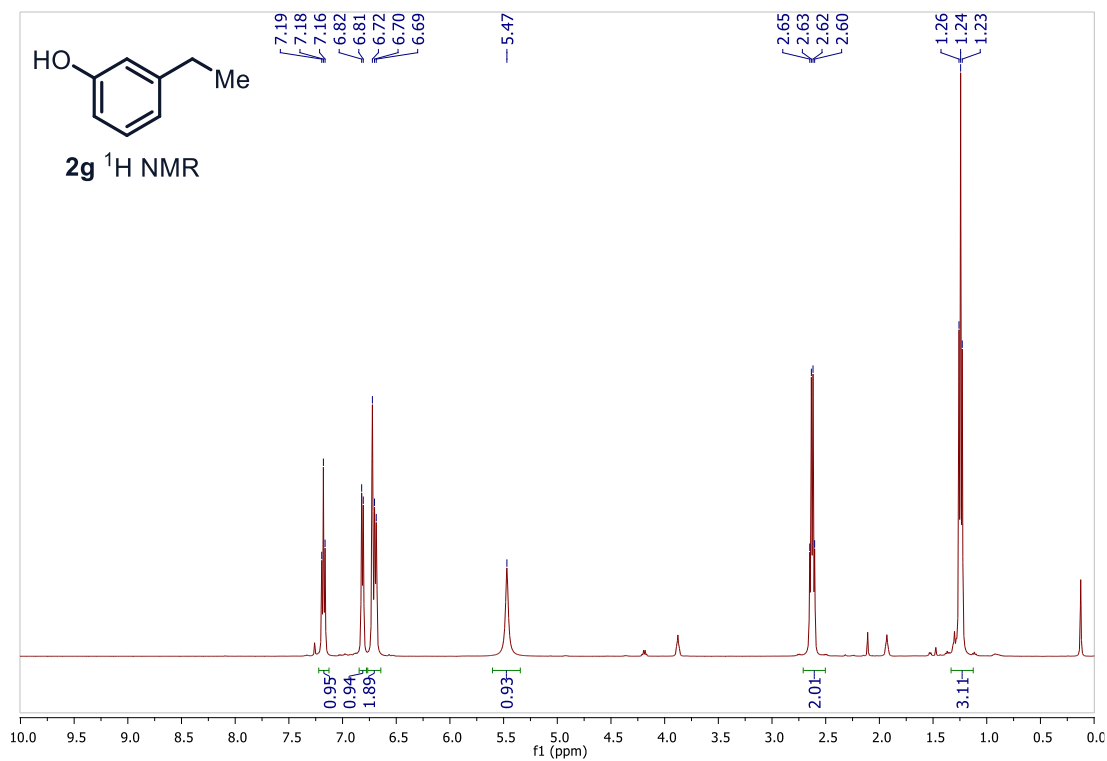


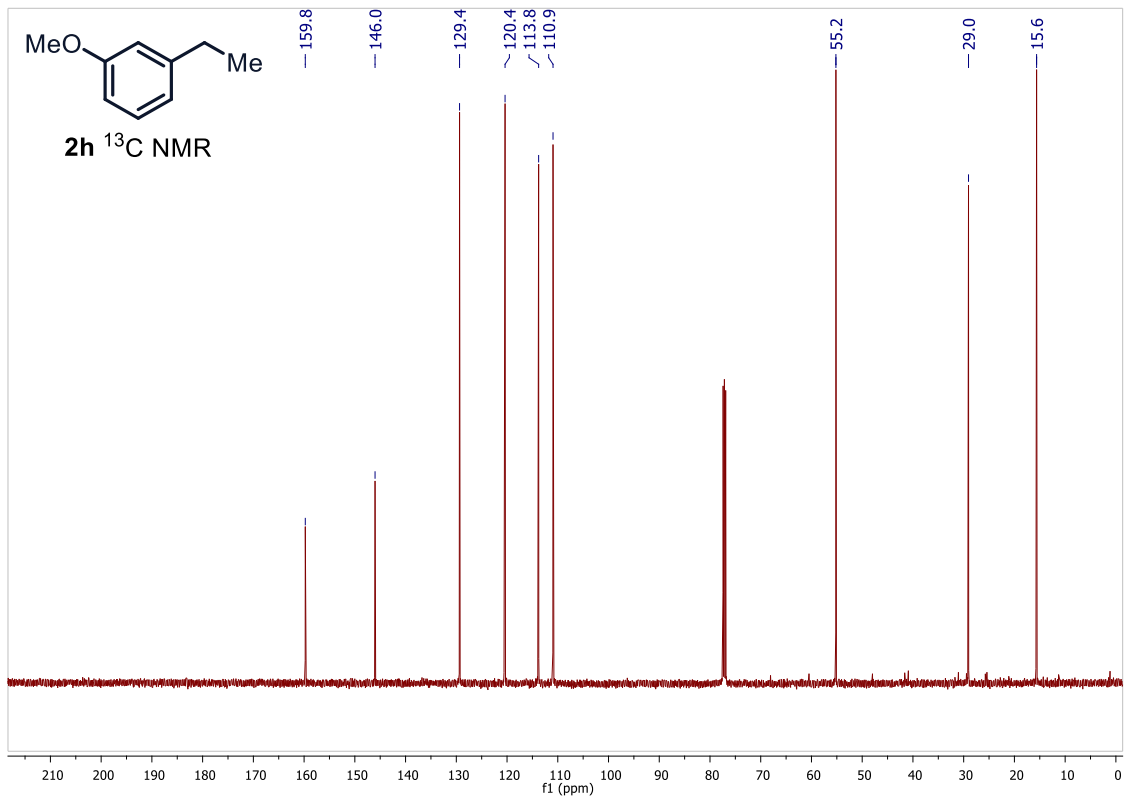
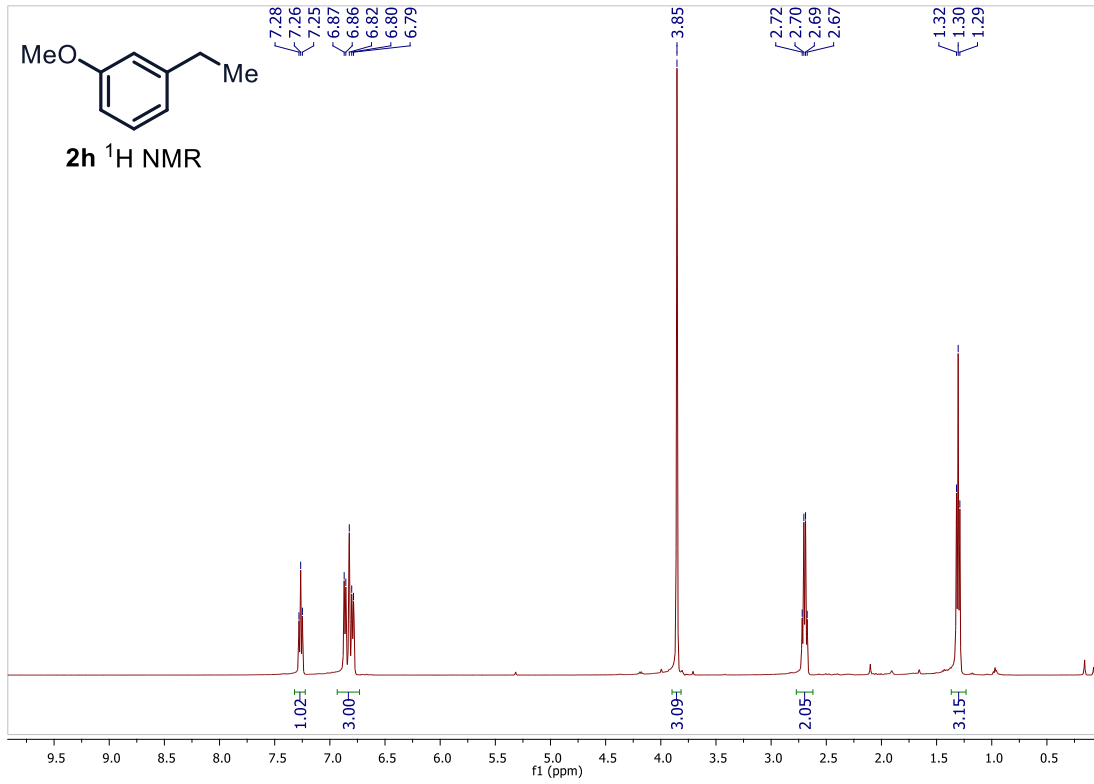


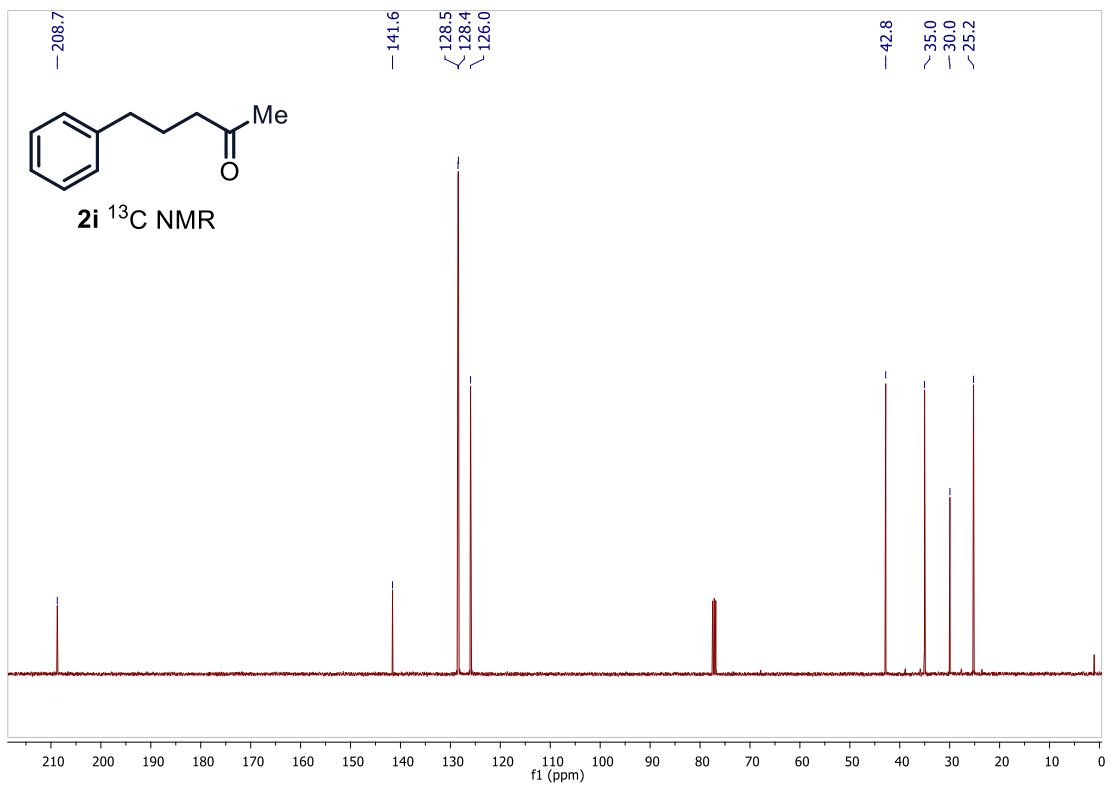
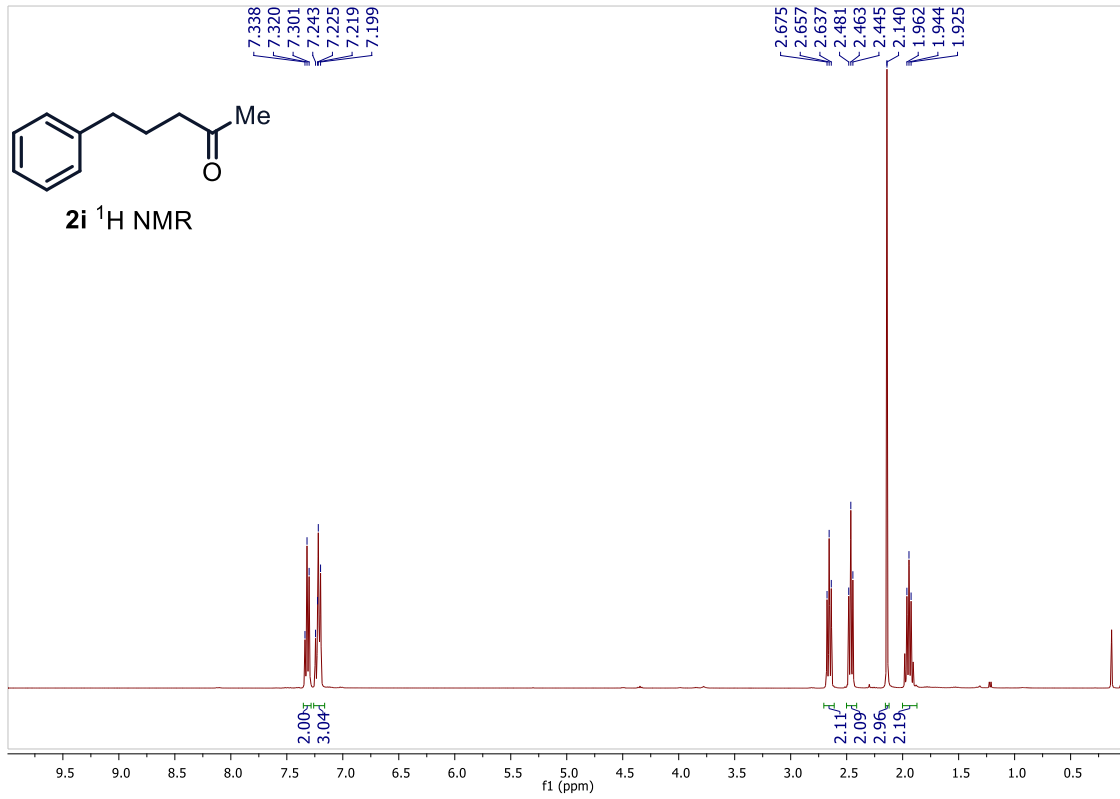


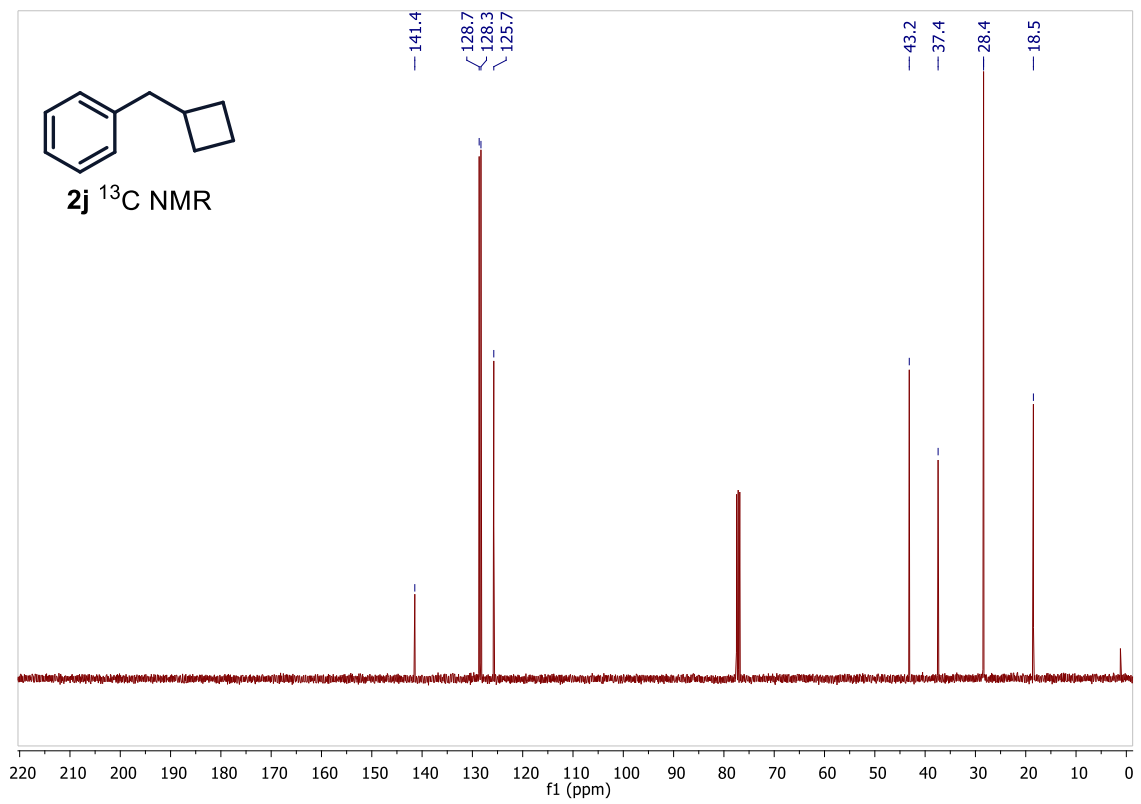
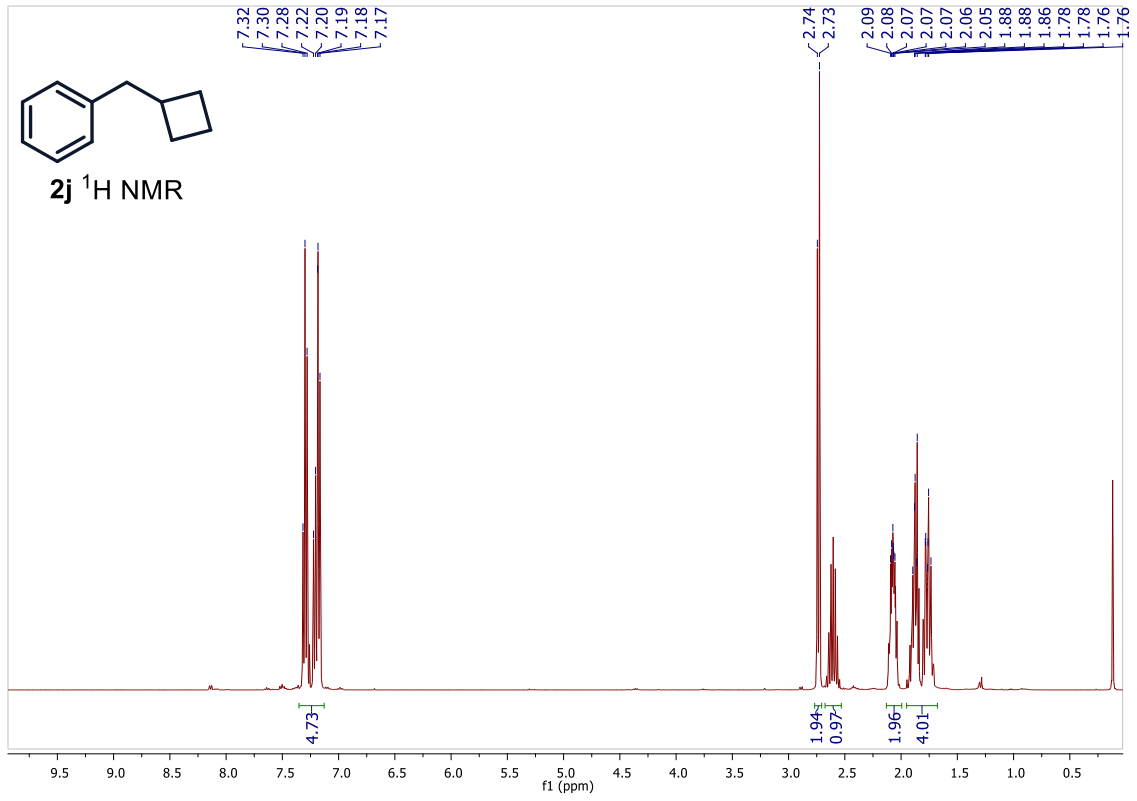


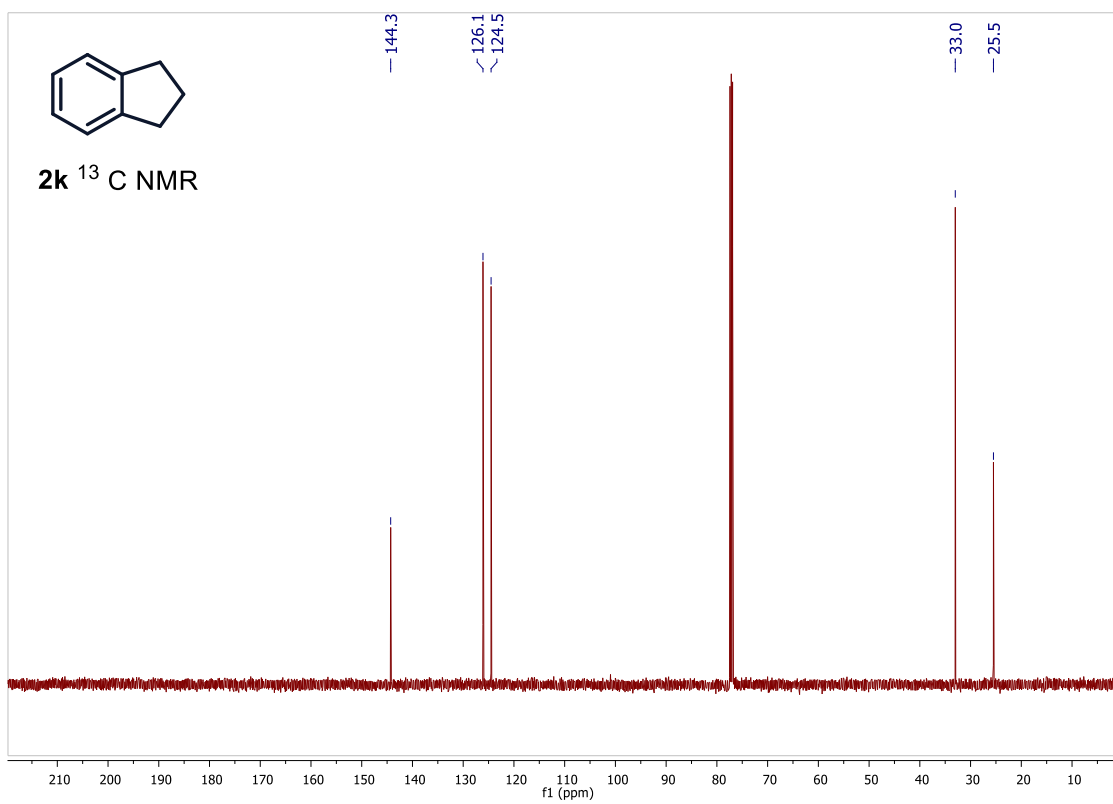
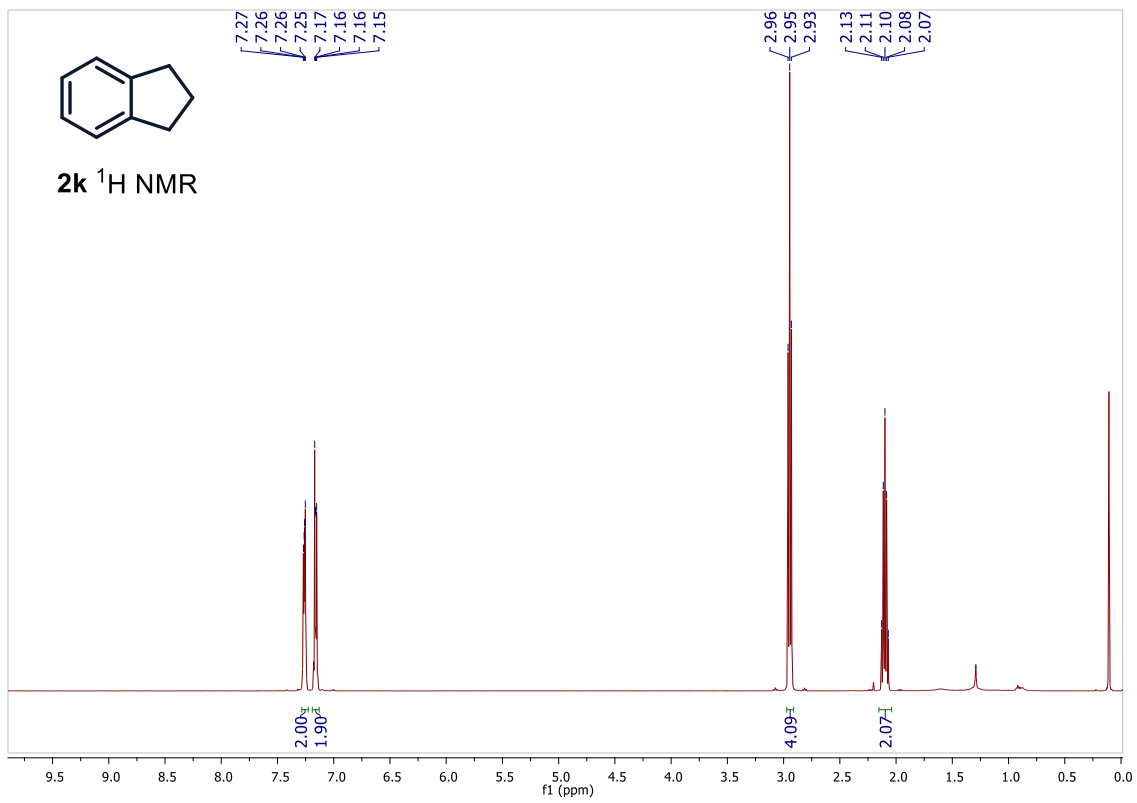


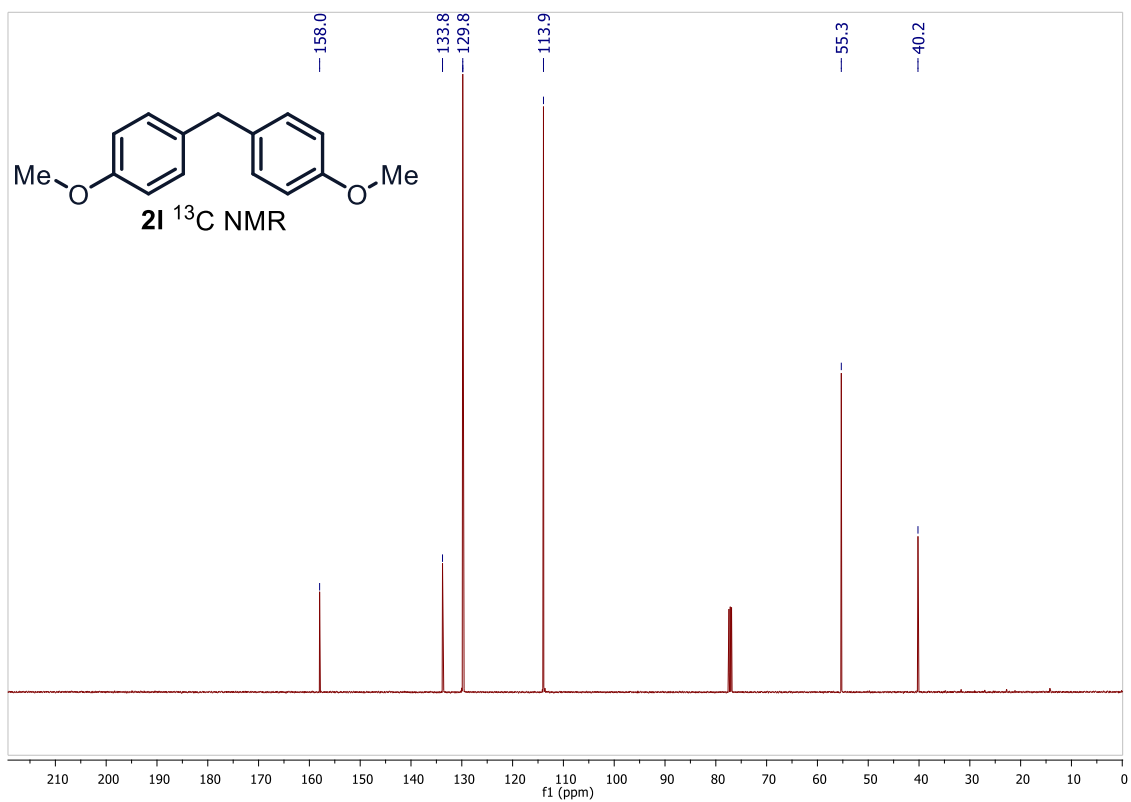
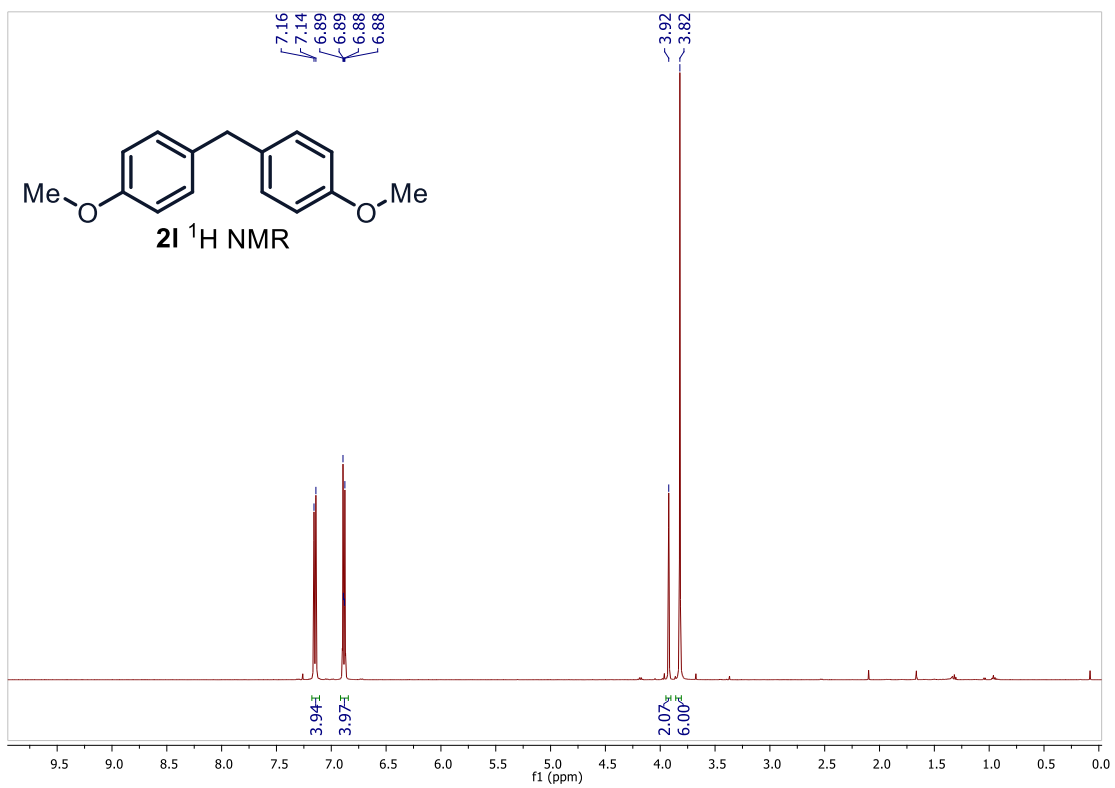


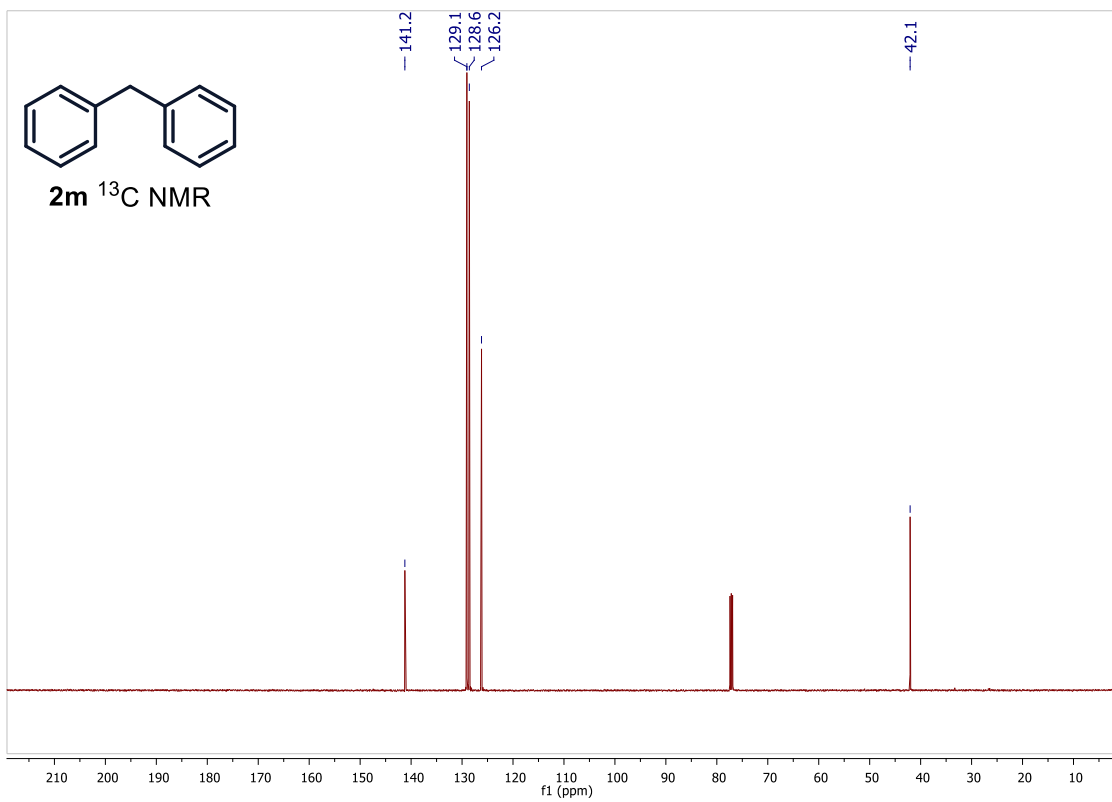
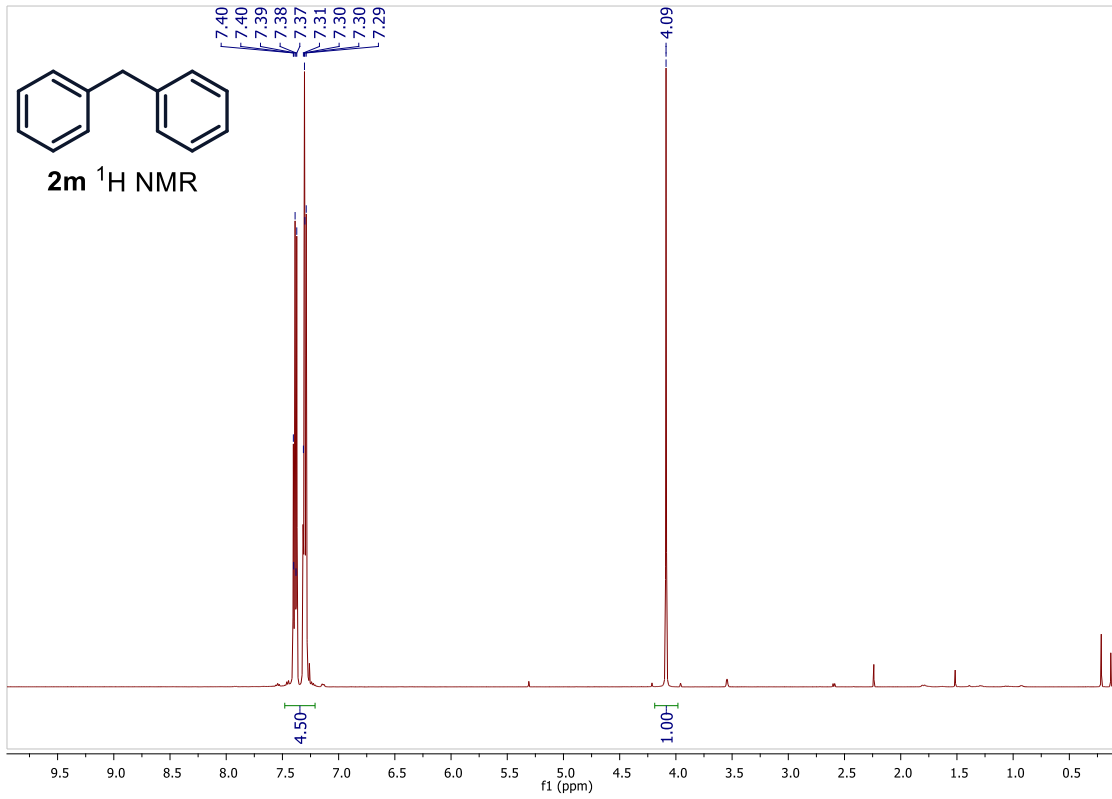


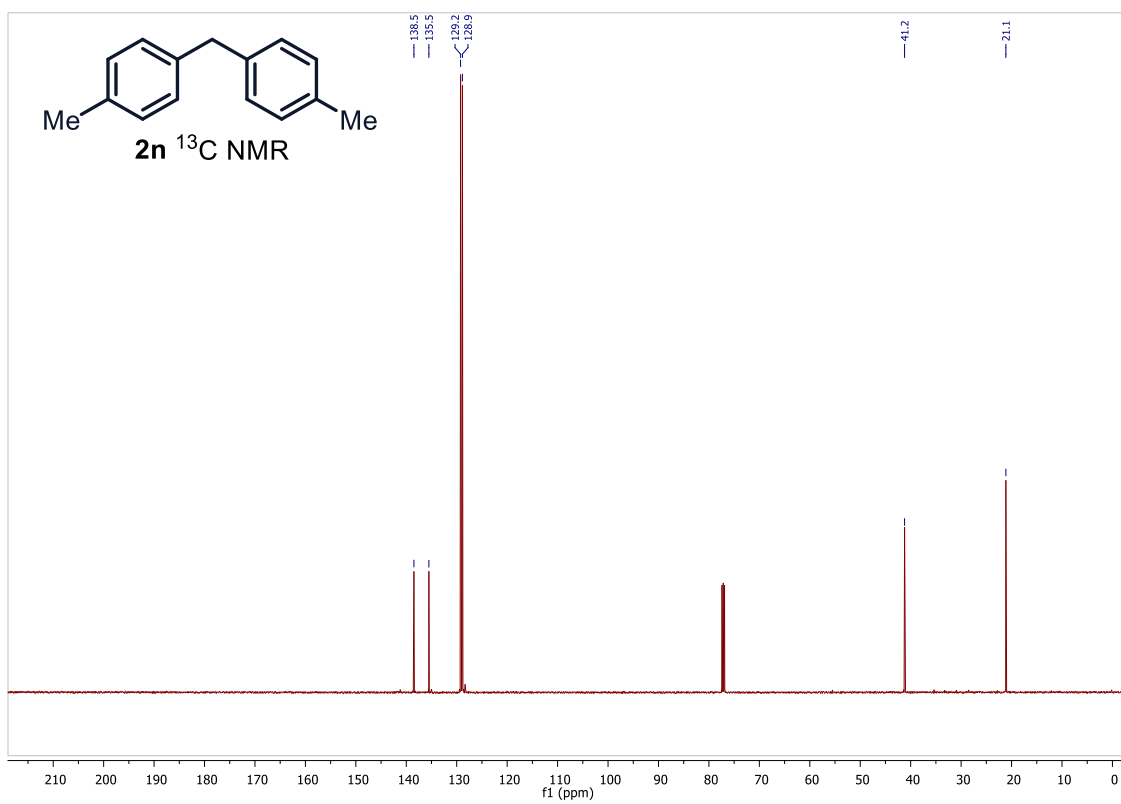
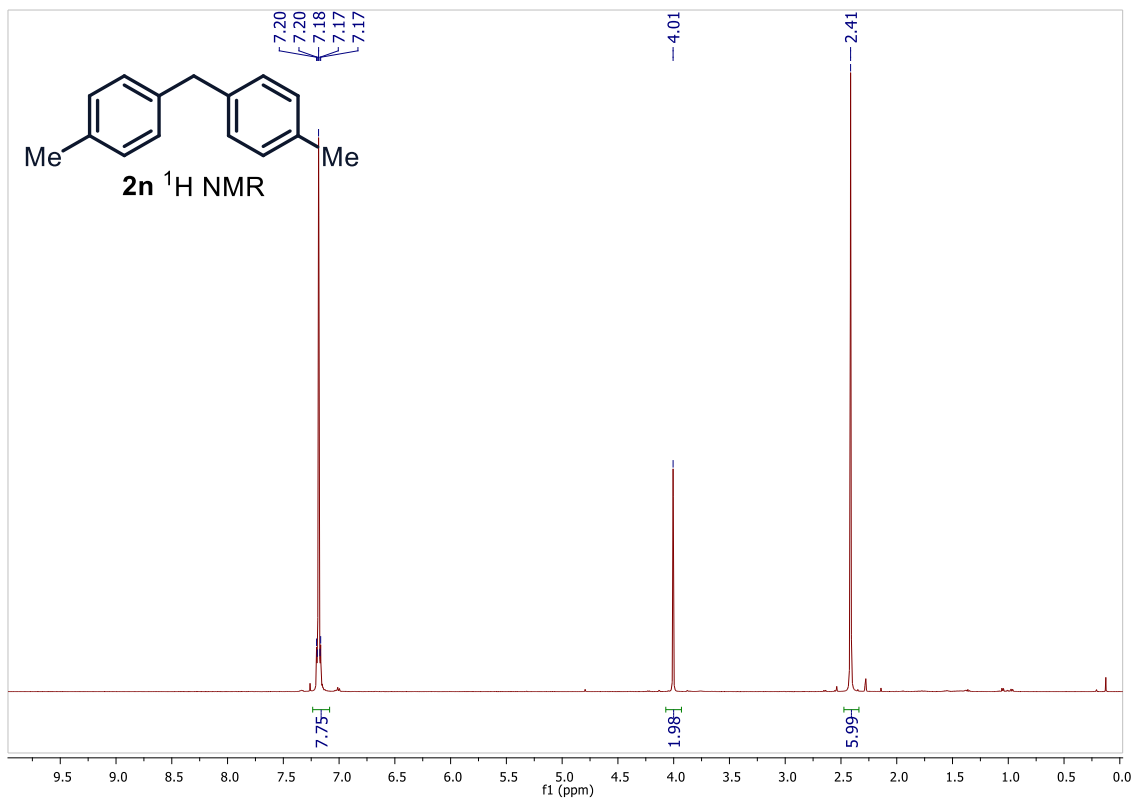


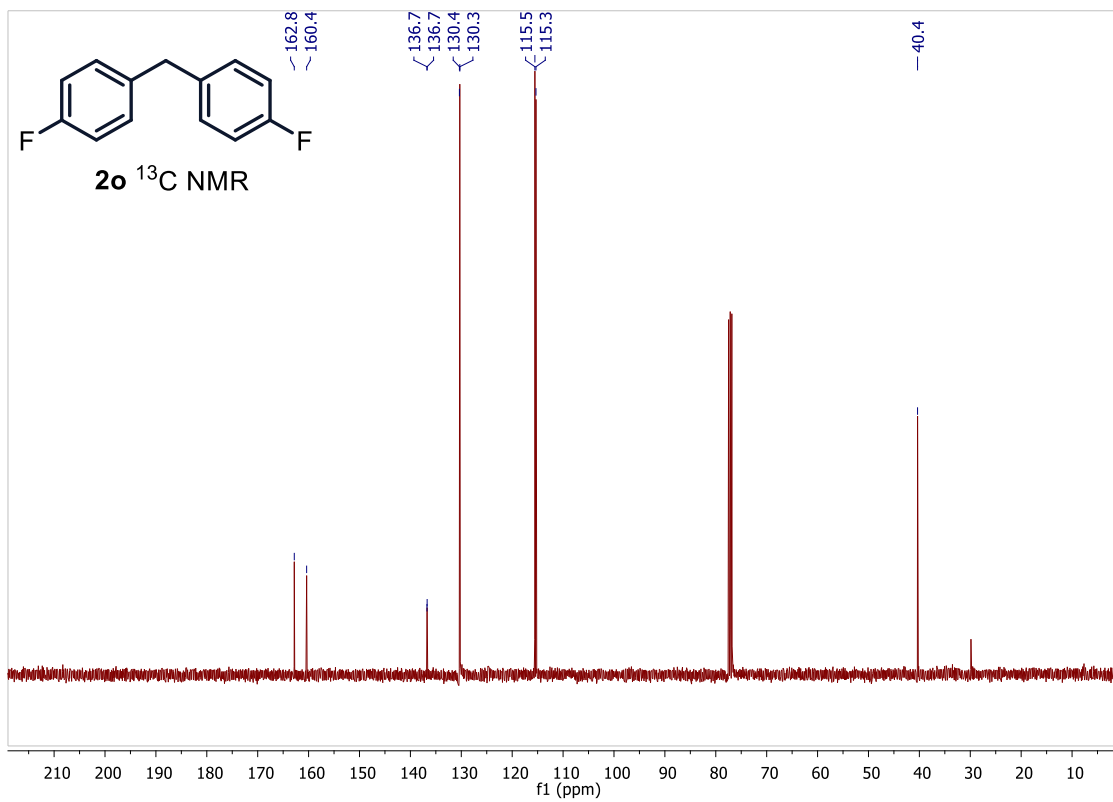
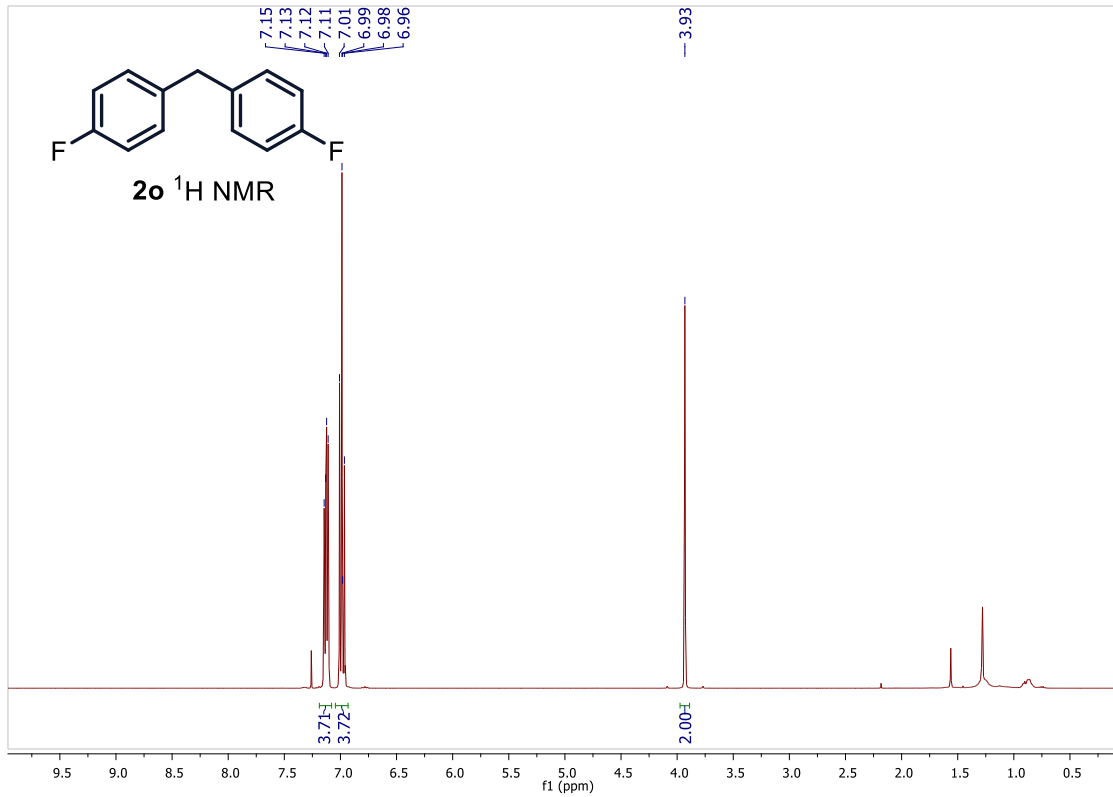


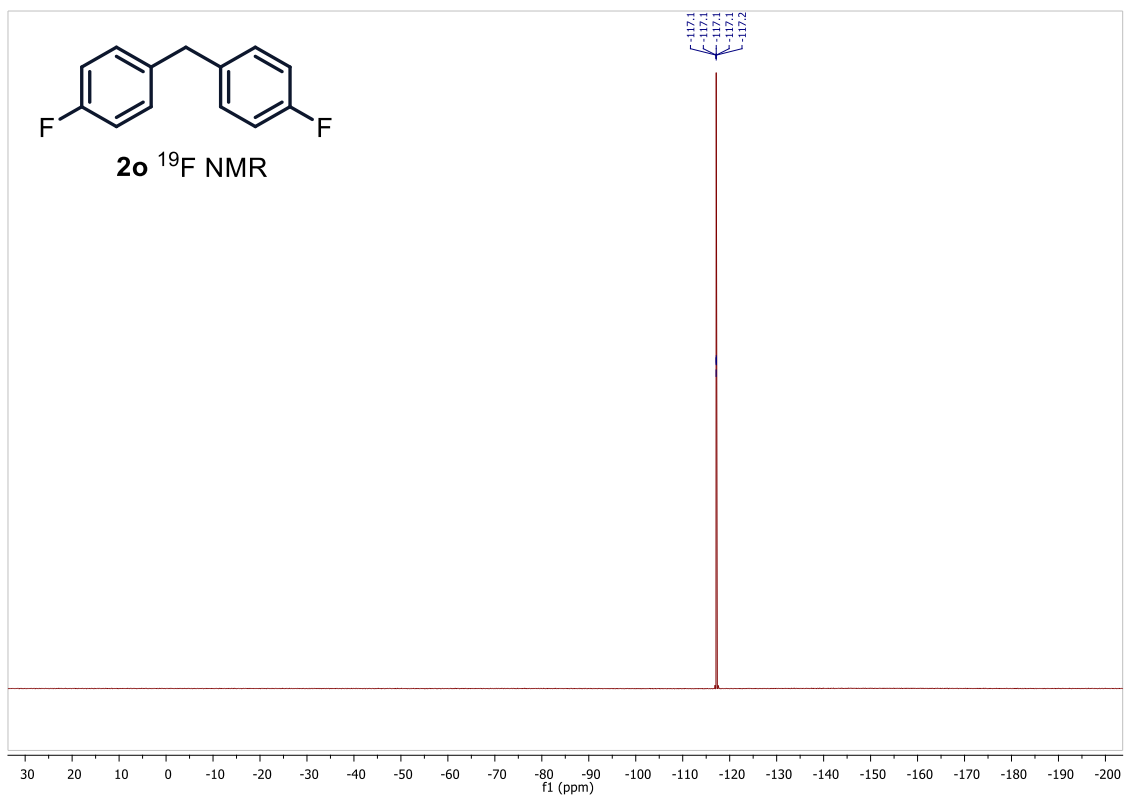


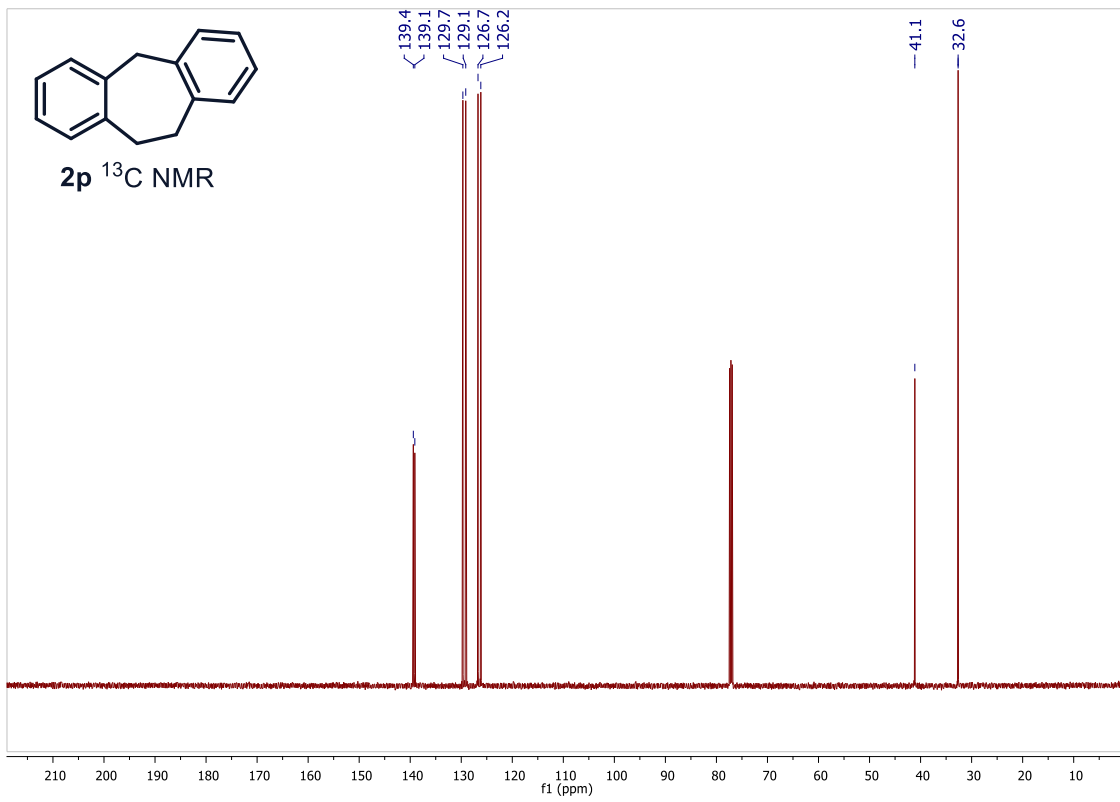
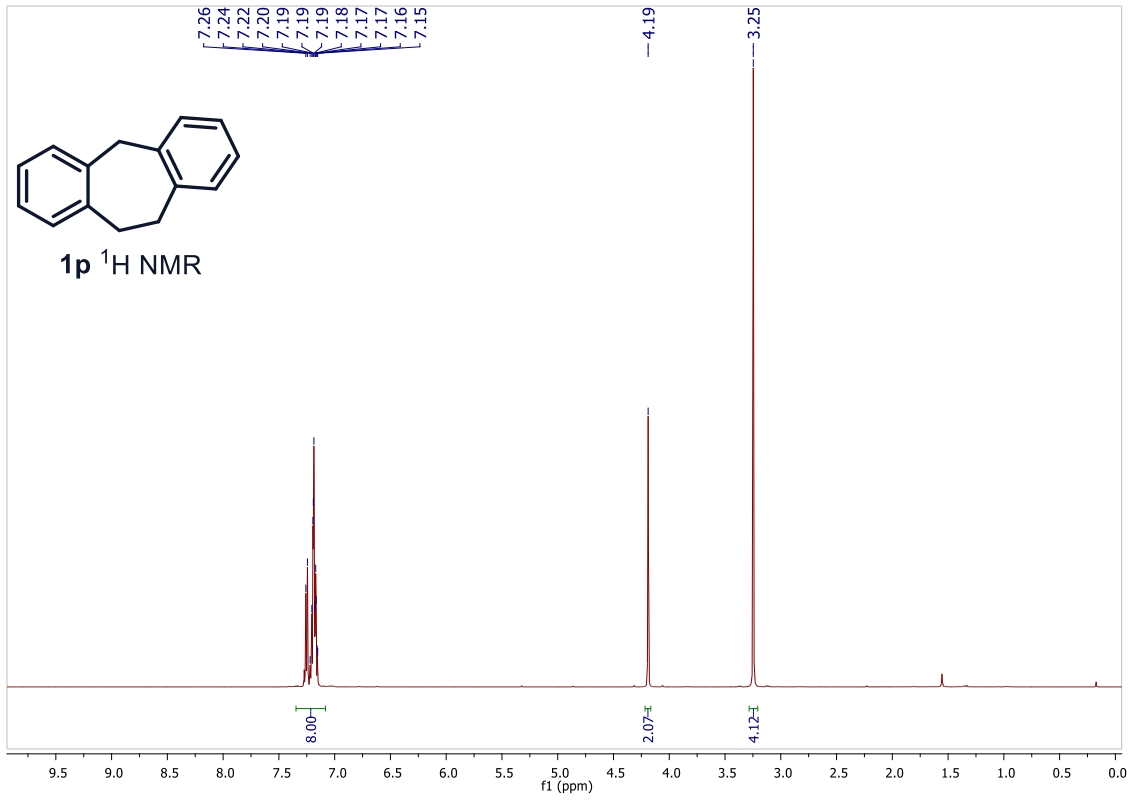


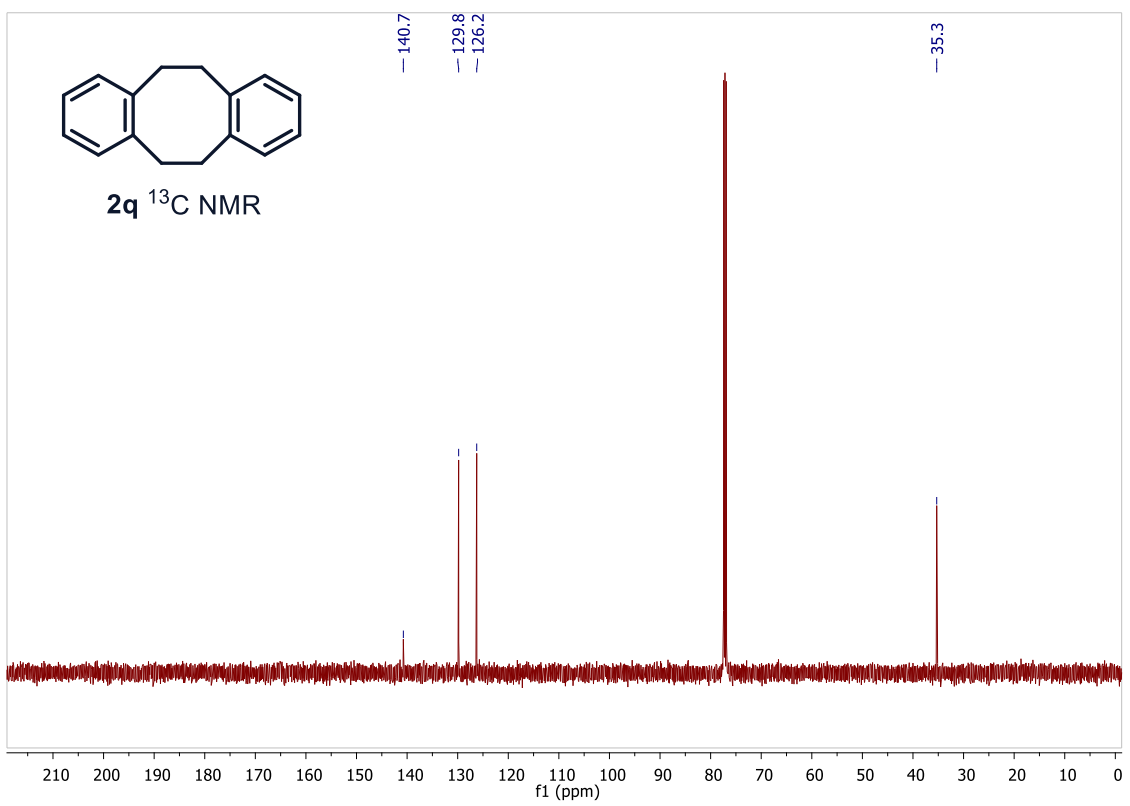
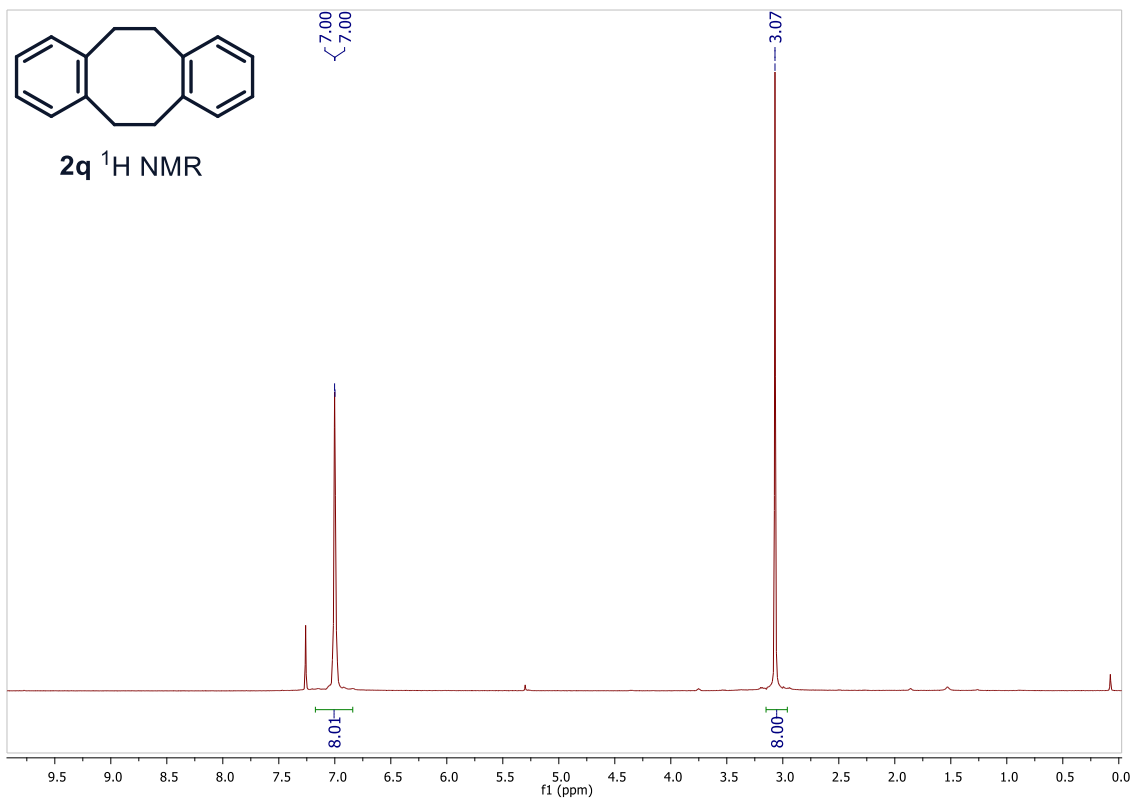


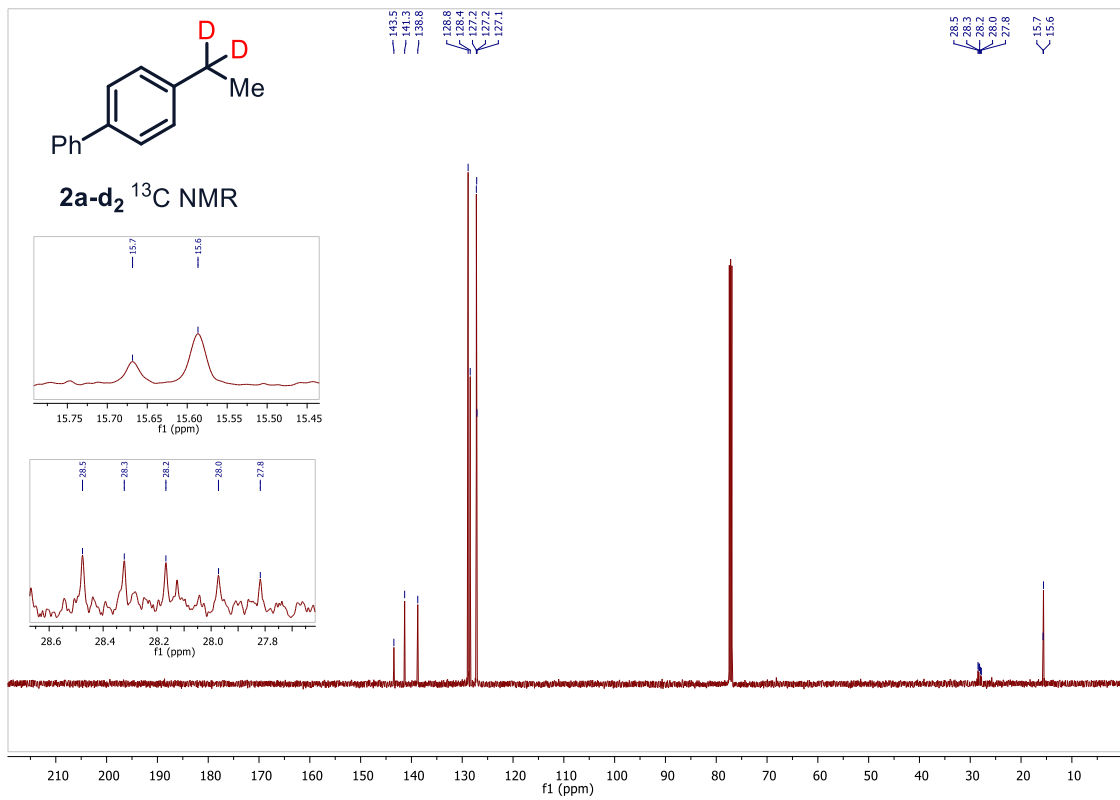
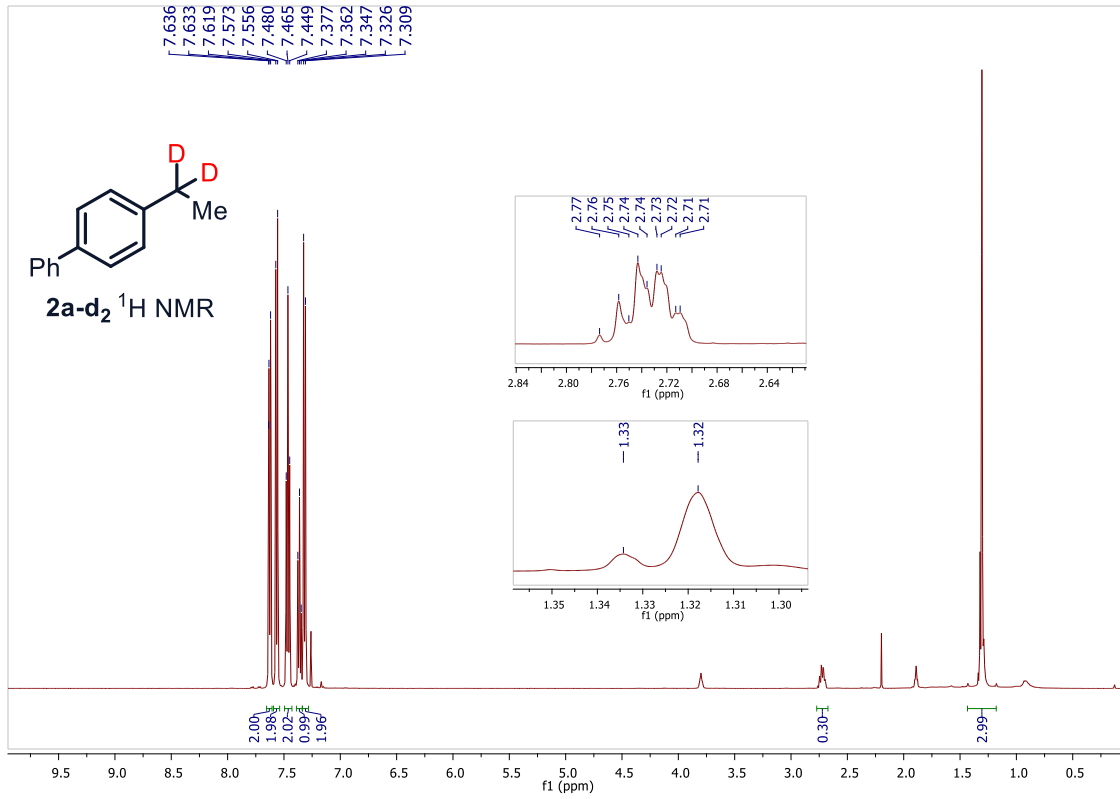


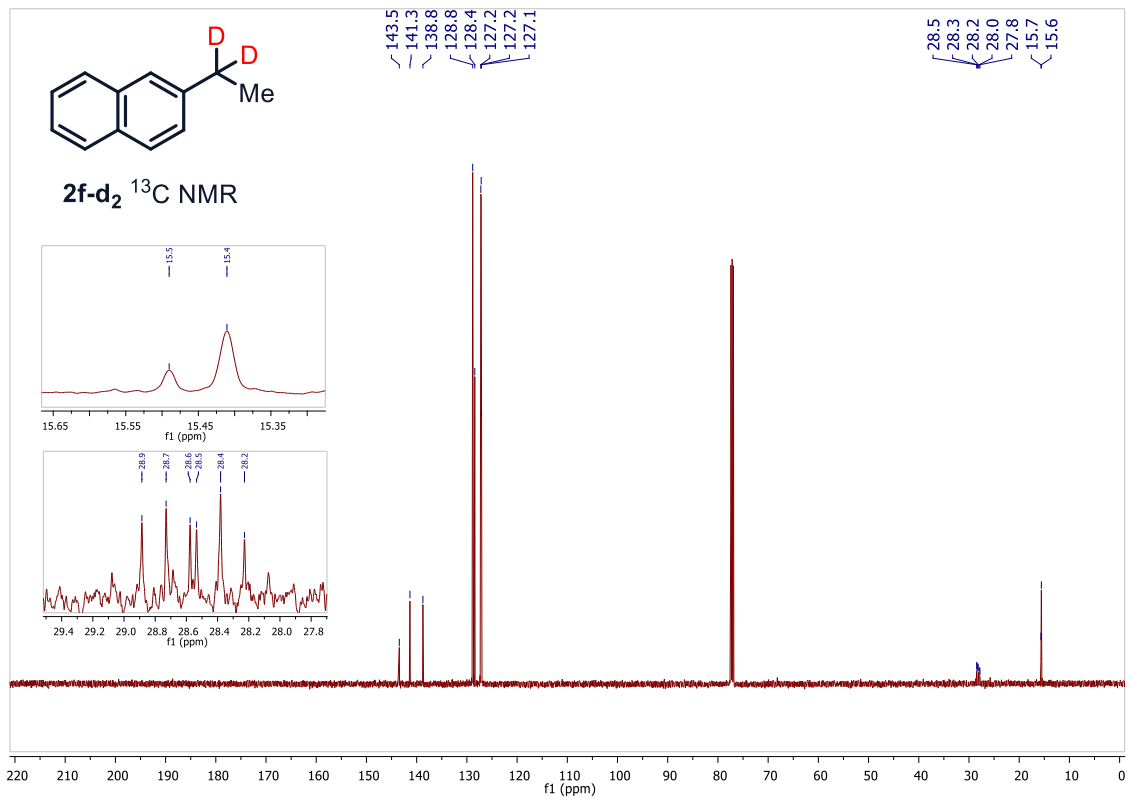
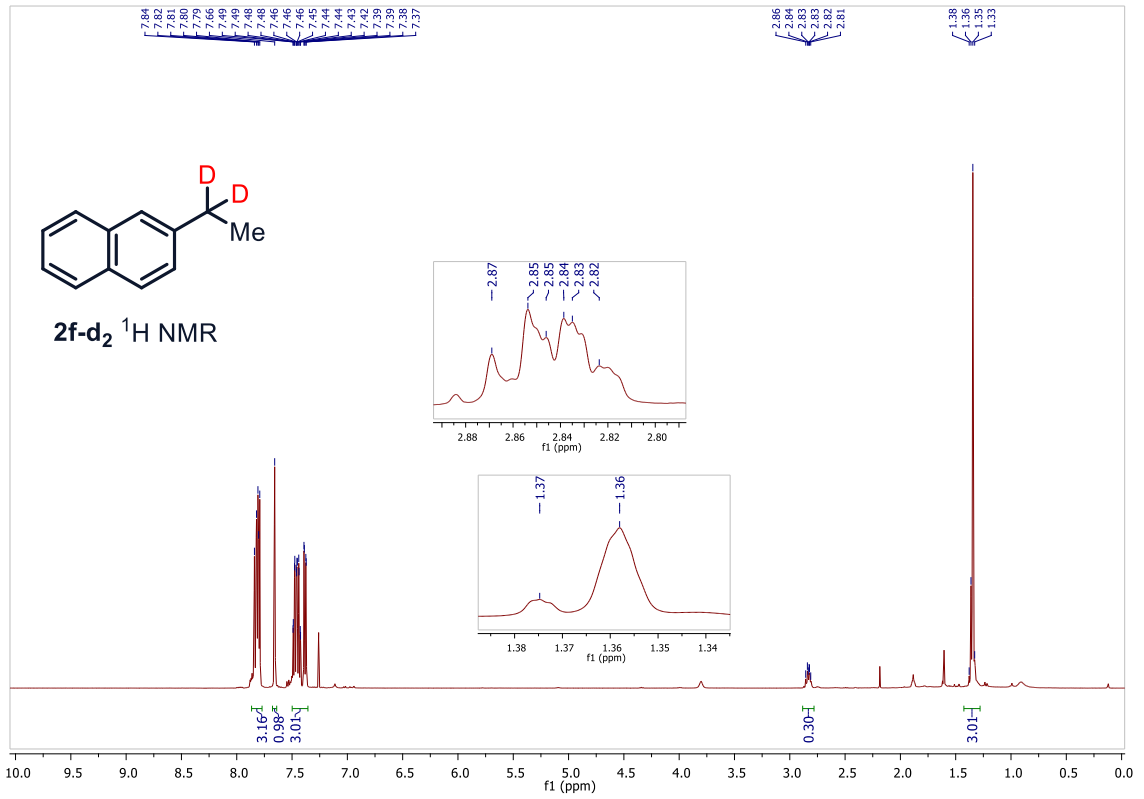


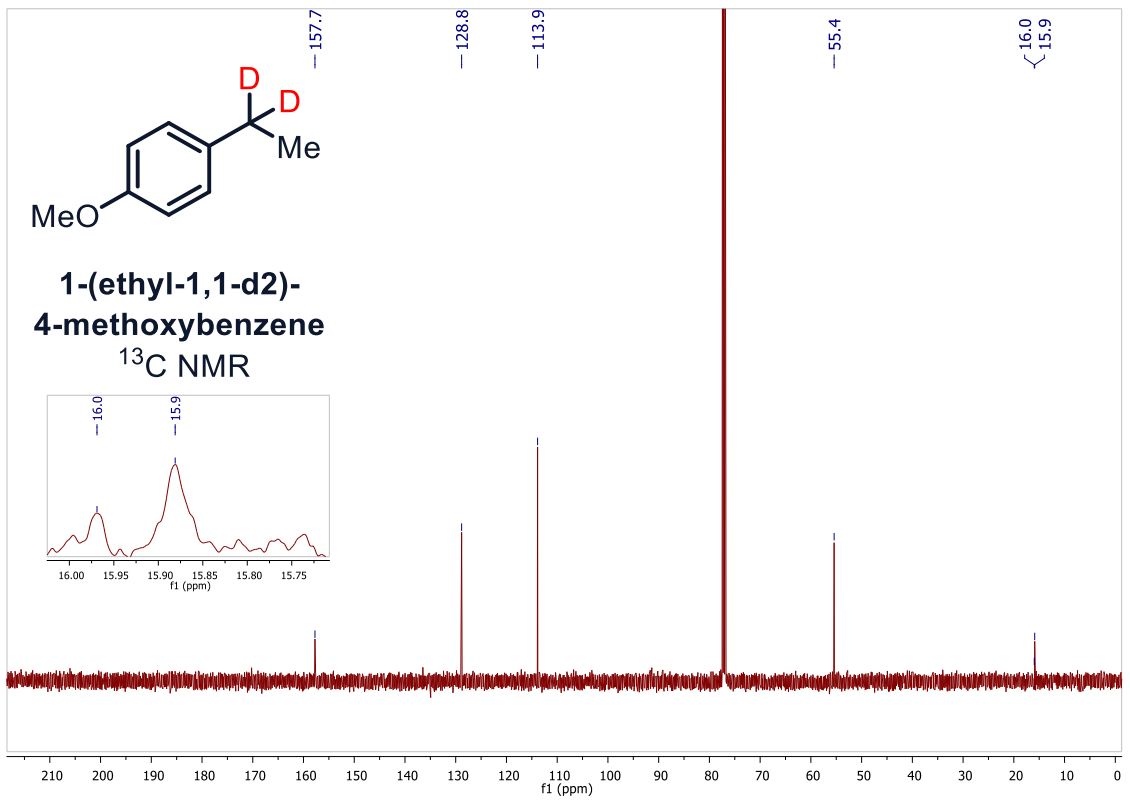
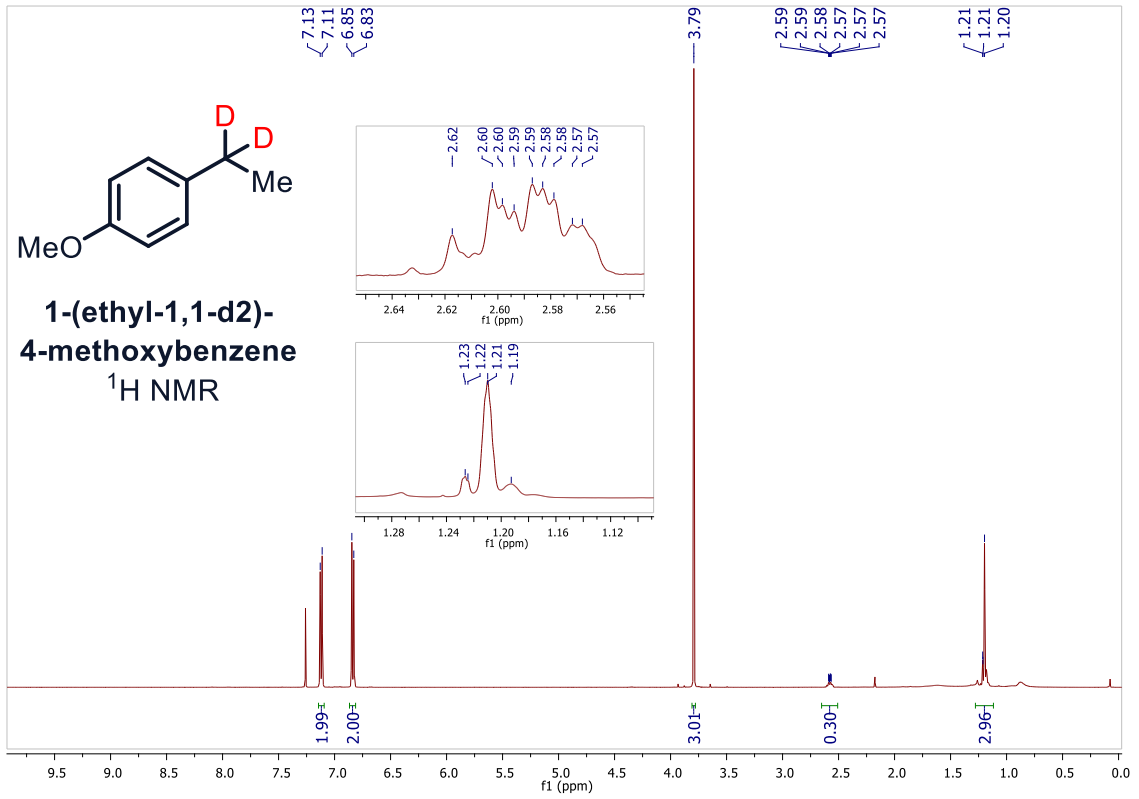












Chapter 2 - Synthesis and characterization of anthracene and pyrene containing DBCOD compounds

Abstract

3 novel compounds based on the DBCOD scaffold for use as functional material are described. These compounds contained pendant polyaromatic hydrocarbons fluorophores and showed promise for reversible excimer formation based on solvent polarity and potentially temperature. Results indicate in a pyrene containing (1-PyreneAmide) compound an excimer emission is unavoidable under all temperature ranges and solvent conditions tested. However, when anthracene in the 2-position (2-AnthraAmide) is substituted an excimer emission ascribable to ‘end-to-end’ overlap is observed in solution and shows dependence to the solvent polarity. Additionally, intriguing solvatochromism is observed in 1-AnthraAmide. To my knowledge, this is the first example a dynamic scaffold exhibiting both a monomer and excimer emission from one compound based on a dynamic scaffold. Initial results will be shown collected on compound 1-AnthraAmide.

Introduction to DBCOD based materials.

Designing stimuli responsive materials has received significant attention in material and chemical science. Molecular design to achieve a shape changing molecule opens the door to the design of many functional materials. In the present case, dibenzo[a]cyclooctadiene (DBCOD) is known to adopt two conformers, boat and chair.¹ The conformational flexibility of the 8-membered ring moiety is shown below in Figure 2.1.

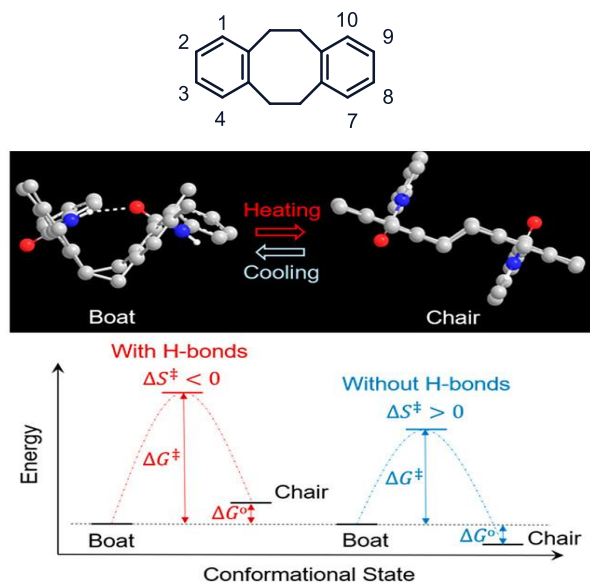


Figure 2.1. Top : Chemical structure of a DBCOD Unit and Possible Substitution Positions (1–10) Bottom: Energy vs. Conformational state diagram of boat to chair conformational change.

This structure has been exploited to drive low energy conformational changes in compounds containing carefully tailored substituents in the 1 and 10 -positions in which an intramolecular hydrogen bond stabilizes the otherwise less stable Boat. These systems can be examined using variable temperature ^1H NMR (VT NMR). The coalescence temperature (T_c) is the temperature where the rate of exchange between the Boat and Chair approaches the NMR timescale and a distinct peak broadening occurs. At temperatures above T_c the NMR spectrum appears to blur indicating fast exchange between the two

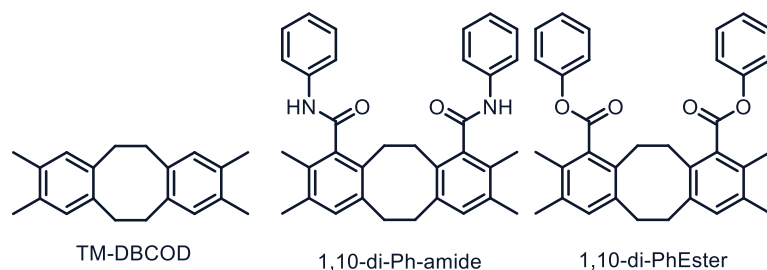


Figure 2.2. Chemical structures of TM-BDCOD (left) 1,10-di-Ph-amide (middle) and 1,10-di-PhEster (right)

conformers. At temperatures below the T_c distinct peaks corresponding to the Boat and Chair conformers arise and quantification is possible through integration of the ^1H NMR spectrum. For example, the unsubstituted TM-DBCOD (**1**) gave a coalescence temperature (T_c) at $-80\text{ }^\circ\text{C}$. In stark contrast, the 1,10-di-Ph-amide exhibited a coalescence temperature at the elevated temperature of $60\text{ }^\circ\text{C}$. Fu and coworkers rationalized this impressive result invoking an intramolecular hydrogen bond $\text{O}=\text{C}-\text{NH}\cdots\text{O}=\text{C}-\text{NH}$ located on the key amide moiety. Ester containing molecule 1,10-di-PhEster was also synthesized, but the chair was overwhelmingly preferred as indicated by T_c of $-35\text{ }^\circ\text{C}$ indicating the ester moiety does little to stabilize the Boat conformer. Very cold temperatures were required to spectroscopically view the Boat conformer in 1,10-di-PhEster. DFT calculations indicated there were repulsive forces between the pendant esters.¹ Solvent polarity was also demonstrated to be an important factor in the conformational dynamics as demonstrated below in Figure 2.3. The inclusion of more nonpolar DCM resulted in the observance of more Boat conformers. This is a result of the strong hydrogen bonding ability of DMSO and its ability to disrupt the intramolecular hydrogen bond. DCM is unable to destabilize the Boat conformer as it is not a hydrogen bond donor or acceptor.

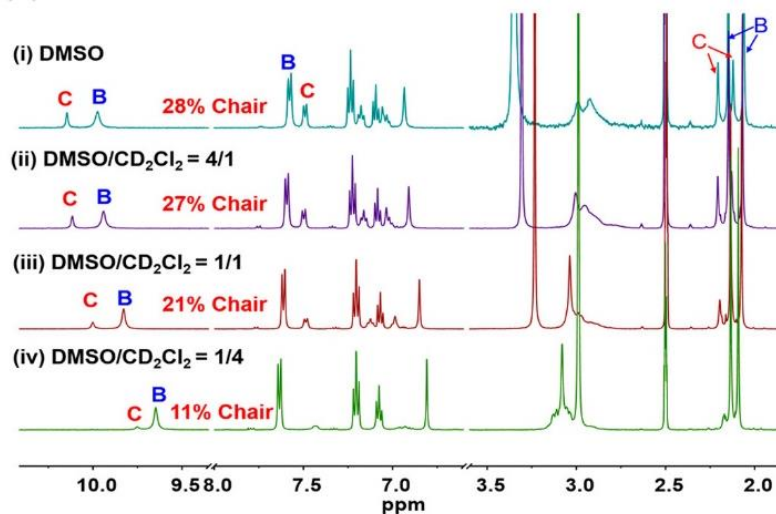


Figure 2.3. ^1H NMR spectra of 2 mg/mL 1,10-di-Ph-amide in different deuterated solvents at 23 °C. B and C denote the Boat and Chair conformations, respectively.

This laid the groundwork for a scaffold in which temperature or solvent polarity can be used to actuate a conformational change in a single molecule. From a molecular engineering standpoint this opens a myriad of possible applications. Herein, I disclose my attempts to design and synthesize a system in which the boat/chair conformation change could be used to reversibly induce the formation of excimers of polyaromatic hydrocarbons such as anthracene and pyrene. The ensuing change from monomer to excimer emission of the pendant fluorophores could serve as a scaffold for a switchable fluorescent material actuated by temperature or solvent polarity. In essence, the color of emission would change as a function of temperature or solvent polarity, as do so reversibly if successful. A schematic of such a design is shown in Figure 2.4. Fluorescence thermometers could be fashioned out of such materials. The structure on the left side of the arrow would, in theory, emit a lower energy wavelength (green light) due to the excimer emission while the chair conformer would emit a higher blue shifted wavelength.

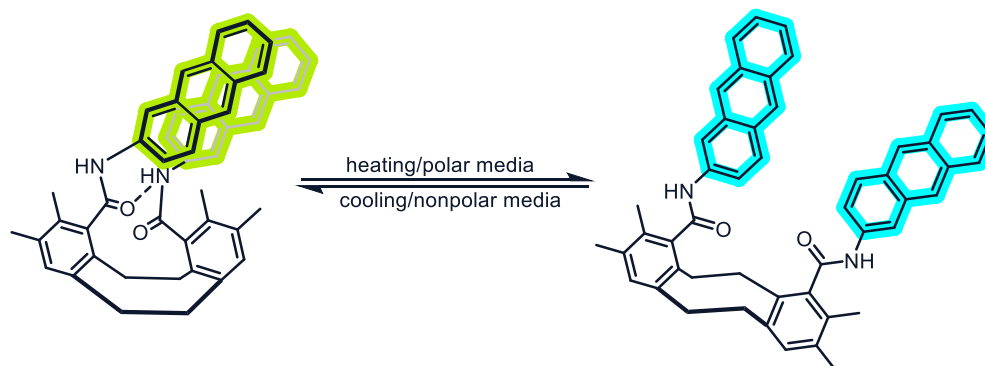


Figure 2.4. Strategy for reversible excimer formation in TM-DBCOD based scaffolds. 2-AnthraAmide is depicted here as the model compound.

Background on excimer formation in pyrene.

The emission spectrum of pyrene in dilute solutions consists of five well-defined peaks at ~375, 379, 385, 385, and 410 nm respectively. Attributed to the $\pi \rightarrow \pi^*$ transitions these well-defined peaks are generally called monomeric emission.² Monomeric emission is defined as a single noninteracting pyrene emission. The same concept applies to anthracene (**An**), which also exhibits well defined peaks in monomer emission. An excimer is a photophysical process in which an excited state of a single molecule interacts with a ground state of the same molecule and the resulting complex has a smaller HOMO-LUMO band gap. The emission of an excimer is structureless red shift band compared to monomer emission and in classic cases unmistakable from the monomer emission. The general MO diagram formation of an excimer is shown in Figure 2.5 (top). When two pyrene molecules are within ~10 Å an excimer will occur. This concept is widely used in labeling biological molecules to determine. Figure 2.5 (bottom) gives an example of a series of spectra exhibiting both the monomer and excimer emissions, which is highly dependent on the concentration of pyrene. When this spatial interaction occurs an excimer emission

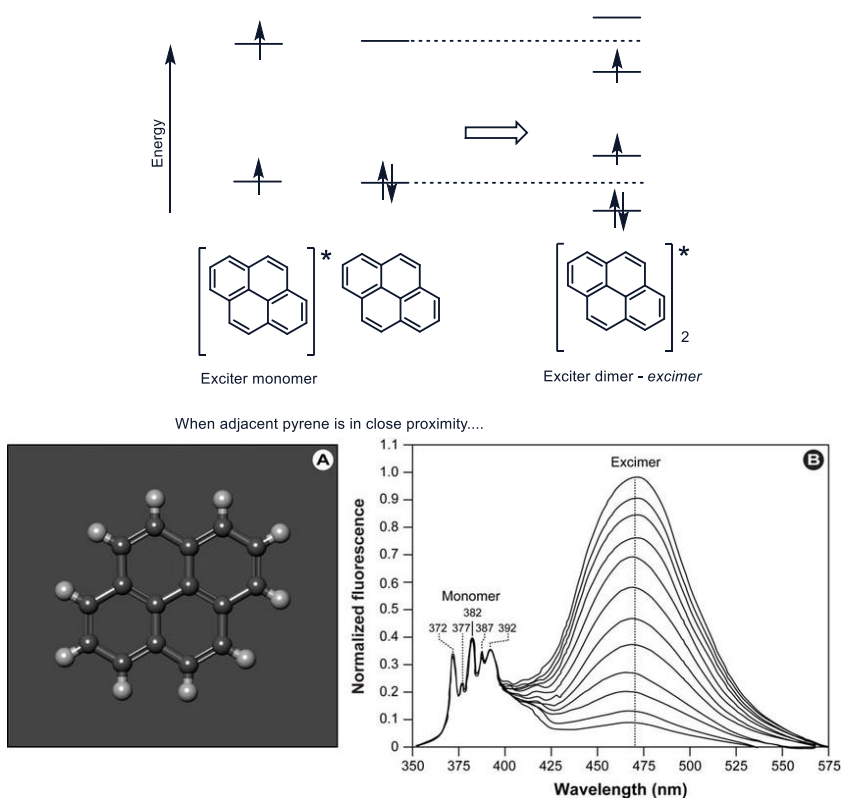


Figure 2.5. Top - Simplified orbital description of excimer formation in pyrene. Bottom - Example spectra showing both the emissions of monomer and excimer.

ranging from 425-550 nm is exhibited as a broad structureless peak. With increasing concentration, the excimer peak increases accordingly.³ In pyrene, the excimer was studied extensively in the 1960's by Birks. In solution, when the concentration of pyrene exceeds

0.1 mM a large peak centered at 482 nm is observed in the emission spectrum, attributable to the excimer. Pyrene is well known in the field of biochemistry for its unique spectral features that allow investigation of protein structure and conformation.^{2,4}

Background of anthracene excimer in solution

The emission spectrum of monomeric anthracene is like that of pyrene and exhibits distinct monomeric peaks, as shown in Figure 2.6 labeled AN in bulk. The excimer of anthracene is well characterized and studied in the solid state. Nominally a distance of 3.4 Å is required for the excimer of anthracene to form. However, the excimer of anthracene (AN) in solution is much less understood and the topic of recent investigation.⁵ The known photodimerization (Figure 2.7) of AN to dianthracene (diAn) is known to erode the photophysical properties of AN adding a difficult problem to overcome in the development of fluorescent AN containing material. Prevention of this dimerization is paramount, as diAn doesn't exhibit fluorescence. To this end, Das and co-workers envisioned a system where a host guest interaction between octaacid and anthracene allowed for preorganization. Octa acid served as a cage in which two anthracenes could be pre-organized with the required π - π overlap to observe excimer formation. Additionally, enclosure in the host octa acid prevented the deleterious photodimerization. This to my knowledge is the only definitive example of an anthracene excimer forming in solution and observation of the associated emission.

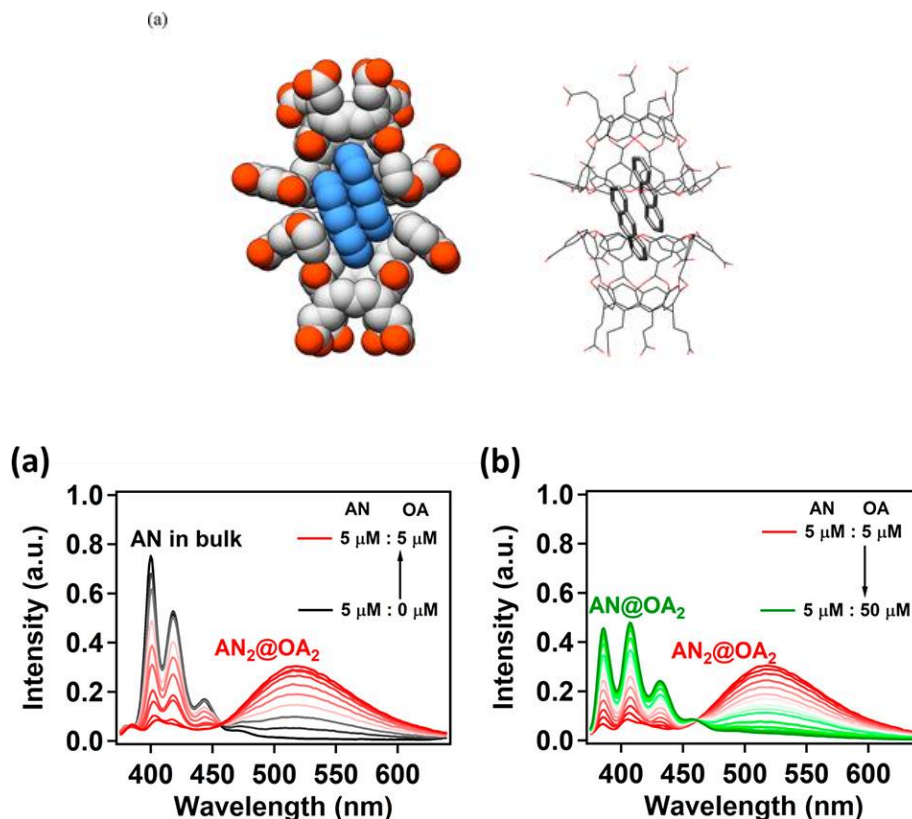


Figure 2.6. Top: Skeletal representation of octaacid and anthracene host guest interaction giving rise to excimer emissions. Bottom: emission of anthracene as a function of octaacid concentration showing increase in redshifted band attributed to excimer.

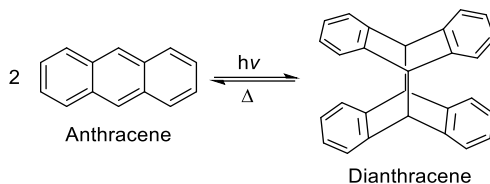


Figure 2.7. Photodimerization of anthracene to dianthracene and thermally reversibility of dimerization

A growing body of literature has investigated compounds like di-anthracene benzene (**DAB**) and similar derivatives. In stark contrast to the pyrene excimer, extremely limited work investigating the nature of the anthracene excimer in solution has been done, due to the intrinsic difficulties associated.

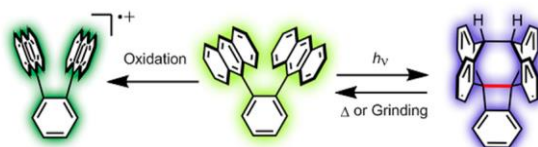


Figure 2.8. Oxidation and photoisomerization of DAB

Anthracene is known to exhibit many different types of excimer emission depending on the degree of overlap between the π - π planes. A pure unsubstituted anthracene will emit around 530 nm but this emission will change dramatically depending on the system and extent of overlap.

Synthesis of tetramethyldibenzocyclooctadiene (TM-DBCOD) scaffold

The synthetic pathway for the synthesis of TM-DBCOD is given below in Figure 2.9. A Diels Alder cycloaddition between 2,3-dimethylbutadiene and methylacetylene dicarboxylate gave the adduct in quantitative yield and subsequent dehydrogenation gave 1,2,4,5 substituted arene that could be reduced using LiAlH_4 to the diol. Subjection of the diol to an equivalent of PBr_3 quantitatively yielded dibenzylbromo-orthoxylylene. Sonication for 3 days in dry THF with excess of lithium metal ribbon yielded the key tetramethyl dibenzocyclooctadiene (TM-DBCOD). This step was far and away the lowest yield with an average of 15% of the desired product. Although TM-BDCOD could be isolated, though painstakingly difficult column chromatography, this was found unnecessary, and the crude mixture could be carried through. The subsequent Reich formylation with TiCl_4 and α,α -dichloromethyl methyl in DCM yielded formylated products and fortunately the desired 1,10-diCHO could be isolated relatively easily from the other products. After isolation of the desired 1,10-diCHO, a Pinnick oxidation affords the di CO_2H in a good yield of around 70%. Next, reflux of the di CO_2H in SOCl_2 until a clear solution is observed and subsequent distillation of excess SOCl_2 afforded the acyl chloride. Suspension of appropriate solvent

and addition of amine with excess freshly distilled TEA would afford the final products. For detailed synthetic procedure see below. All steps preceding the synthesis of the final compounds have been described in literature.^{1,4}

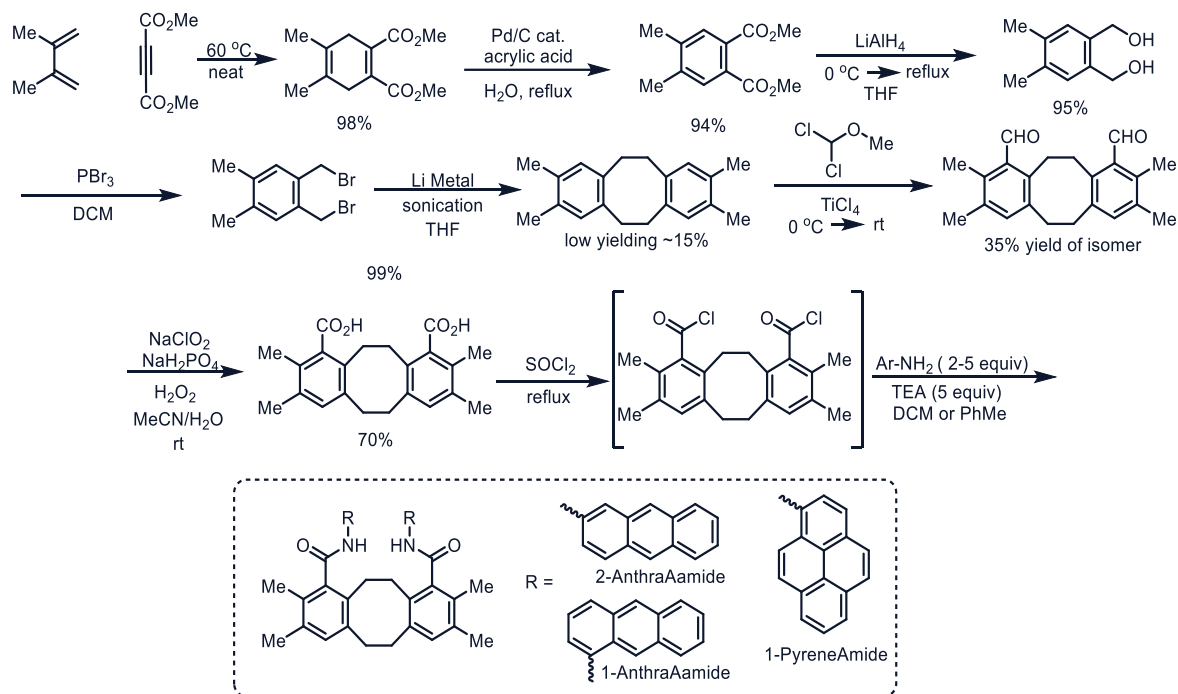


Figure 2.9. Synthetic Scheme for the synthesis of DBCOD based compounds appended with pyrene or anthracene.

Fortunately, the 2-aminoanthracene is available commercially but the 1-aminopyrene must be prepared through a nitration-hydrogenation, which is described in the literature.⁹ The synthesis of 9-aminoanthracene was attempted but rapid oxidation thwarted its use in this chemistry. Note that 1,10 substitution on the TM-DBCOD scaffold is assumed in the naming convention of these compounds thus they are named based on the position of the amine on the pyrene or anthracene as denoted on Figure 2.9 in the boxed final structures.

Synthesis of 1-PryeneAmide

As discussed above, pyrene is the most well studied excimer former, thus made sense to incorporate into this system. Below is the characterization of the titular compound.

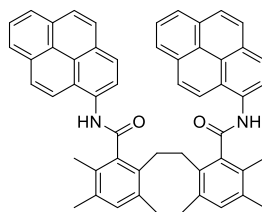


Figure 2.10 Skeletal structure of 1-PyreneAmide

164 mg of diCO₂H (0.514 mmol) was refluxed in 10 ml of SOCl₂ overnight under air resulting in a clear solution. The excess SOCl₂ was removed under vacuum distillation resulting in a grey/brown powder. The resulting acyl chloride was immediately protected under N₂ and immersed in an ice-water bath. 10 ml of dry DCM was added to the flask and vigorously stirred resulting in a cloudy solution. 444 mg (2.05 mmol, 4 equivalents) of 1-aminopyrene and 0.207 ml (2.05 mmol, 4 equivalents) of freshly distilled triethylamine dissolved in 10 ml of dry DCM were added drop wise under the protection of N₂. Upon full addition the ice water bath was removed, and the solution was allowed to warm to room temperature. Solvent was then removed by rotary evaporation and ~30 ml of distilled water was added, and the resulting suspension collected through vacuum filtration. This step removed the TEA-HCl from the crude product. Drying under vacuum and assessment of the resulting powder dissolved in DCM by thin layer chromatography showed 2 products with pure DCM as the eluent when viewed under irradiation at 365nm (longwave) with the suspected product appearing green on the TLC plate with an rf of ~0.05 in pure DCM. The other compound present (rf = 0.6 in pure DCM) appeared blue under irradiation at 365 nm. The bottom spot was isolated using column chromatography and a solvent system of DCM -> 10% MeOH:DCM once the top spot had fully eluted. The product was isolated as an orange powder in 25% yield. Observed Mass 751.329 m/z. Calculated Mass 751.332 m/z. ¹H NMR (500 MHz, CDCl₃) 8.60 (N-H), 8.27, 8.18, 8.11, 8.09, 7.97, 7.88, 7.79, 7.67, 6.87, 3.52, 3.22, 2.28, 2.21.

Results and discussion on 1-PyreneAsmide

Upon synthesis and spectroscopic verification of 1-PyreneAmide the temperature dependance of this compound was examined and results discussed below.

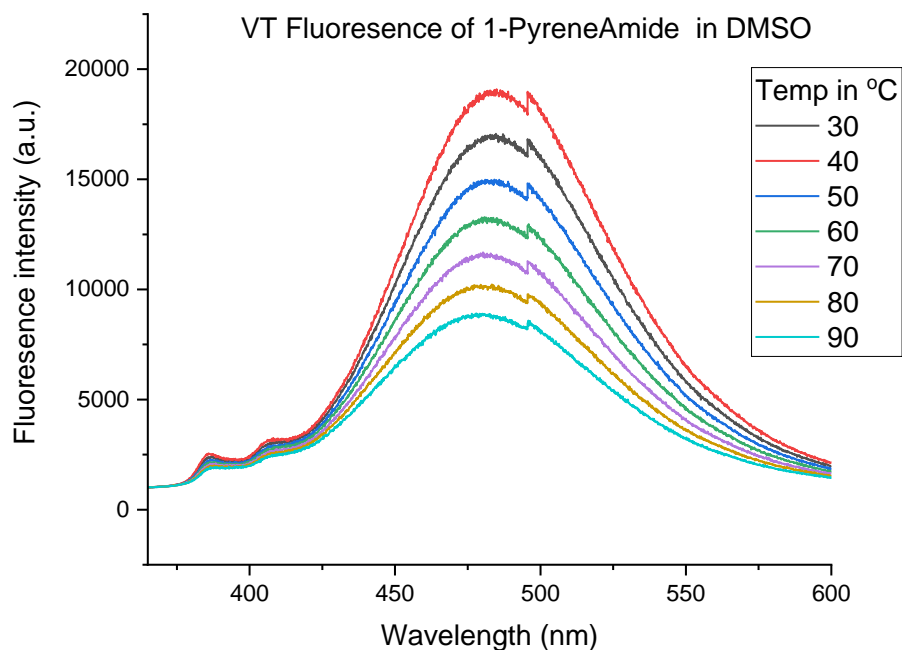


Figure 2.11. Variable temperature fluorescence of 1- PyreneAmide in DMSO (10 μ M) and 340 nm excitation 1 mm slit width.

From Figure 2.11 it is clear 1-PyreneAmide did not exhibit the desired dual monomer-excimer emission as a function of temperature. It should be noted the concentration required to observe an excimer is around 0.1 M. The concentration of 1-PyreneAmide is 5 orders of magnitude lower than the required concentration for intermolecular excimer formation, thus the observed emission is presumed to be result of an intramolecular interaction between the pendant pyrenes, and not a bimolecular interacting between two molecules. From the variable temperature ^1H NMR (Figure 2.17) coalescence of the peaks occurs around 60 $^\circ\text{C}$ suggesting fast interconversion between the boat and chair conformation. A similar coalescence temperature was observed in the 1,10 di-PhAmide by Fu and coworkers.¹ The only observed change in fluorescence spectra was a loss in intensity, which is to be expected with increasing temperature. Additional experiments in which ratios of DMF:water from (from 10:0 \rightarrow 0:10) were employed as solvent also only rendered the excimer emission. Additionally, the fluorescence intensity was greatly attenuated with increasing fraction of water indicating aggregation induced quenching could be occurring. Also of note is that in CDCl_3 a clean spectrum could not be acquired despite being chromatographically purified 1-PyreneAmide. This could be due to the lower solubility but was not thoroughly investigated. This compound was not further pursued.

NMR Characterization of 1-PyreneAmide

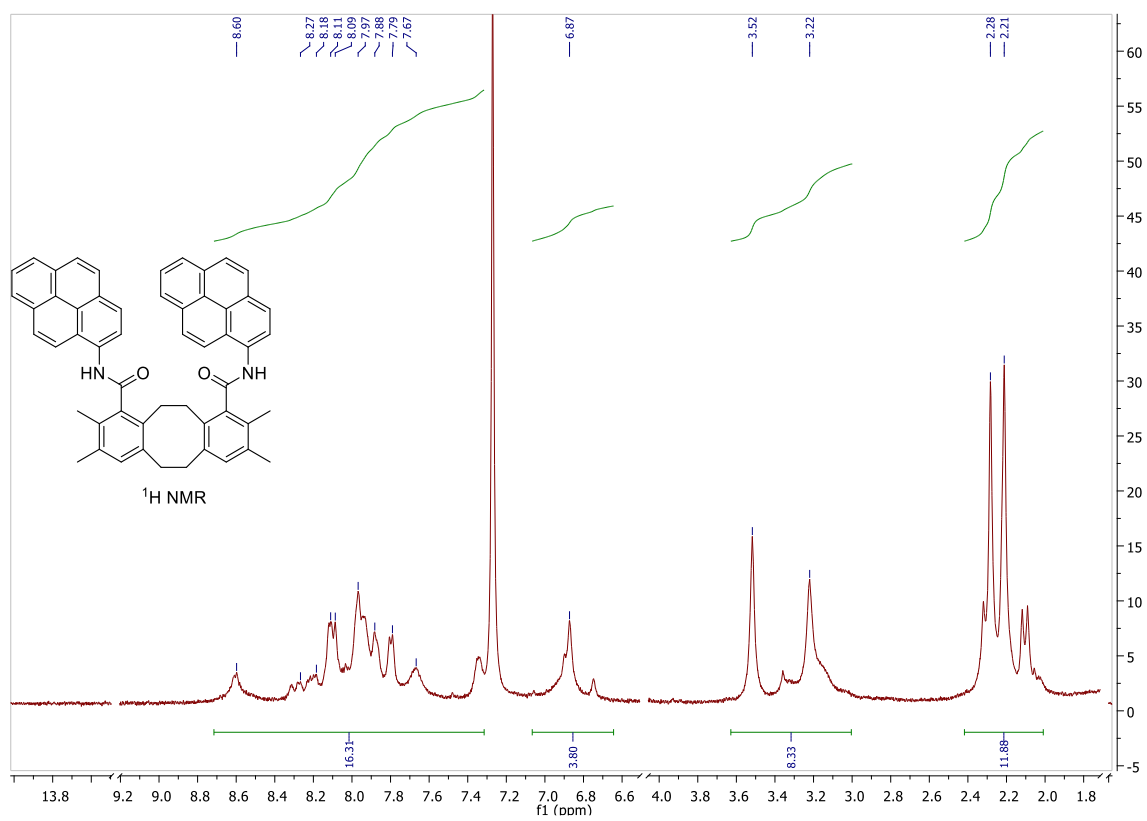


Figure 2.12. ¹H NMR (500 MHz, CDCl₃) spectrum of 1-PyreneAmide

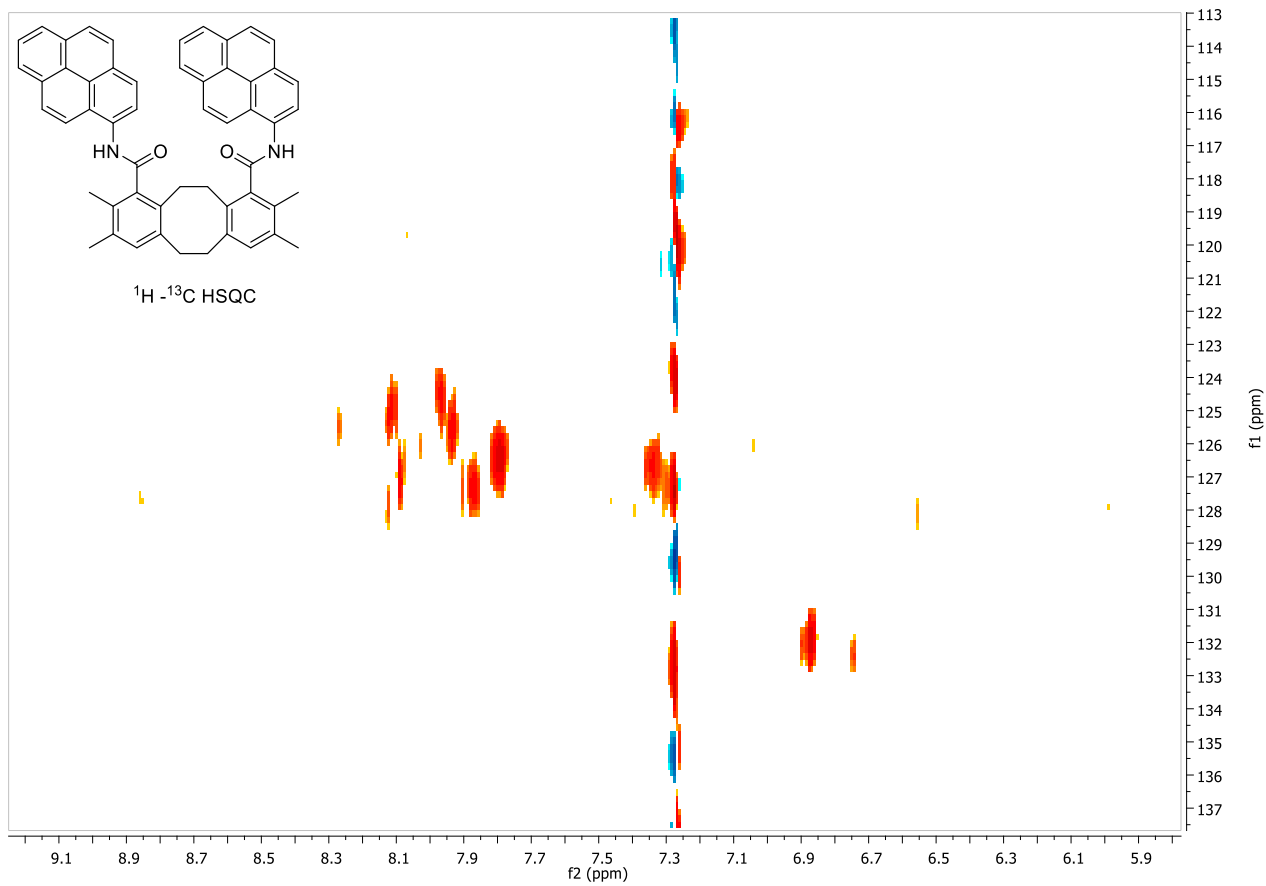


Figure 2.13 $^1\text{H} - ^{13}\text{C}$ HSQC (500 MHz, CDCl_3) of 1,10-PyreneAmide in the aromatic region

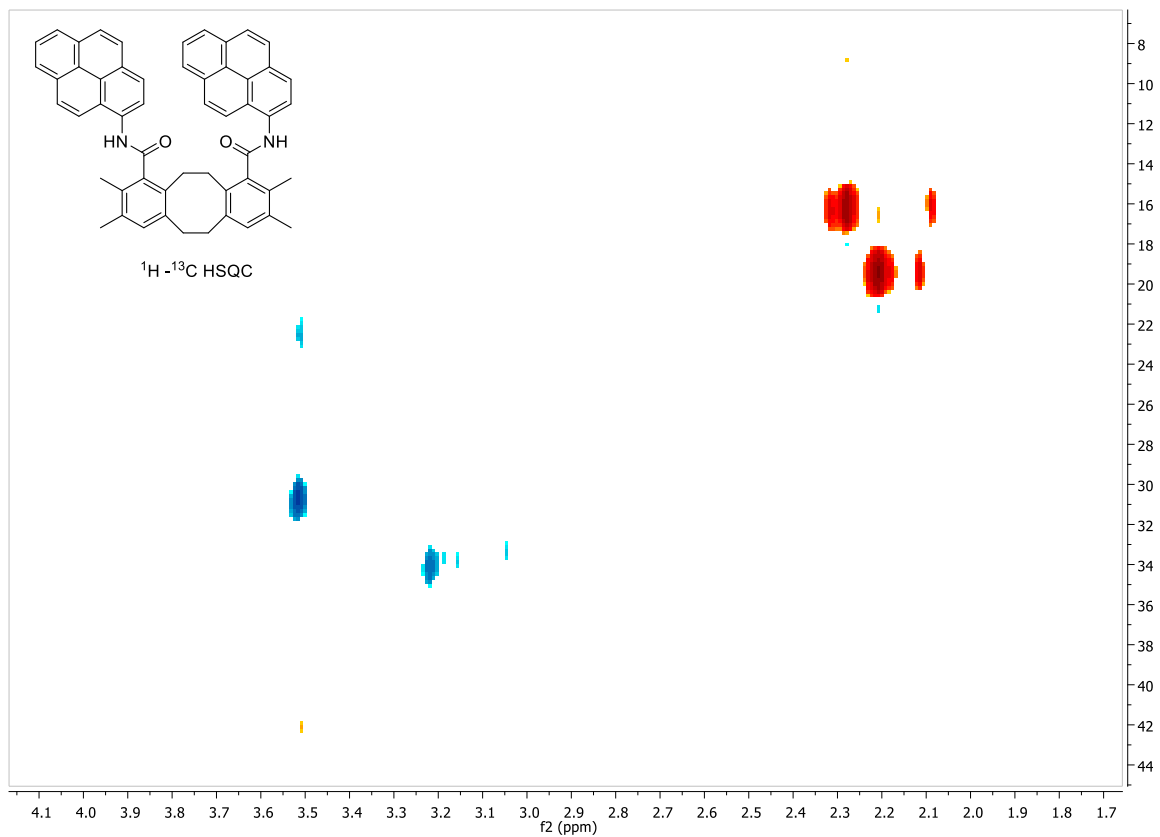
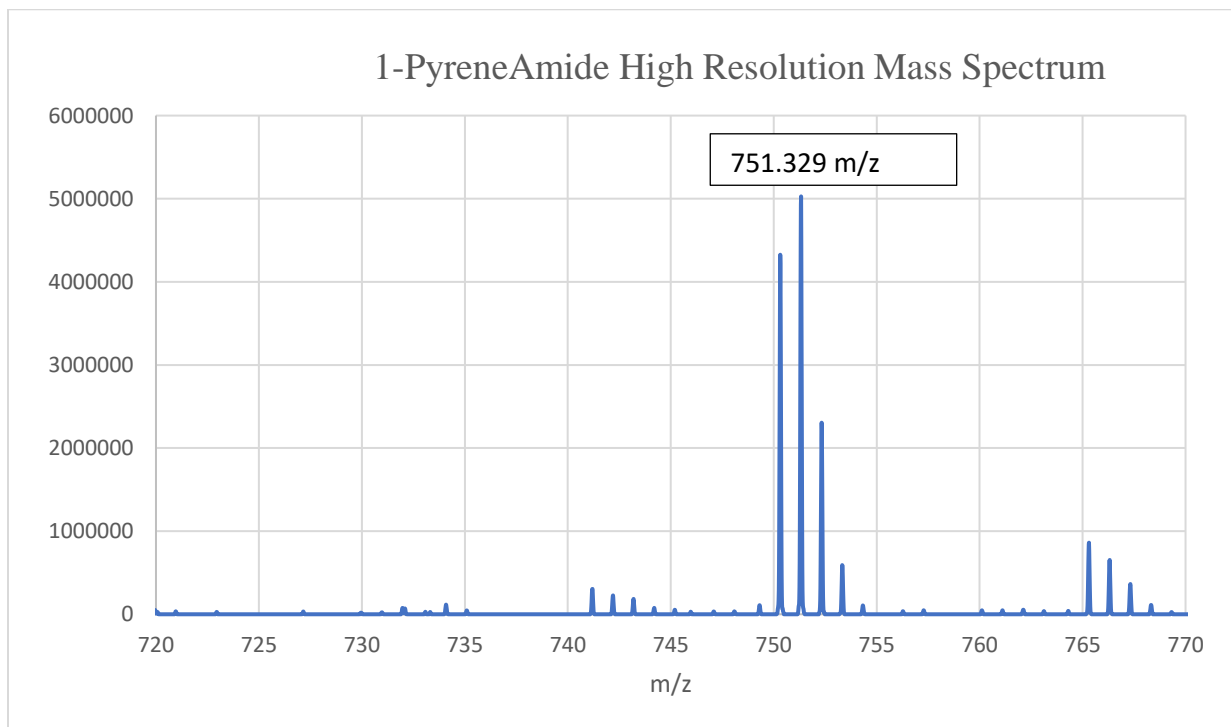
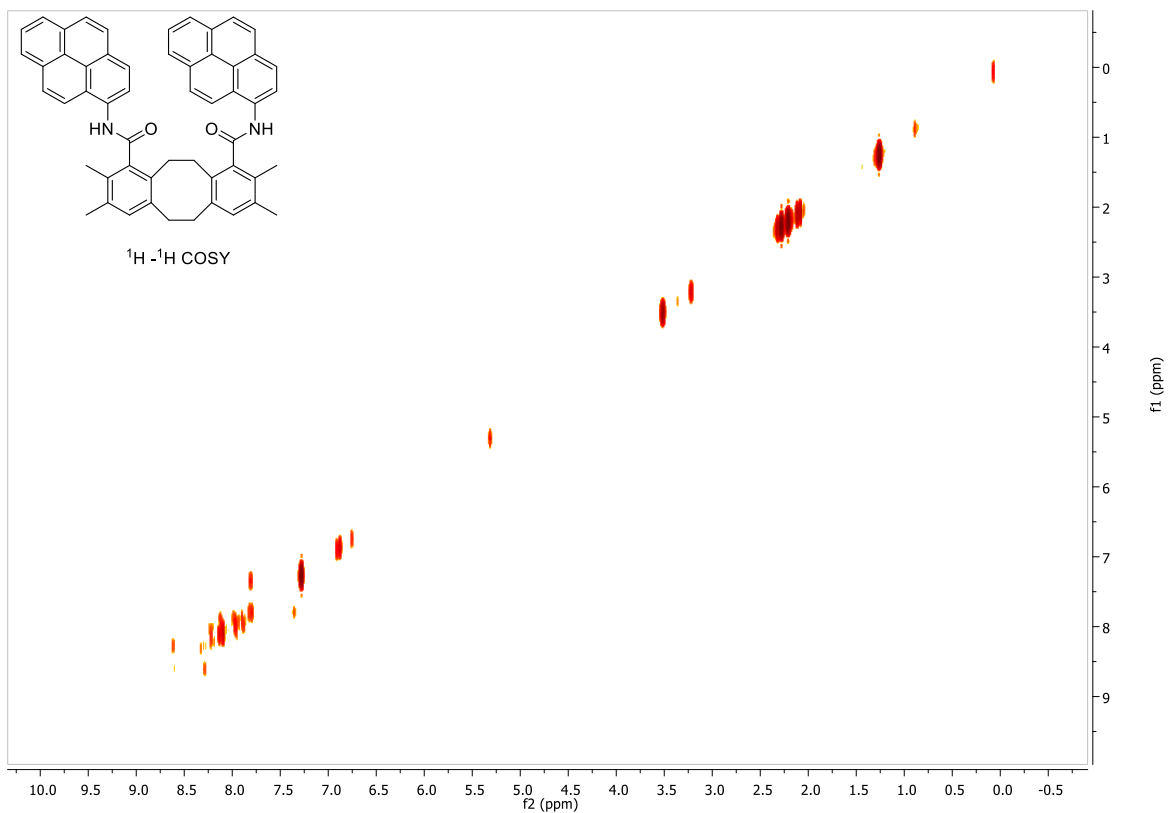


Figure 2.14. $^1\text{H} - ^{13}\text{C}$ HSQC (500 MHz, CDCl_3) of 1-PyreneAmide in the methylene and methyl region



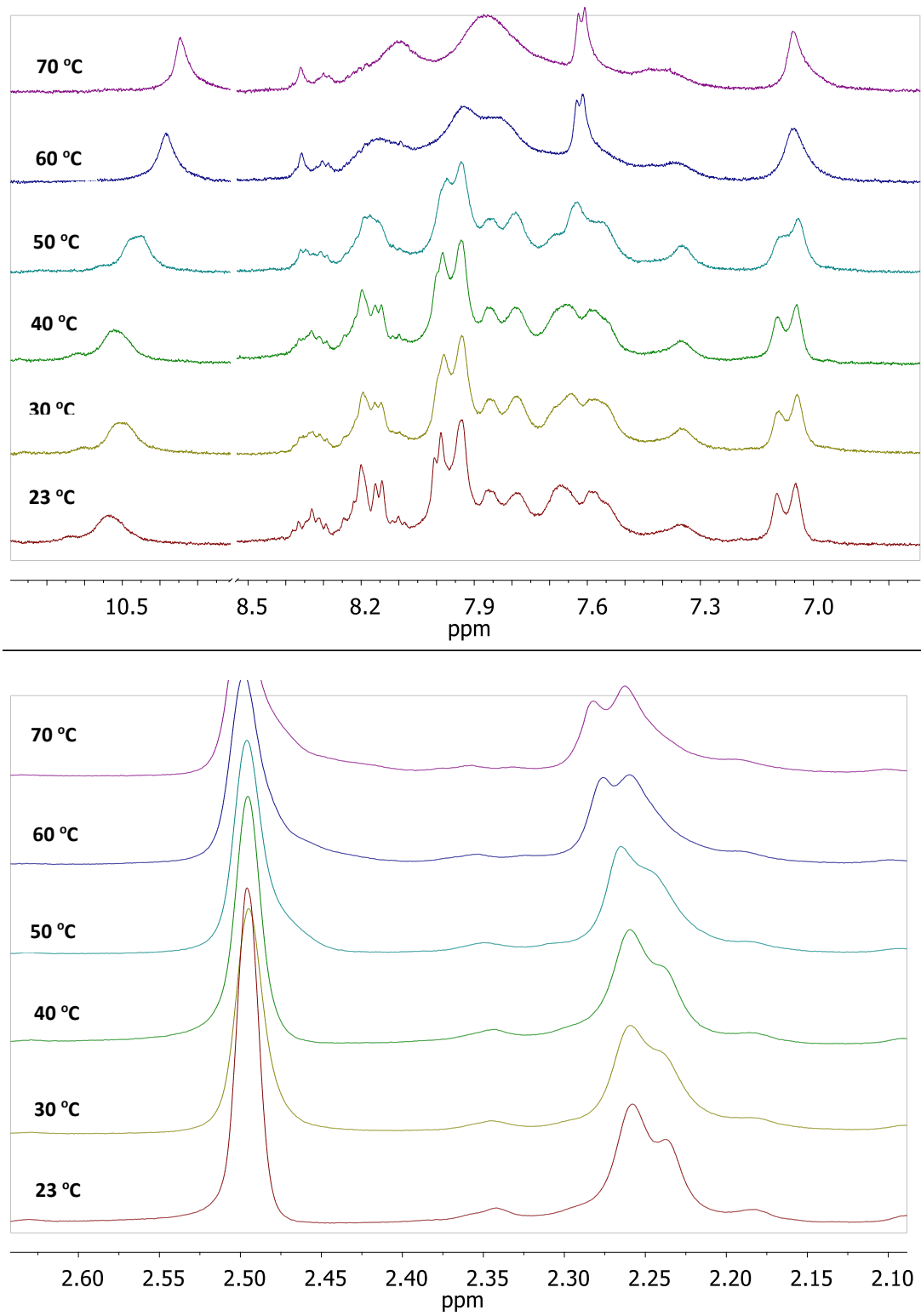


Figure 2.17. Variable temperature ^1H NMR (500 MHz, CDCl_3) of 1-PyreneAmide

After having synthesized 1-PyreneAmide and concluding pyrene was not a suitable fluorophore for this purpose, I directed efforts to synthesize an analogue containing anthracene. Synthesis and purification of this compound was much more difficult than its pyrene counterpart, due to the very low solubility of both the product and starting material 2-aminoanthracene in many common solvents. Extremely dry solvents and freshly distilled TEA are essential for the success of the following procedure.

Synthesis of 2-AnthraAmide

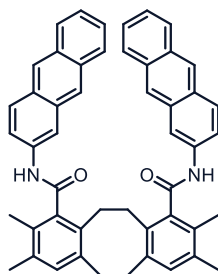


Figure 2.18. Skeletal structure of 2-AnthraAmide

In a 100 ml round bottom flask 172 mg of diCO₂H was refluxed in 10 ml SOCl₂ overnight rendering a transparent solution. The excess SOCl₂ was removed by vacuum distillation and the resulting acyl chloride was protected immediately under an atmosphere of N₂ and suspended in 15 ml of a mixture of DCM : PhMe (1:2) and immersed in an ice bath. of 2-aminoanthracene 235 mg (2.5 equivalents, 0.488 mmol) and 338 μ L (5 equivalents, 246 mg, 0.976 mmol) of freshly distilled triethylamine were mixed with 20 ml of DCM : PhMe (1:2) and added drop wise to the flask. 2-aminoanthracene is not fully soluble and a suspension will form, rinse as thoroughly as possible and be aware clogging of the syringe may occur. Note – TEA freshly distilled from CaH₂ appeared essential for the success of this reaction. After addition the mixture was allowed to warm to room temperature and the solvent removed by rotary evaporation. 20 ml of DCM was added to the flask and the flask sonicated to suspend all the contents. The power was collected by vacuum filtration and continued to be washed until the filtrate was colorless yielding a green powder found to be 2-AnthraAmide. This compound is sparingly soluble in DCM and the washing removes the starting materials and side products while leaving the product. ¹H NMR (500 MHz, DMSO-d₆) δ 10.2, 8.69, 8.55, 8.05, 7.99, 7.85, 7.45, 7.29, 7.11, 7.05, 6.89, 2.28, 2.24. High resolution mass spectroscopy - Calculated: 703.332 m/z. Found : [M+H⁺] 703.328 m/z (see figure 2.19)

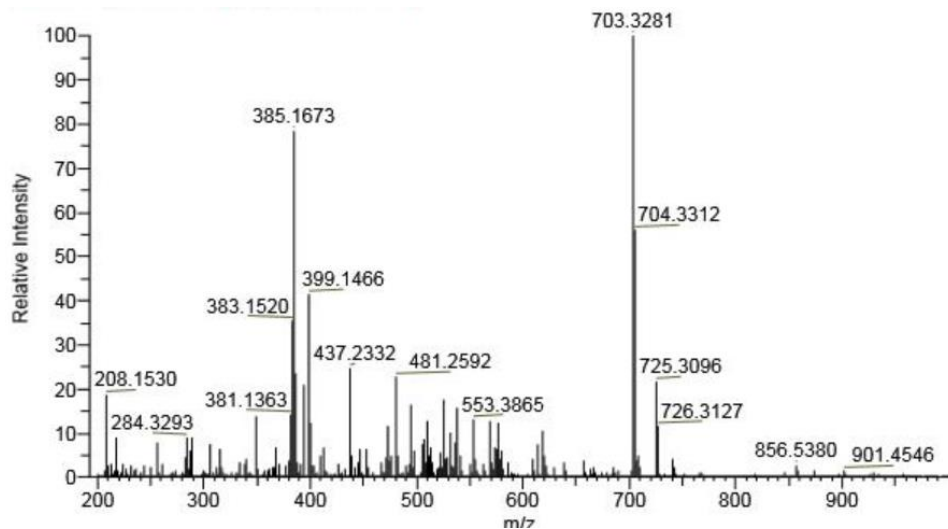


Figure 2.19. High resolution mass spectrum of 2-AnthraAmide confirming the molecular weight as 703.32 g/mol.

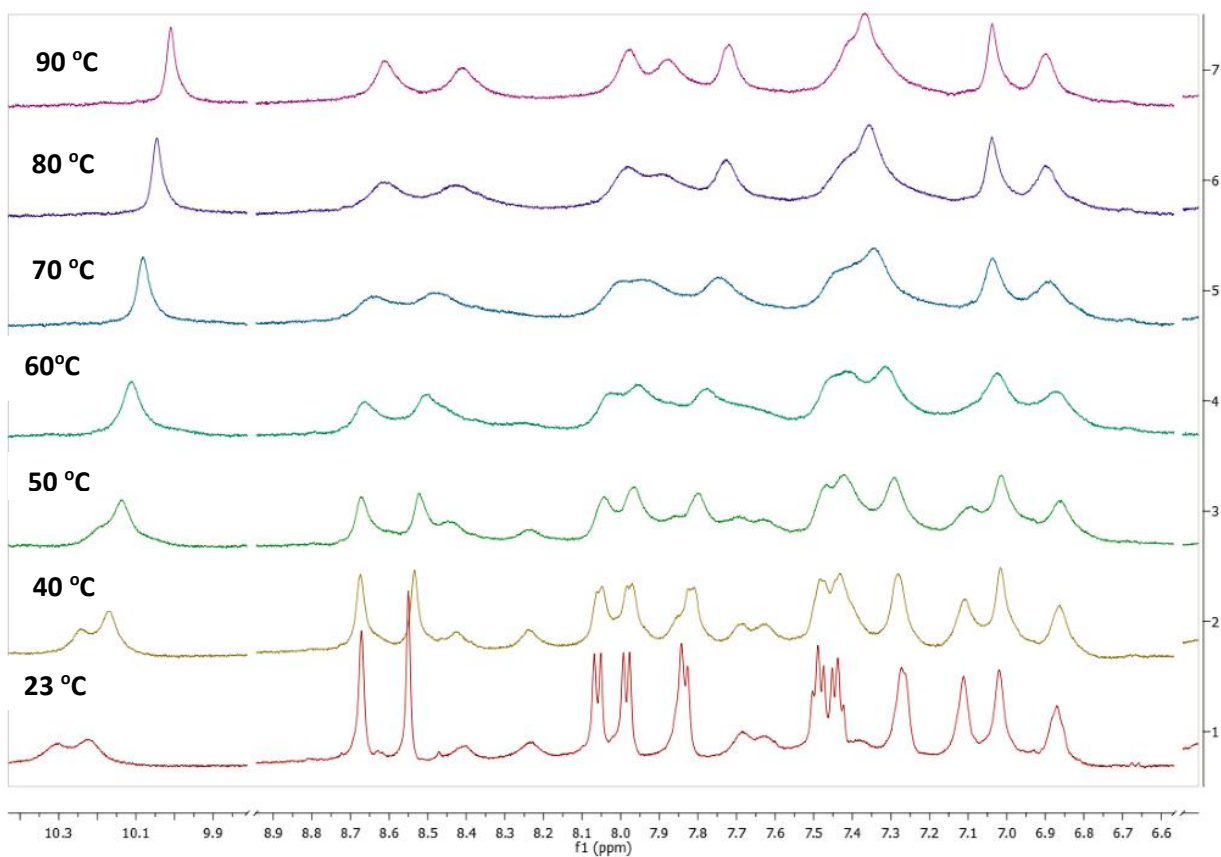


Figure 2.20. VT- ¹H NMR (500 MHz, DMSO-d₆) of aromatic region of 2-AnthraAmide

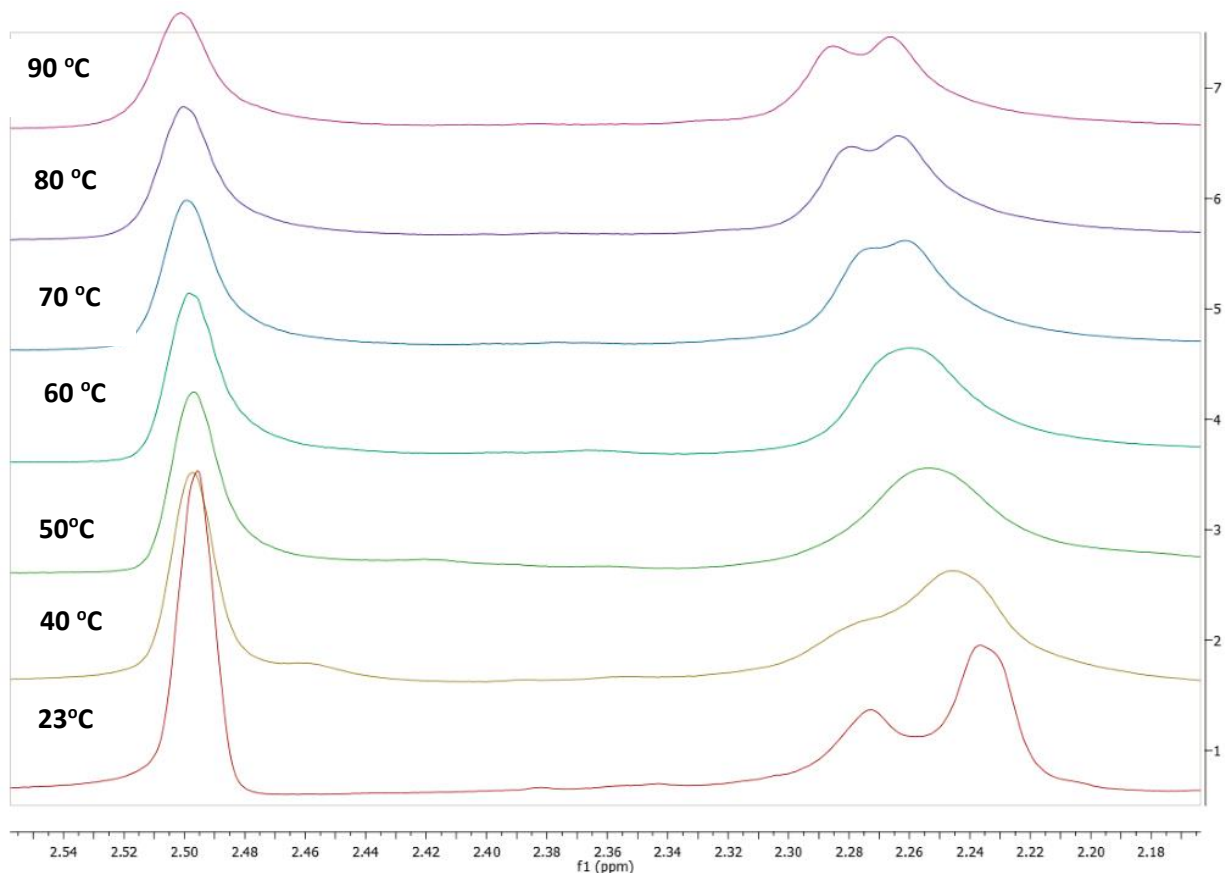


Figure 2.21. VT- ^1H NMR (500 MHz, DMSO- d_6) of methyl region of 2-AnthraAmide

Results and discussion on 2-Anthraamide

Variable temperature NMR revealed coalescence of peaks around 60 °C in DMSO- d_6 . Interestingly 2 sets of peaks ascribable to the boat and chair conformers were not observed in this system. The explanation for this is unknown and precluded assigning ratios of conformers by simple NMR spectroscopy, as in previous work with the phenyl amide. Regardless variable temperature fluorescence was conducted in N-Methyl pyrrolidine (NMP) in 50 μM concentration. 2 distinct features were observed centered around 440 nm and 485 nm respectively with smaller features observed around 410 nm and 520 nm. The ratio of the 2 peaks never changed throughout the course of the variable temperature experiment, with only thermal attenuation of the peaks observed. While disappointingly the desired thermal responsiveness was not observed, it appeared the two major features could be ascribed to 2 different photophysical processes. To this end I decided to examine the effects of differing solvent polarity

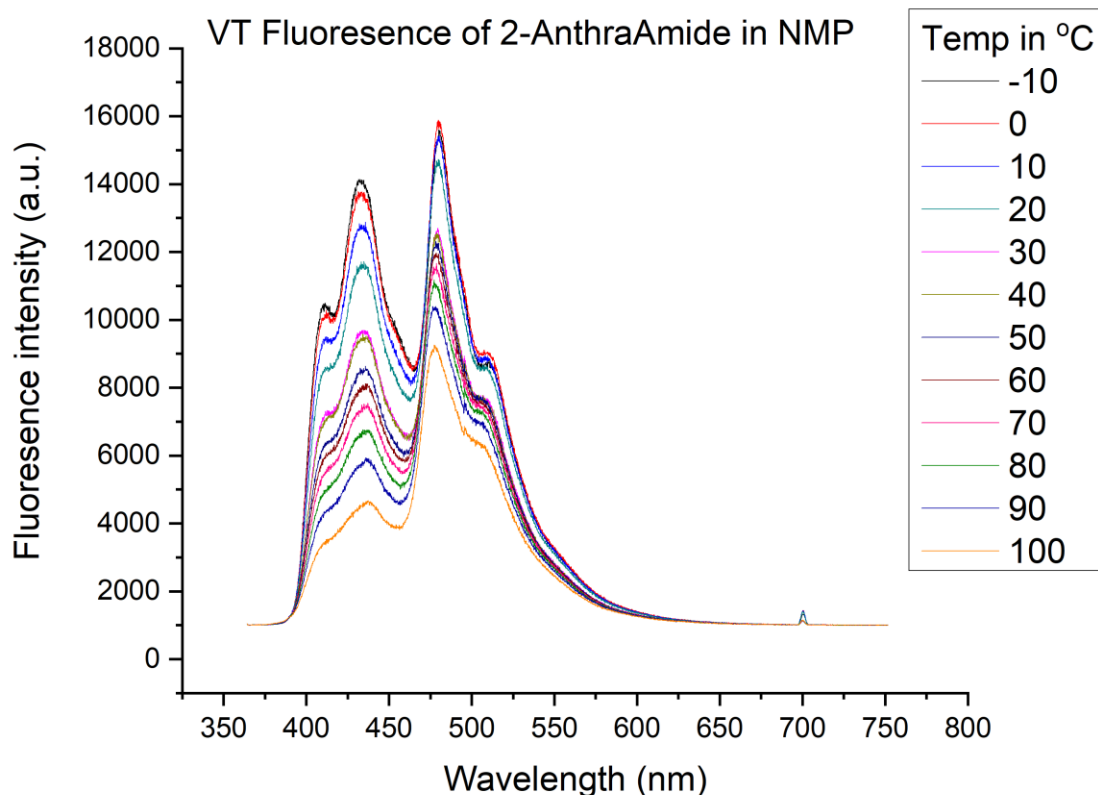


Figure 2.22. Variable temperature (°C) fluorescence spectrum of 2-Anthraamide in N-Methylpyrrolidone (NMP)

Fluorescence in 4 different solvents (Figure 2.23) shows a strong dependence on the polarity on the emission of 2-AnthraAmide. It appears to give rise to 2 different features in all the solvents tested but at drastically different ratios. Structureless monomer emission centered at 445 nm and a structureless peak centered at 480nm which has been described as a twisted & end-overlapped excimer are observed.⁶ Another feature is observed around 500 nm which could be presumably another excimer attributed to a conformation that allows better overlap, thus red shifted emission. In the less polar solvents such as TCE and 1,2, dichlorobenzene (DCB) (dielectric constants 8.42 and 9.33 respectively) the presumed monomer peak is much smaller. In more polar solvents and better hydrogen bond donating/accepting solvents NMP and Dioxane the peak at 450 nm is larger relative to the peak at 480 nm, suggesting the pendant anthracenes are separated as a function of solvent polarity or hydrogen bond/donating capability of the solvent. This trend also contradicts the classic solvatochromism effect which states the more polar a solvent will cause a bathochromic (red shift) in emission.

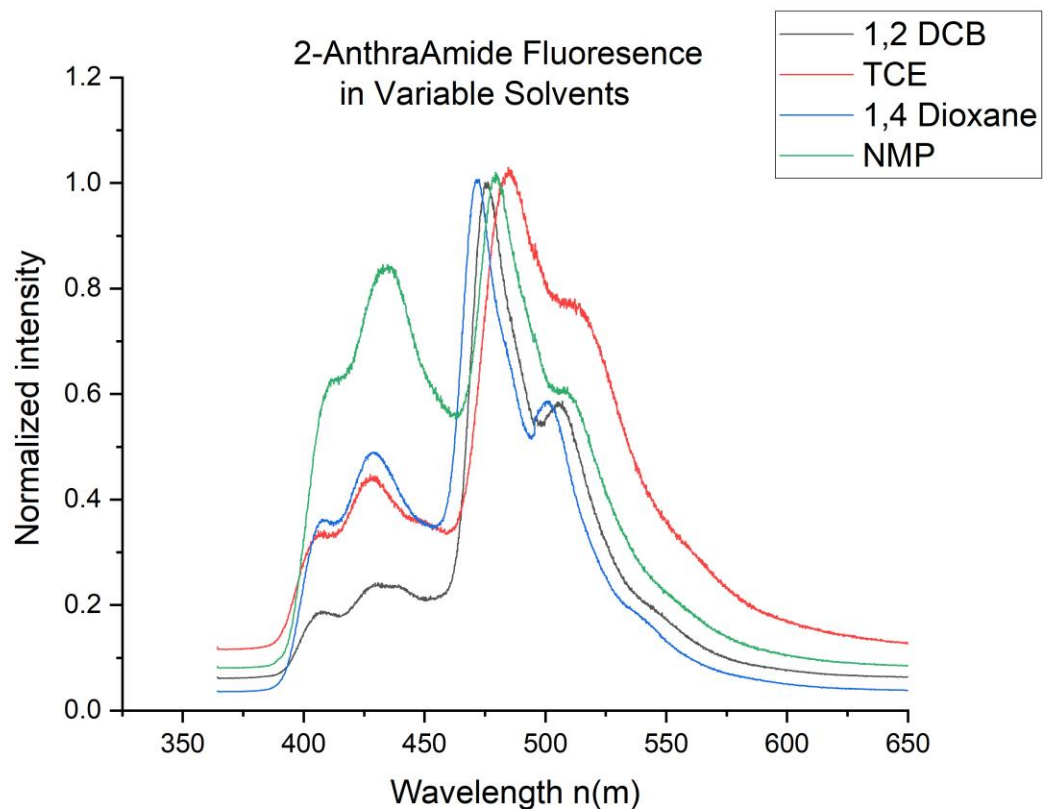


Figure 2.23. Fluorescence spectrum of 2-anthraamide in various solvents. 1 nm slit width and 345 nm excitation.

Next, the possibility of an intramolecular isomerization giving rise to a photoisomer was investigated. One could envision if 2-anthraamide were photoexcited while occupying the Boat state, the [4+4] cycloaddition may occur to give the compound depicted below in Figure 2.25. To this end, I took a freshly prepared sample and took an ^1H NMR spectrum (Figure 2.24 top) of 2-anthraamide and upon irradiation the distinctive brown/green color began to fade. ^1H -NMR analysis after irradiation with a TLC lamp at 365 nm overnight revealed a completely different spectrum. All aromatic peaks were shifted up-field (Figure 2.24, middle). This combined with the fact the color had faded led me to postulate the photo-isomer had been formed, since breaking of the aromaticity on the central ring of anthracene would lead to these observations and spectrum. The [4+4] cycloaddition is reported to be thermally reversible and upon heating of the NMR tube in an oil bath at 160 °C for 48 hours the original spectrum was observed. The thermally reversible nature of an intramolecular [4+4] cycloaddition of anthracene has recently been described in the literature but only been described twice to my knowledge.^{5,8} This would be the first example outside of the Dianthracene benzene family of molecules. Additionally, given the propensity for endoperoxides to form under photoexcitation when oxygen is present this must be considered a possibility. However, since complete reversibility back to the original compound was observed, I do not believe an endoperoxide

or oxygen is playing a role, since an oxygenated compound would result, and reversibility would not be observed.

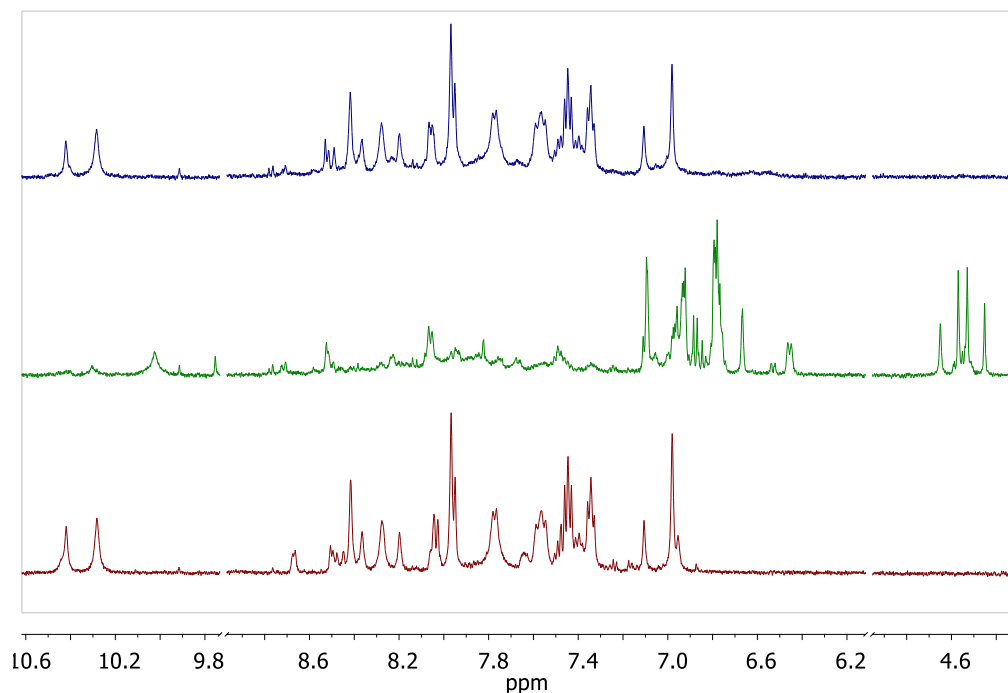


Figure 2.24. 2-AnthraAmide ¹H-NMR in DMSO-*d*₆. Middle : after irradiation at 365 nm for 24 hr. Bottom - After heating at 160 °C in oil bath for 48 hr. New peaks at ~4.5 ppm are ascribed to photo-isomer shown in **Figure 2.25** below.

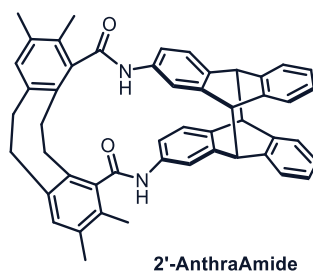


Figure 2.25. Proposed structure of the photo-isomer of 2-AnthraAmide.

This kind of reversible switch is of interest to many scientific communities and could find utility as a photoswitch or other molecular photoswitch. The quantitative reversion back to the 2-AnthraAmide without any deleterious side reactions is certainly an interesting result and could be further pursued.

Synthesis of 1-AnthraAmide and initial results

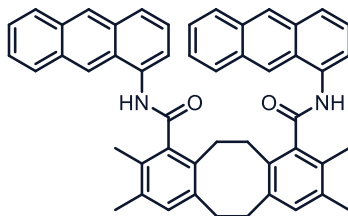


Figure 2.26. Skeletal structure of 1-AnthraAmide

1-AnthraAmide was prepared using the same general procedure as for the 1-PyreneAmide with 333mg of 1-aminoanthracene and 250 mg of di-CO₂H. 1-aminoanthracene is soluble in DCM, thus 500 μ l and 5 ml of DCM were used add the amine dropwise into the acid chloride after the distillation step. The reaction mixture was allowed to stir overnight and warm to room temperature. The solvent removed and the crude reaction suspended in DCM and filtered. This step removes any unreacted di-CO₂H which can be recycled for future use. TLC (5% MeOH in DCM) revealed a compound with a retention factor of 0.50. This spot was isolated with column chromatography and determined to be the desired product by NMR spectroscopy. The ¹H NMR spectrum is presented below in Figure 2.27. Up to 60 °C coalescence is not clearly observed. Mass of this compound was not confirmed in this work, although the ¹H NMR spectrum fully supports the proposed structure.

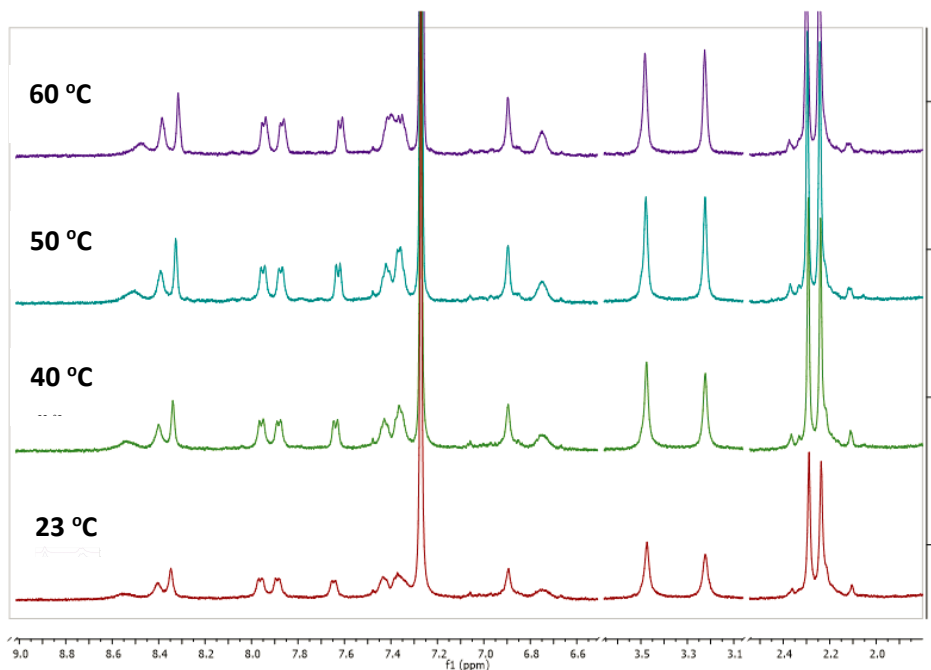


Figure 2.27. VT ¹H NMR (500 MHz, CDCl₃) of 1-AnthraAmide

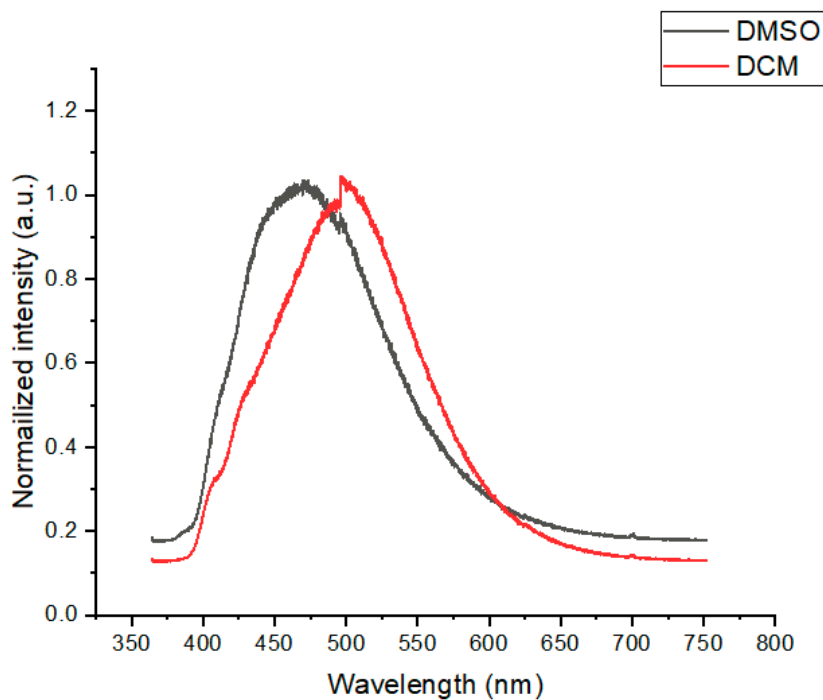


Figure 2.28. Fluorescence spectrum of 1-AnthraAmide in DCM and DMSO.

Interestingly the spectrum in DMSO is blue shifted compared to in DCM. DCM exhibits emission at 500 nm while DMSO at 460 nm (Figure 2.28). This is counter intuitive as classic solvatochromism states more polar solvents will lead to a red shifted emission. Studies on the excimer emission of pyrene-3-carboxaldehyde state the fluorescence maxima in nonpolar solvents is around 530 nm and in polar solvents about 560 nm, indicating a bathochromic shift would be expected. Additionally, increasing the fraction of water in mixtures of H₂O: dioxane also exhibit a marked red shift with the increase of water in the system.¹³ This shift observed in 1-AnthraAmide may be attributed to the increased polarizability of DCM over DMSO, but this was not determined for this system. Further experiments would be required to determine the true dependence of solvent polarity on the emissive properties of this compound.

Conclusions on chapter 2

3 novel DBCOD based compounds containing pyrene and anthracene were synthesized in an attempt to exploit the conformational dynamics to reversibly control the nature of the emissive properties. 1-PyreneAmide exhibited excimer emission up to the limits of temperature in our fluorimeter (90 °C). This suggests the TM-DBCOD scaffold wasn't large enough to separate the pyrenes the >10Å required to form monomeric emission, even in the chair conformer. VT ¹H NMR in CDCl₃ confirmed coalescence around 60 °C, thus suggesting that even interconversion between the Boat and Chair

conformers in occurring in solution but it doesn't attenuate the excimer emission. While neither of the compounds exhibited the desired thermal response, 2-AnthraAmide exhibited an intriguing response to solvent polarity and photo-thermal isomerization. 1-AnthraAmide exhibited an interesting solvent dependence that warrants further investigation. While these compounds are in their infancy the prospect of developing responsive materials based on the DBCOD scaffold remains an extremely promising avenue of research. The main problem to overcome in developing anthracene-based systems will be to prevent the [4+4] photoisomerization, substitution on the anthracene ring may prevent this. Additionally, the 1-AnthraAmide compound needs to be more thoroughly characterized. Shown below in Figure 2.29 is a proposed solution to preventing the photoisomerization of these compounds, since substitution on the 9 positions of anthracene is known to suppress the [4+4] cycloaddition. Additionally, during the course of this work, care was not taken to exclude oxygen, which could be playing an unforeseen role in the emissive properties of these compounds.

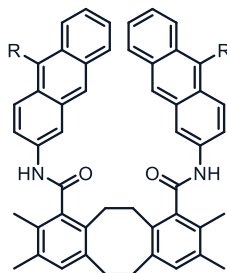


Figure 2.29. Proposed substitution on 2-AnthraAmide to prevent deleterious photoisomerization.

References for chapter 2

1. W.; Alam, T. M.; Li, J.; Bustamante, J.; Lien, T.; Adams, R. W.; Teat, S. J.; Stokes, B. J.; Yang, W.; Liu, Y.; Lu, J. Q. Arene Substitution Design for Controlled Conformational Changes of Dibenzocycloocta-1,5-dienes. *J. Am. Chem. Soc.* **2020**, 142 (39), 16651–16660
2. Bains, G. K.; Kim, S. H.; Sorin, E. J.; Narayanaswami, V. The Extent of Pyrene Excimer Fluorescence Emission Is a Reflector of Distance and Flexibility: Analysis of the Segment Linking the LDL Receptor-Binding and Tetramerization Domains of Apolipoprotein E3. *Biochemistry* **2012**, 51, 6207–6219
3. Birks, J. B.; Christophorou, L.G. Excimer fluorescence spectra of pyrene derivatives. *Spectrochim. Acta* **1963**, 19, 401–410s
4. Bains, G.; Patel, A. B.; Narayanaswami, V. Pyrene: A Probe to Study Protein Conformation and Conformational Changes. *Molecules* **2011**, 16 (9), 7909–7935.
5. Das, A., Danao, A., Banerjee, S., Raj, A. M., Sharma, G., Prabhakar, R., Srinivasan, V., Ramamurthy, V., & Sen, P. Dynamics of Anthracene Excimer Formation within a Water-Soluble Nanocavity at Room Temperature *J. Am. Chem. Soc.*, **2021** 143(4), 2025–2036

6. Nishiuchi, T.; Uno, S.; Hirao, Y.; Kubo, T. Intramolecular Interaction, Photoisomerization, and Mechanical C–C Bond Dissociation of 1,2-Di(9-anthryl) benzene and Its Photoisomer: A Fundamental Moiety of Anthracene-Based π -Cluster Molecules. *J. Org. Chem.* **2016**, 81, 2106–2112
7. Tomohiko Nishiuchi, Kazuki Kisaka, Takashi Kubo. Synthesis of Anthracene-Based Cyclic π -Clusters and Elucidation of their Properties Originating from Congested Aromatic Planes. *Angew. Chem. Int. Ed.* **2021**, 60 (10) , 5400-5406.
8. Yasukawa, N.; Yokoyama, H.; Masuda, M.; Monguchi, Y.;Sajiki, H.; Sawama, Y. *Green Chem.* **2018**, 20, 1213
9. Zhao, C.; Cai, X.; Ma, Z.; Shi, J.; Xu, L.; Wang, H. Excimer Formation from Partially Overlapped Anthracene Dimer Based on Saddle-shaped Cyclooctatetrathiophene as Spacer. *J. Photochem. Photobiol., A* **2018**, 355, 318–325.
10. Wannasiri, C.; Chanmungkalakul, S.; Bunchuay, T.; Chuenchom, L.; Uraisin, K.; Ervithayasuporn, V.;Kiatkamjornwong, S. Cross-Linking Silsesquioxane Cages with Polyaromatics as Fluorescent Porous Polymers for Fluoride Sensing and Removal. *ACS Appl. Polym. Mater.* **2020**, 2, 1244–1255
11. Tomohiko Nishiuchi, Kazuki Kisaka, Takashi Kubo. Synthesis of Anthracene-Based Cyclic π -Clusters and Elucidation of their Properties Originating from Congested Aromatic Planes. *Angew. Chem. Int. Ed.* **2021**, 60 (10) , 5400-5406.
12. J. Frommer; B. Karg; K. Weisz; S. Müller, Preparation and characterization of pyrene modified uridine derivatives as potential electron donors in RNA. *Org.Biomol.Chem.* **2018**, 16,7663–7673
13. Kalyanasundaram, K.; Thomas, J. K. Solvent-Dependent Fluorescence of Pyrene-3-carboxaldehyde and Its Applications in the Estimation of Polarity at Micelle-Water Interfaces. *J. Phys. Chem.* 1977, 81, 2176–218

Chapter 3. H-BPin/KO^tBu mediated palladium catalyzed hydrogenation of trans-stilbene and discovery of benzo-oxetenes side product in B₂(OH)₄ mediated deoxygenation of aromatic ketones – Side Projects

Abstract

During the studies outlined in chapter 1 I envisioned a novel method for the hydrogenation of olefins that employed an alternative hydrogen atom source. To my knowledge, borohydride had not been employed in palladium catalysis for the hydrogenation of olefins. I showed that under palladium catalysis the addition of potassium tertbutoxide to pinacol borane is capable of hydrogenation of trans-stilbene to dibenzyl. The addition of an external oxidant appeared to close the catalytic cycle allowing for catalytic palladium to affect this transformation. While this reaction was not further developed, this strategy could hold promise in asymmetric hydrogenation of unactivated olefins, one of the most difficult transformations in all synthetic chemistry. Additionally, I describe the isolation and initial characterization of a unique benzo-oxetane side product discovered during the work done in chapter 1. The unique strained ring of this product has yet to be described in any literature. Spectroscopic characterization is presented supporting the unexpected structure.

Hydride mediated alkene hydrogenation

In 2018 Webster and coworkers showed an β -diketiminate iron(II) precatalyst with HBpin and a sacrificial amine could be used to hydrogenation unactivated olefins Figure. 3.1. Although this method uses a 1st row transition metal, the catalyst preparation is laborious and requires use of ⁿBuLi and air free techniques. This method could be extended to hydrogenate even terpene natural products as well as aminoalkanes. Trisubstituted α -methylstyrene did require 90 °C for 4hr for complete conversion.

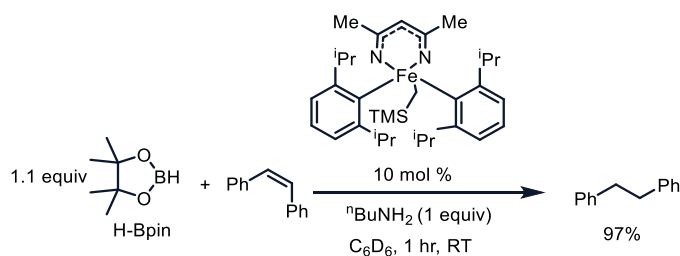


Figure 3.1. β -diketiminate iron (II) catalyzed hydrogenation of alkenes using H-Bin.³

The strategy of employing an activated hydride of H-BPin and a catalytic alkali alkoxide base (NaOEt) was first employed by Clark in a metal free reduction of ketones to alcohols in 2011. The Thomas Group used a similar system for the activation of 1st row transition metal catalysts for hydroboration and other reactions. I envisioned this species could be used as a hydride source in a palladium catalyzed olefin

hydrogenation. In 2018 the Thomas Group showed that boranes in the presence of many nucleophiles decomposes into BH_3 , which in turn can be used in hydroboration of unsaturated C-C bonds. The authors investigated a myriad of nucleophiles including LiO^tBu , NaO^tBu , and KO^tBu finding a 7.5 M solution with 0.5M solution of the nucleophile afforded only a 0.02 M solution of BH_3 . This surprising result that BH_3 is formed under these conditions is relevant to the reaction discussed next.

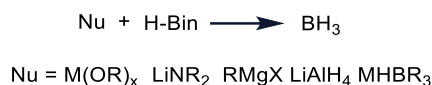


Figure 3.2. Nucleophile promoted decomposition of HBpin to form BH_3 as demonstrated by Thomas⁻²

Table 3.1. Optimization and Proposed mechanism of H-Bin/ KO^tBu Palladium Catalyzed Hydrogenation of Trans-Stilbene

Entry	Pd source	Pd loading [%]	Oxidant (equiv)	Conversion to 6b
1	$\text{Pd(P}^t\text{Bu}_3)_2$	5	none	>5
2	Pd(OAc)_2	20	none	20
3	Pd(OAc)_2	100	none	100
4	Pd(OAc)_2	20	BQ (1.1)	70
5	PdCl_2	5	none	>5
6	PdCl_2	5	BQ (1.1)	70
7 ^a	Pd(OAc)_2	10	BQ (1.1)	100

a. Reaction in benzene. Conversion determined by $^1\text{H-NMR}$

B

Benzoquinone (BQ)

Possible Mechanism

Table 3.1 outlines the reactions run to test this hypothesis if palladium could be used in this manner to conduct a catalytic reaction. A mixture of palladium salts, H-BPin, KO^tBu, and an oxidant was examined in the presence of model substrate trans-stilbene. First, Pd(P^tBu₃)₂ was screened, and it showed very little activity under these conditions giving only a trace conversion to **2b** (Table 3.1, entry 1). No hydroboration products were detected in entry 1 suggesting BH₃ formation is suppressed as it would likely lead to hydroboration. Next, a high catalyst loading of 20 mol% of Pd(OAc)₂ (entry 2) gave the interesting and peculiar result of 20% conversion to **2b**. Intrigued by this result a stoichiometric reaction in which 100 mol% of Pd(OAc)₂ gave a full conversion to **2b**. This result and the failure of a zero valent palladium catalyst strongly suggested a Pd(II) species is the active catalyst involved in engaging the borohydride to begin product formation. Obviously stoichiometric palladium is not amenable to a practical method for the hydrogenation of an alkene, thus I sought to make the reaction catalytic by enabling turnover of the palladium catalyst. Reductive elimination is likely the product determining step of this reaction, as with traditional palladium catalyzed hydrogenations. Since Pd(P^tBu₃)₂ (Table 3.1, entry 1) proved to be an inactive catalyst under these conditions I proposed it the catalytic dead end. To this end, I employed the oxidant benzoquinone (BQ) to re-oxidize the Pd(0) to Pd(II) and hopefully complete the catalytic cycle. BQ is known to act as an oxidant in palladium catalyzed C-H functionalization reactions, in reactions such as the oxidative Heck, to reoxidize a Pd(0) species back to Pd(II). Upon inclusion of 1.1 equivalents of BQ the yield increased to quantitative hydrogenation using 10 mol% Pd(OAc)₂ making this method catalytic (Table 3.1, entry 4). The byproduct fate of the benzoquinone was not established and could potentially give insight into the nature of the presumed oxidation. The mild oxidant Selectfluor was also screened but gave very low yield presumably unable to effectively re-oxidize the generated Pd(0) back to Pd(II). Additionally, there were no hydroboration products observed during this study in any reaction mixture. However, hydroboration and subsequent deborylation-protiation cannot be ruled out under the current understanding of this reaction, especially given the likely formation of BH₃ in the reaction mixture. It is my hope that these results will help inform someone attempting a similar method.

Although this work was not further pursued, it could lay the groundwork for development of an asymmetric hydrogenation of unactivated olefins if a chiral phosphine ligand is incorporated into the reaction mixture. The use of a more atom economical alkoxide like sodium methoxide could help improve the atom economy. Also, to this end, screening mild oxidants added over the course of the reaction could also help improve this reaction. This work was not expanded to screen the functional group tolerance of this method, which could reveal a robust method for asymmetric hydrogenation of unactivated olefins, which remains a difficult problem in synthetic chemistry.

Isolation and identification of a novel benzo-oxetane product in the diboron mediated deoxygenation of aromatic ketones

Through the course of all this work, no side products of observable quantity were observed when THF was employed as the solvent. However, in MeCN an additional product was observed by thin layer chromatography in levels in anhydrous conditions. The identity of this compound remained unknown for some time until careful isolation by column chromatography and subsequent NMR and high resolution mass spectroscopy revealed it to be the odd benzo-oxetane (**5a**, Figure 3.4). This structure had never been reported, although a similar structure was recently synthesized summarized in Figure 3.4. 2'-hydroxyacetophenones were found to cyclize into benzo-oxetes using sulfonyl fluoride at high temperatures in DMSO.³

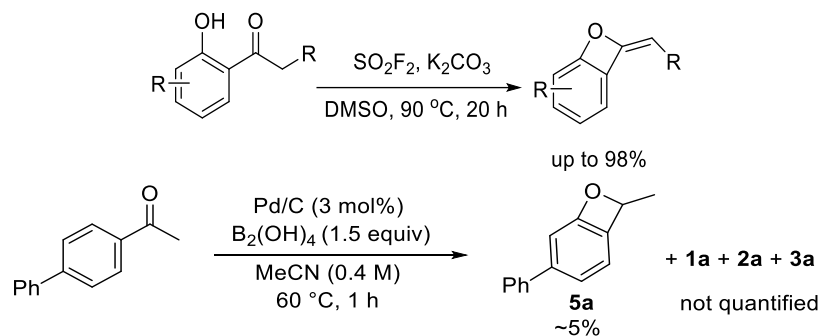


Figure 3.3. (Top) Sulfonyl fluoride mediated synthesis of benzo-oxetes from 2'-acetophenones. (Bottom) Side product of benzo-oxetane when MeCN is employed as solvent.

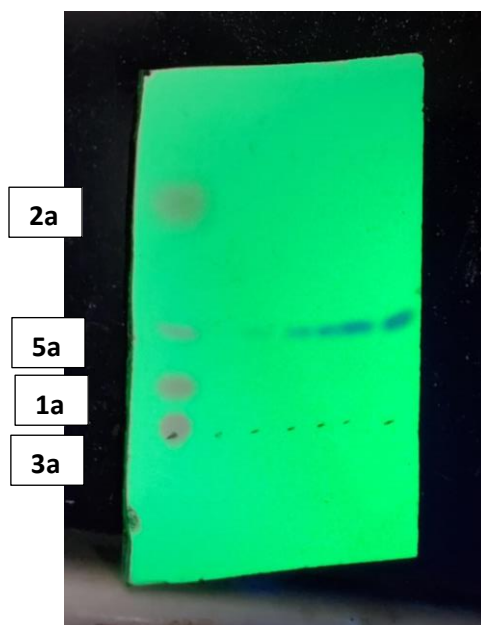


Image 3.1 . Picture of TLC plate of reaction depicted in **Figure 3.4 bottom** in the left most lane . The other lanes are from fractions of the column chromatography used to isolate the unknown product. Eluent - EtOAc:Hexanes (1:4).

From observing the TLC plate it was apparent a new product was being formed in significant quantities under slightly altered condition from those optimized for deoxygenation. A picture of the TLC plate is given as **Figure 3.4** above. Strangely, the new product when viewed under 254nm excitation of the UV lamp glowed violet blue, which was distinctly different from the other spots on the plate. Typically most organic compounds show as pink under the TLC lamp. Qualitatively aryl ethers and phenols also exhibit this color when viewed on a TLC plate. This observation began a series of structural determination experiments.

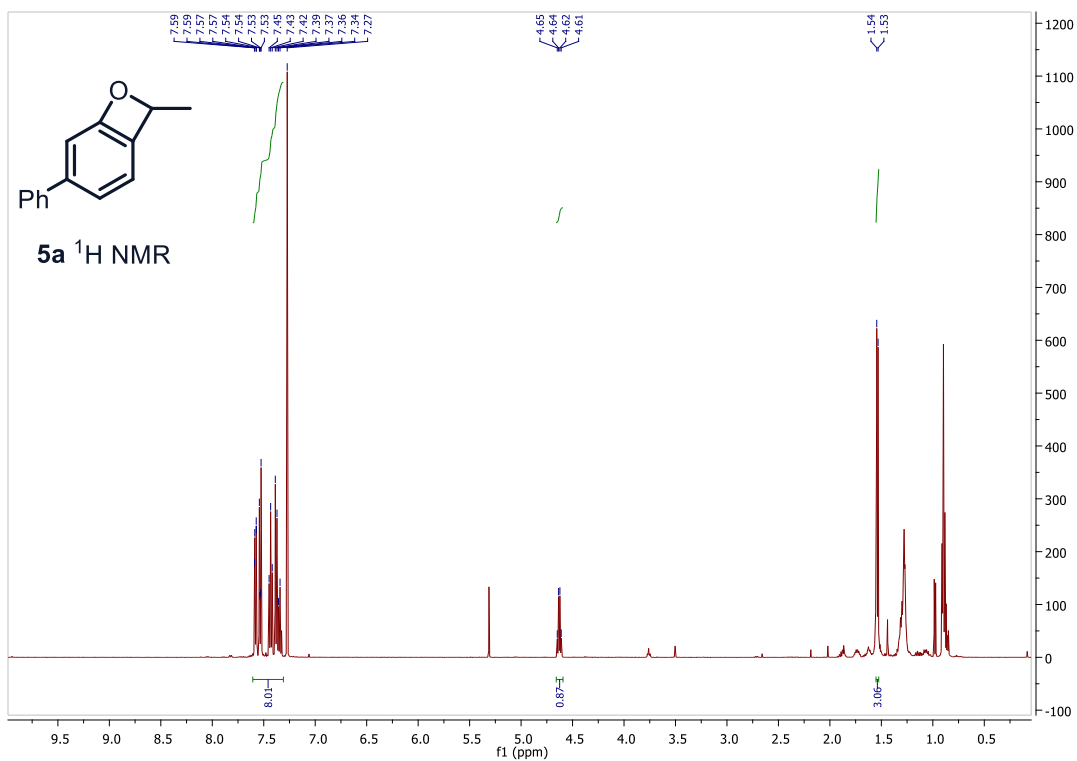


Figure 3.4. ^1H NMR (500 MHz, CDCl_3) of isolated **5a**

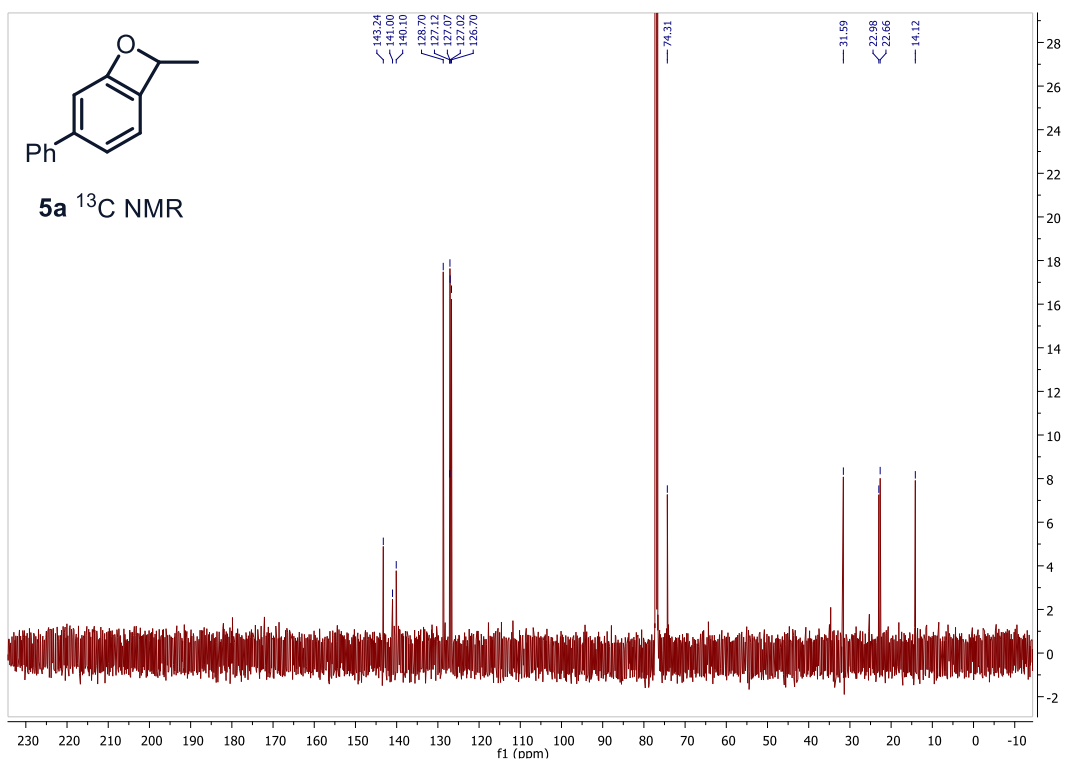


Figure 3.5 ^{13}C NMR (101 MHz, CDCl_3) of isolated **5a**

The doublet at 1.54 ppm integrated to 3 hydrogens and quartet at 4.62 ppm integrated to 1 hydrogen. These distinct features of this compound immediately rule out the characterized **2a**, **3a** and **4a**. The integration of the aromatic peaks at eight hydrogens immediately stood out as being lower than expected with nine hydrogens being in the starting material. The doublet at 1.54 ppm clearly indicated only 1 hydrogen on the neighboring carbon. ^{13}C NMR revealed the spectrum presented in Figure 3.5. A peak at 22.98 ppm and 74.31 ppm are observed. The resonance of 74.31 ppm is indicative of an ethereal carbon, which led me to believe a C-O bond could have potentially been formed, with signals in that region corresponding to ethereal carbons. To help elucidate the correlation between the observed peaks ^{13}C - ^1H HSQC was conducted (Figure 3.6) revealing cross peaks 4.62-74.31 ppm and 1.53-22.71 ppm. ^{13}C - ^1H HMBC (Figure 3.7) showed multiple bond correlation between the 1.51-74.24 ppm indicating the presumed methyl hydrogen is on the carbon adjacent to the methyl, confirming the connectivity of the atoms giving rise to those signals. A cross peak at 4.60-126.68 ppm indicated the presumed ethereal proton is multiple bonds away from the aromatic ring. None of these data disproved the proposed structure of **5a**.

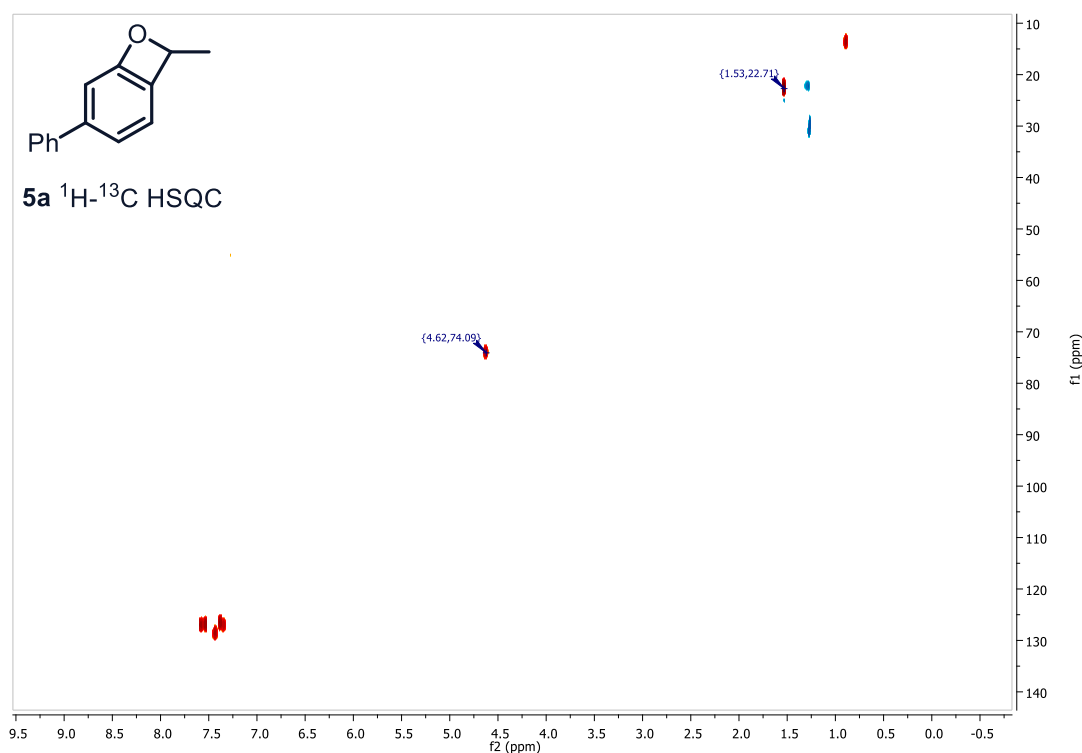


Figure 3.6 . ^{13}C - ^1H HSQC (500 MHz, CDCl_3) of **5a**.

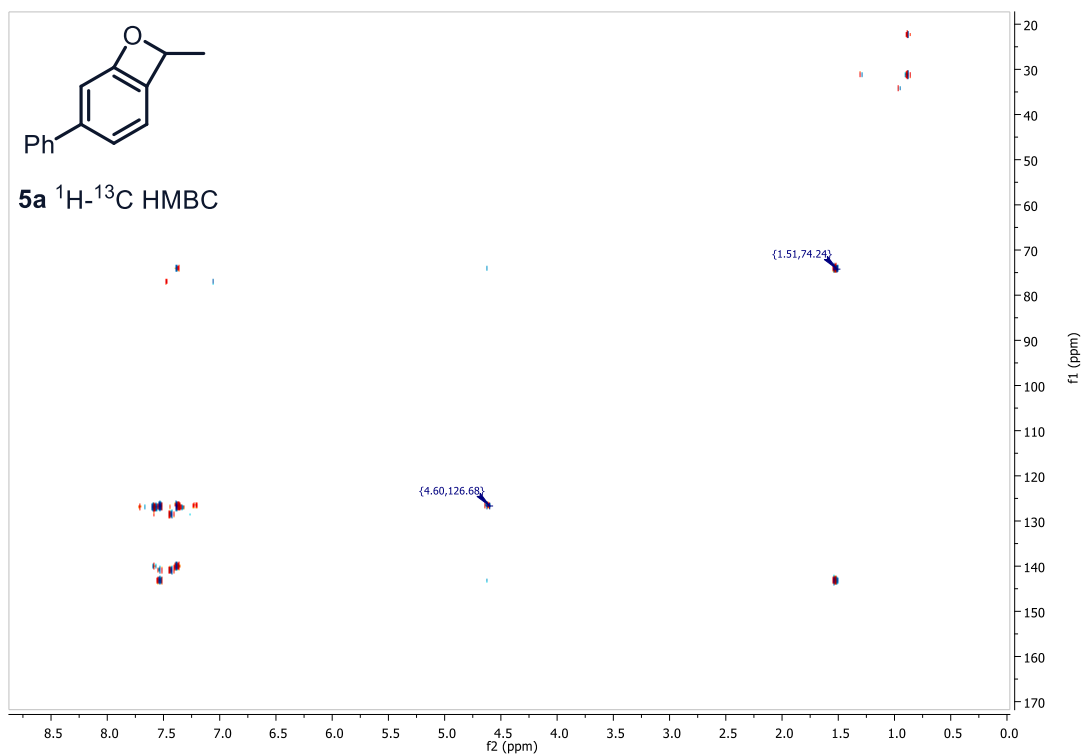


Figure 3.7. ^{13}C - ^1H HMBC (500 MHz, CDCl_3) of **5a**.

After gathering these data through NMR spectroscopy, high resolution mass spectroscopy was performed revealing a compound with an m/z of 197.0959 which perfectly agrees with the structure of **5a** which would exhibit an exact mass of 197.097 m/z when protonated (Figure 3.8) providing almost definitive proof to the identity of **5a**.

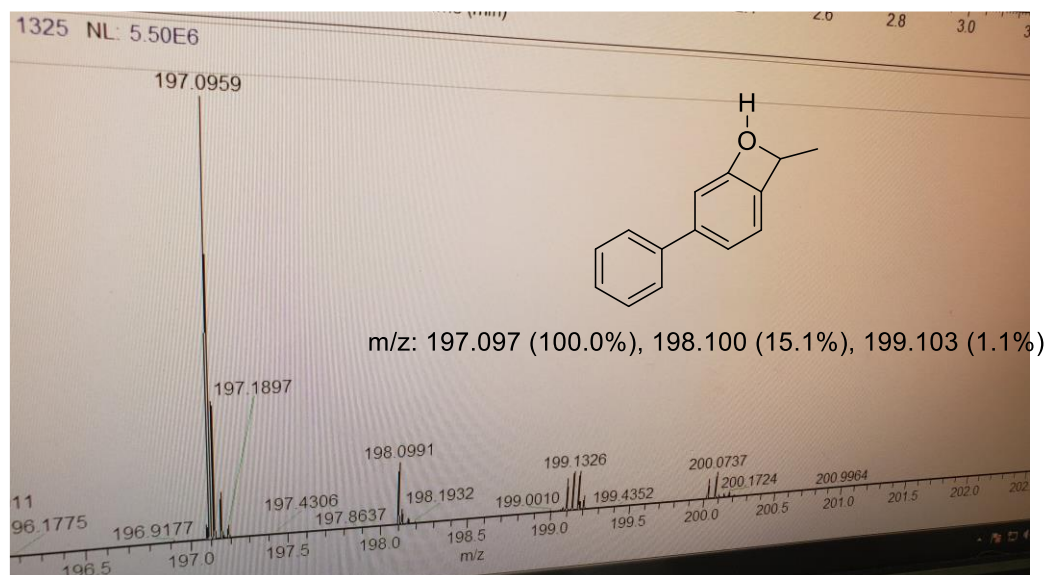


Figure 3.8. High resolution mass spectrum of **5a** showing an $m/z = 197.0959$.

Conclusions to chapter 3

First discussed, the method for hydrogenation of unactivated olefins described in the former section of this chapter represents an interesting and potentially useful method to be developed further by future researchers. The obvious drawback of this method is the atom economy. Use of a more atom economical oxidant than benzoquinone to achieve catalytic turn over could be a good place to begin investigation. Additionally, this reaction was not tested using a simple borane adducts (BH_3) which if successful could lead to a significantly improved atom economy. And finally, the inclusion of a prochiral substrate with an asymmetric palladium complex may afford the coveted asymmetric hydrogenation of unactivated olefins if successful.

On the later section of this chapter, optimizing the formation of the benzo-oxete product would be a worthwhile endeavor. While this structure has never been investigated or previously reported, traditional oxetanes are known to engender desirable changes in pharmaceutical compounds when compared to ketones. While it is unknown what appending an oxetane fused to a benzene ring like this would have since it has never been synthesized, it stands to reason compounds with this moiety would be worth investigating for their bioactivity. The mechanistic pathway for the formation of this compound was not postulated but I suspect the intermediate borate ester (**4a**) may play a key role in its formation since **5a** was only observed under anhydrous conditions. Borate ester **4a** rapidly converts to **3a** in the presence of water or any protic source and thus couldn't be transformed into **5a**. Isolation of the borate ester and subjection to various conditions could yield answers to the origin of the C-O bond forming step.

References for Chapter 3

1. Espinal-Viguri, M.; Neale, S. E.; Coles, N. T.; Macgregor, S.A.; Webster, R. L. Room temperature iron-catalyzed transfer hydrogenation and regioselective deuteration of carbon-carbon double bonds. *J. Am. Chem. Soc.* **2019**, 141, 572–582
2. Bage, A. D.; Nicholson, K.; Hunt, T. A.; Langer, T.; Thomas, S. P. The Hidden Role of Boranes and Borohydrides in Hydroboration Catalysis. *ACS Catal.* **2020**, 10, 13479–13486.
3. R. Lekkala, B. Moku, K.P.Rakesh and H. L. Qin, SO_2F_2 -mediated transformation of 2'-hydroxyacetophenones to benzo-oxetes. *Beilstein J. Org. Chem.*, **2019**, 15, 976

End of Document